

UNIVERSIDADE DE LISBOA
FACULDADE DE FARMÁCIA



Nanoencapsulation of New Compounds with Potential Antileishmanial Activity

João Pedro Vitorino Quintas

Tese orientada pelo Professor Doutor António José Leitão das Neves Almeida
Coorientada pela Professora Doutora Francisca da Conceição Lopes

Dissertação apresentada à Faculdade de Farmácia da Universidade de Lisboa com vista à
obtenção do grau de Mestre em Química Farmacêutica e Terapêutica

Lisboa

2016

UNIVERSIDADE DE LISBOA
FACULDADE DE FARMÁCIA



Nanoencapsulation of New Compounds with Potential Antileishmanial Activity

João Pedro Vitorino Quintas

Tese orientada pelo Professor Doutor António José Leitão das Neves Almeida
Coorientada pela Professora Doutora Francisca da Conceição Lopes

Dissertação apresentada à Faculdade de Farmácia da Universidade de Lisboa com vista à
obtenção do grau de Mestre em Química Farmacêutica e Terapêutica

Lisboa

2016

***“Every disadvantage has its
advantage.”***

Johan Cruyff

Aos meus pais

Acknowledgements

Durante o percurso até à finalização dos estudos conducentes ao grau de mestre existiram desafios, intelectuais e pessoais, que só foram possíveis de ultrapassar com a entreaajuda de todos aqueles que contribuíram para este caminho. Não querendo esquecer ninguém, a todos, o meu sincero agradecimento.

Em primeiro lugar gostaria de expressar toda minha gratidão aos meus orientadores Prof.^a Francisca Lopes e Prof. António Almeida pela permanente disponibilidade, pelos seus sábios conselhos, crítica perspicaz, pelo tempo que dedicaram ao constante aperfeiçoamento da presente dissertação e encorajamento que me ajudou a atingir os objectivos propostos.

À Doutora Manuela Colla gostaria de expressar os meus sinceros agradecimentos pela ajuda nos ensaios de viabilidade celular e actividade *in vitro*. À Doutora Lúcia Gonçalves agradeço a disponibilidade e partilha de conhecimentos.

A todos os colegas de ambos os grupos, e de um modo especial, à Joana Magalhães, André Dias, Diana Gaspar, Paulo Roque Lino e Joana Marto agradeço o espírito de grupo, a amizade e boa disposição, o sentido de entreaajuda e humor dentro e fora dos laboratórios, e pelo permanente apoio que me ajudou a ultrapassar as fases mais difíceis.

Aos meus amigos de sempre Mário Cardoso, Rudi Silva, Mauro Cardoso, Diogo Lourenço, João Meireles e Miguel Rosa pela sua inestimável amizade ao longo destes anos.

Um especial agradecimento à minha namorada, Joana Oliveira por todo o apoio, amizade e motivação que foi crucial ao longo deste percurso.

A toda a minha família que sempre me encorajou a prosseguir com a minha vida académica. Um especial obrigado aos meus pais, pela compreensão, apoio e força incansáveis não só ao longo destes anos, mas sempre. Aos meus irmãos por toda a boa disposição e alegria. Aos meus avós por todos os valores que me transmitiram e às minhas tias pelo apoio permanente.

Abstract

Infectious diseases caused by viruses, parasites and bacteria are currently the second cause of mortality worldwide. One of these parasites is *Leishmania sp.*, the protozoa responsible for leishmaniasis, which is highly susceptible to oxidative stress where trypanothione reductase is an enzyme that plays a crucial role in the antioxidant defense. Endoperoxide compounds such as tetraoxanes are known to be reductively activated by iron(II)-heme to form carbon-centered radicals that will create oxidative stress in the parasite. Following this concept, new tetraoxane compounds intended as antileishmanial drugs were designed and synthesized. The synthesis reaction occurred in two steps: first the suitable ketones or aldehydes were treated with hydrogen peroxide and formic acid to give the corresponding gem-dihydroperoxide; then, *trans*-cinnamaldehyde and Re_2O_7 were added to complete conversion into 1,2,4,5-tetraoxane. Two novel tetraoxanes (**23** and **24**) were synthesized, characterized and loaded in solid lipid nanoparticles in order to improve the targeting capacity and effective delivery to infected macrophages. These nanosystems, composed of natural triacylglycerols are among the most promising nanostructured particulate carriers with proven *in vivo* efficacy in the treatment of experimental leishmaniasis, while reducing adverse side effects in non-target organs. Solid lipid nanoparticles were prepared by emulsion-solvent evaporation method, using tripalmitin as the lipid component and sodium deoxycholate, Tween[®] 20 and lecithin as surfactants. Particle mean diameters of solid lipid nanoparticles loaded with compounds **23** and **24** were 118 nm and 125 nm, respectively. A narrow polydispersity index and a negative surface charge were achieved for both formulations, which is suitable for their physical stability and desirable for macrophage targeting. Particle mean diameter, polydispersity index and surface charge remain unchanged after storage during 20 days at 4°C. Encapsulation efficiencies of 87% and 88% were obtained for compounds **23** and **24**, respectively. The *in vitro* study showed a very promising activity of formulation loaded with compound **23** against leishmania infected THP-1 cells when compared with the standard anti-leishmanial drug miltefosine. Using this strategy, new therapeutically active tetraoxanes were synthesized and loaded in solid lipid nanoparticles, demonstrating their potential as anti-leishmanial agents.

Keywords: Leishmaniasis; Tetraoxanes; Solid lipid nanoparticles; *in vitro* evaluation.

Resumo

As doenças infecciosas causadas por vírus, bactérias e parasitas são atualmente a segunda causa de mortalidade em todo o mundo. Um destes parasitas é a *Leishmania sp.*, o protozoário responsável pela doença leishmaniose. Embora seja reportada como a nona doença infecciosa mais grave em todo o mundo, a leishmaniose continua a fazer parte do grupo das doenças negligenciadas, afetando sobretudo as regiões equatoriais mais pobres do globo.

Segundo a Organização Mundial de Saúde, 98 países são endêmicos para a leishmaniose onde estão cerca de 350 milhões de pessoas em risco de contraírem a doença, gerando aproximadamente 2 milhões de novos casos todos os anos.

São conhecidas mais de 20 espécies de *Leishmania* infecciosas para o Homem sendo as mais comuns as seguintes: *L. donovani*, *L. infantum*, *L. siamensis*, *L. braziliensis* and *L. guyanensis*. A doença é transmitida através da picada de uma mosca fêmea do género *phlebotomine*.

Existem principalmente três formas de leishmaniose: i) leishmaniose visceral, que constitui a forma mais severa da doença e que tem uma taxa de mortalidade a rondar os 100% na falta de medicação adequada; ii) leishmaniose cutânea, que representa a forma mais comum da doença; iii) leishmaniose mucocutânea que é a forma mais destrutiva da doença.

Durante mais de 70 anos, a primeira linha de tratamento nos países mais afetados foram os injetáveis de antimônio pentavalente (Pentostam[®] and Glucantime[®]). No entanto, este tratamento é doloroso, potencialmente tóxico, de longa duração e tornou-se ineficaz em algumas regiões, devido ao aparecimento de resistências. A pentamidina, a paromomicina e anfotericina B fazem parte dos fármacos de segunda linha usados no tratamento da leishmaniose, mas a sua utilização é limitada devido à toxicidade e também ao aparecimento de resistências. O medicamento mais atrativo e eficaz é a formulação lipídica da anfotericina B, o Ambisome[®], que apesar do índice terapêutico elevado e ausência de efeitos secundários é bastante caro e, desta forma, inacessível para os países endêmicos, que são na sua maioria pobres. Finalmente, o primeiro fármaco eficaz de administração oral, a miltefosina, está associada a teratogenicidade e atividade hemolítica, e o seu tempo de semi-vida é muito longo, o que pode também originar o aparecimento de resistências. Por estas razões, e na ausência de uma vacina eficaz e

barata, a necessidade de novos medicamentos eficazes contra a leishmaniose é mais urgente que nunca.

A *Leishmania* é muito suscetível ao *stress* oxidativo, situação em que a enzima tripanotiona redutase desempenha um papel fundamental na defesa antioxidante. Compostos com função endoperóxido como os tetraoxanos, inicialmente desenvolvidos para o tratamento da malária, são conhecidos por serem redutivamente ativados pelo ferro (II)-heme para formarem radicais centrados no carbono e espécies reativas de oxigênio (ROS) que irão criar *stress* oxidativo no parasita.

Seguindo este conceito, foram sintetizados novos tetraoxanos destinados a atuarem como fármacos antileishmaniose através de um mecanismo de ação duplo. Sendo assim, após a ativação do tetraoxano pelo ferro (II), por quebra da ligação peroxídica, irão formar-se dois compostos: uma primeira molécula radicalar, altamente reativa, que poderá alquilar biomoléculas essenciais para a sobrevivência do parasita, ao mesmo tempo que contribui para o aumento do *stress* oxidativo; forma-se também uma segunda molécula com um carbonilo α,β -insaturado na sua estrutura, que funcionará como possível inibidor da enzima tripanotiona redutase.

Para obtenção dos compostos pretendidos recorreu-se a um processo de síntese que ocorreu em duas etapas: em primeiro lugar compostos carbonílicos (cetonas ou aldeídos) reagiram com peróxido de hidrogénio na presença de ácido fórmico, à temperatura ambiente, para formar o correspondente *gem*-dihidroperóxido; de seguida este intermediário reagiu com aldeído *trans*-cinâmico com catálise de Re_2O_7 , a 0°C, para completar a conversão no 1,2,4,5-tetraoxano. Dois novos tetraoxanos (**23** e **24**) foram assim sintetizados, purificados e caracterizados. O rendimento final da reação de síntese do composto **23** foi de 71% e o do composto **24** foi de 47%. Ambos os compostos foram caracterizados por ressonância magnética nuclear de próton (^1H -RMN), de carbono (^{13}C -RMN) e por técnicas bidimensionais (COSY, HMQC, HMBC), espectroscopia de infravermelho, análise elementar e ponto de fusão.

Os valores de análise elementar estão de acordo com os valores teóricos calculados e os pontos de fusão são 132-135°C e 96-100°C para os compostos **23** e **24**, respetivamente e foram concordantes em duas técnicas diferentes (método de fusão instantâneo e DSC).

Desde que foram descritas, no início dos anos 90, as nanopartículas lipídicas sólidas são vistas como uma excelente alternativa, eficaz e não tóxica, aos transportadores de fármacos coloidais mais conhecidos, como por exemplo, os lipossomas. As nanopartículas lipídicas podem ser preparadas com lípidos normalmente utilizados como

excipientes farmacêuticos. As duas primeiras formas de produção destes transportadores foram a homogeneização a alta pressão e a microemulsão.

A natureza coloidal e de liberação controlada permitem a proteção dos fármacos encapsulados pelas nanopartículas lipídicas sólidas, e a administração parentérica e não parentérica. Estes nano-sistemas combinam as vantagens dos lipossomas e das nanopartículas poliméricas numa só tecnologia farmacêutica.

Os novos tetraoxanos foram então encapsulados em nanopartículas lipídicas sólidas, com o objetivo de melhorar a veiculação controlada e direcionada até aos macrófagos infectados. Estes nano-sistemas, constituídos por triacilgliceróis naturais estão entre os veículos mais promissores, com eficácia comprovada *in vivo* no tratamento da leishmaniose, reduzindo os efeitos secundários em órgãos não infectados.

As nanopartículas lipídicas sólidas foram preparadas pelo método de emulsão e evaporação de solvente, utilizando a tripalmitina como componente lipídica e o desoxicolato de sódio, Tween[®] 20 e lecitina como tensioativos. O diâmetro médio das partículas para as formulações com os compostos **23** e **24** encapsulados foi de 118 nm e 125 nm, respetivamente. Foi obtido um índice de polidispersão baixo e potencial zeta negativo para ambas as formulações. Estes valores são adequados para a sua estabilidade física, e desejáveis para vectorização para os macrófagos. O diâmetro médio das partículas, o índice de polidispersão e o valor de potencial zeta permaneceram inalterados após o armazenamento durante 20 dias a 4°C. Após esterilização por autoclave o diâmetro médio das partículas baixou consideravelmente, assim como a carga de fármaco. Este fenómeno foi identificado por DLS, uma vez que quando a temperatura se elevava acima do ponto de fusão da tripalmitina os tetraoxanos saíam do interior da matriz lipídica, resultando na redução do diâmetro médio das partículas. Foram obtidas eficiências de encapsulação de 87% e 88% para os compostos **23** e **24**, respetivamente. Os estudos de liberação comprovaram que a formulação com o composto **23** é mais estável aos valores de pH testados (7.4 e 1.0) mas que ambas têm de ser melhoradas de forma a aumentar a gastro resistência, uma vez que estas formulações têm como fim a administração oral.

Os estudos de viabilidade celular mostraram que ambos os compostos não têm toxicidade associada. O estudo *in vitro* em células THP-1 infectadas com *L. infantum* revelou atividade bastante promissora, do composto **23** encapsulado, quando comparado com a miltefosina (fármaco aprovado com atividade antileishmaniose). Esta estratégia permitiu a descoberta de novas formulações lipídicas com tetraoxanos encapsulados, como potenciais candidatos a fármacos contra a leishmaniose.

Palavras-chave: Leishmaniose; Tetraoxanos; Nanopartículas lipídicas sólidas; Avaliação *in vitro*.

Table of contents

Chapter 1 – State of the Art	3
1. Leishmaniasis	3
2. <i>Leishmania</i> spp. life cycle	5
2.1. Amastigotes morphology.....	7
2.2. Promastigotes morphology	8
3. Current leishmaniasis treatments	9
3.1. Pentavalent antimonials.....	9
3.2. Pentamidine	11
3.3. Amphotericin B	12
3.4. Paromomycin.....	14
3.5. Miltefosine.....	15
3.6. Ketoconazole	16
3.7. Allopurinol	17
3.8. Dinitroanilines	18
4. <i>Leishmania</i> iron	20
5. Tetraoxanes	22
5.1. Mechanism of action	23
6. Trypanothione reductase	24
7. Nanoparticulate Drug Carriers	27
8. Work's aim	30
9. References	32
Chapter 2 – Synthesis and characterization of 1,2,4,5-tetraoxanes derived from <i>trans</i>-cinnamaldehyde	43
1. Introduction	43
2. Materials and methods	46
2.1. Reagents	46
2.2. Solvents	46
2.3. Chromatography.....	46
2.4. Equipment.....	47
2.5. General procedures for the synthesis of the tetraoxanes	47
2.5.1. (E)-3-phenyl-6-styryl-1,2,4,5-tetraoxane (23).....	47
2.5.2. (E)-3-styryl-1,2,4,5-tetraoxaspiro [5.5] undecane (24).....	48

2.5.3. Attempt to synthesize (1r,5R,7S)-4'-((E)-styryl)spiro[adamantane-2,1'-cyclohexane] (25).....	49
3. Results and discussion	50
3.1. Synthesis methodology	50
3.1.1. Optimization of adamantane-tetraoxane synthesis.....	51
3.2. Benzaldehyde-tetraoxane (23) characterization	53
3.3. Cyclohexane-Tetraoxane (24) characterization	56
4. References	59
Chapter 3 - Lipid nanoparticles containing tetraoxanes for the treatment of leishmaniasis.....	63
1. Introduction.....	63
2. Materials and methods	65
2.1. Reagents.....	65
2.2. Solubility of tetraoxanes in the lipid matrix.....	65
2.3. Preparation of SLN	66
2.4. SLN characterization.....	66
2.4.1. Measurement of particle size and zeta potential	66
2.4.2. Determination of tetraoxanes encapsulated in SLN.....	66
2.4.3. Encapsulation efficiency and drug loading	67
2.5. Stability studies.....	68
2.5.1. Stability in suspension	68
2.5.2. Effect of sterilization.....	68
2.6. Differential scanning calorimetry (DSC) studies.....	68
2.7. Dynamic light scattering (DLS) studies.....	69
2.8. Transmission electron microscopy (TEM).....	69
2.9. In vitro Release Study.....	69
2.10. Cell viability study	70
2.11. In vitro activity studies.....	70
3. Results and discussion	71
3.1. Development of SLN formulations as carriers for tetraoxanes 23 and 24	71
3.2. Characterization of SLN formulations	72
3.3. TEM study	74
3.4. DSC study	75
3.5. Physical stability	77
3.6. DLS study	78

3.7. In vitro Release study	80
3.8. Cell viability studies	82
3.9. In vitro activity studies	84
4. References	87
Concluding remark and future work.....	91
Chapter 4 - Concluding remark and future work	93
1. Concluding remarks	93
2. Future work.....	94
Chapter 5 - Annexes	99

List of Figures

Chapter 1 – State of the Art

Figure 1- World map representing the status of endemicity of VL until 2013.....	4
Figure 2- World map representing the status of endemicity of CL until 2013..	5
Figure 3- Life cycle of <i>Leishmania</i> parasites.....	6
Figure 4- Illustration of promastigotes (A) and amastigotes (B).....	8
Figure 5- Structures of the most common pentavalente antimonials.....	10
Figure 6- Structure of pentamidine.	12
Figure 7- Structure of amphotericin B.	14
Figure 8- Structure of paromomycin.....	15
Figure 9- Structure of miltefosine.....	16
Figure 10- Structure of ketoconazole.....	17
Figure 11- Structure of allopurinol.	18
Figure 12- Structures of trifluralin and oryzalin.	19
Figure 13- Schematic representation of iron acquisition pathways in <i>Leishmania</i>	21
Figure 14- Chemical structure of 12- Artemisinin; 13- 1,2,4-trioxane; 14- 1,2,4,5-tetraoxane.....	22
Figure 15- TR-catalyzed reduction.	25
Figure 16- GR-catalyzed reduction.....	25
Figure 17- Ribbon drawing of the trypanothione reductase dimer..	27
Figure 18- Solid lipid nanoparticle general structure.....	29
Figure 19- Tetraoxanes specific designed for the purpose of this work.	30

Chapter 2 – Synthesis and characterization of 1,2,4,5-tetraoxanes derived from trans-cinnamaldehyde

Figure 1- Tetraoxanes compounds designed for this study.....	43
Figure 2- Tetraoxanes retrosynthetic scheme..	45
Figure 3- Benzaldehyde-tetraoxane (23) ¹ H-NMR spectra.....	54
Figure 4- Benzaldehyde-tetraoxane (23) ¹³ C-NMR spectra.	54
Figure 5- Benzaldehyde-tetraoxane (23) HMQC spectra.	55

Figure 6- Cyclohexane-tetraoxane (24) ¹ H-NMR spectra.....	56
Figure 7- Cyclohexane-tetraoxane (24) HMQC spectra.	57

Chapter 3 - Lipid nanoparticles containing tetraoxanes for the treatment of leishmaniasis

Figure 1- Calibration curves of the estimation of tetraoxanes 23 and 24..	67
Figure 2- SLN formulations photos obtained by TEM.....	75
Figure 3- DSC thermograms of formulations SLN 23 and SLN 24.....	76
Figure 4- Variation of the average diameter of SLN 23 formulation.....	79
Figure 5- Variation of the average diameter of SLN 24 formulation.....	79
Figure 6- Release studies of SLN 23	80
Figure 7- Release studies of SLN 24	81
Figure 8- Cellular viability of THP-1 cells after 24 h of incubation.....	82
Figure 9- Cellular viability of THP-1 cells after 48 h of incubation.....	83
Figure 10- Activity against <i>L. infantum</i> parasite of the free tetraoxanes 23 and 24	84
Figure 11- Activity against <i>L. infantum</i> parasite of SLN 23 and SLN 24	85

List of Tables

Chapter 1 – State of the Art

Table 1- Overview of existing drugs for VL treatment.....	20
--	----

Chapter 2 – Synthesis and characterization of 1,2,4,5-tetraoxanes derived from trans-cinnamaldehyde

Table 1- Theoretical Log P.....	44
Table 2- Summary of the synthesis reactions.....	51
Table 3- Different reactions for the synthesis of the adamantane-tetraoxane.....	53

Chapter 3 - Lipid nanoparticles containing tetraoxanes for the treatment of leishmaniasis

Table 1- Composition of SLN 23 and SLN 24 formulations	72
Table 2- Characterization of formulation 1 for SLN 23 and SLN 24	73
Table 3- Characterization of formulation 2 for SLN 23 and SLN 24	74
Table 4- Characterization of formulation 2 for SLN 23 and SLN 24 after 20 days at 4°C	77
Table 5- Characterization of formulation 2 for SLN 23 and SLN 24 after sterilization by autoclaving.....	77
Table 6- Cellular toxicity of free tetraoxanes 22 and 24 at different incubation times..	83

List of Schemes

Chapter 1 – State of the Art

Scheme 1- Activation of the peroxidic bond by free Fe²⁺ or heme 23

Chapter 2 – Synthesis and characterization of 1,2,4,5-tetraoxanes derived from trans-cinnamaldehyde

Scheme 1- Synthetic procedure used to obtain the Tetraoxanes compounds..... 45

Scheme 2- Scheme of the approach used for the synthesis of the desired tetraoxanes .. 50

Scheme 3- Scheme of the approach used to optimize the synthesis of the adamantane-tetraoxane..... 52

List of Mechanisms

Chapter 2 – Synthesis and characterization of 1,2,4,5-tetraoxanes derived from trans-cinnamaldehyde

Mechanism 1- Proposed mechanism for the synthesis of the desired tetraoxanes. 50

Abbreviations

ACN- acetonitrile

ATP- adenosine triphosphate

CL- cutaneous leishmaniasis

DL- loading capacity

DLS- Dynamic light scattering

DMSO- dimethyl sulfoxide

DSC- Differential scanning calorimetry

EE- encapsulation efficacy

EC₅₀- half maximal effective concentration

FAD- flavin adenine dinucleotide

FLP- frataxin-like protein

GR- glutathione reductase

HCl- hydrochloric acid

MFLP- mitoferrin like-protein

ML- mucocutaneous leishmaniasis

m.p.- melting point

NMR- nuclear magnetic resonance

o/w- oil in water

PBS- phosphate-buffered saline

PdI- polydispersity index

PMA- phosphomolybdic acid

ppm- parts per million

ROS- reactive oxygen species

r.t.- room temperature

SLN- solid lipid nanoparticle

SLN 23- solid lipid nanoparticle with compound 24 encapsulated

SLN 24- solid lipid nanoparticle with compound 24 encapsulated

TEM- transmission electron microscopy

THP-1- human acute monocytic leukaemia cell line

TR- trypanotone reductase

Uv/Vis- ultraviolet–visible spectroscopy

VL- visceral leishmaniasis

Chapter 1



State of the Art

Chapter 1 – State of the Art

1. Leishmaniasis

Infectious diseases caused by viruses, parasites and bacteria are currently imposing a substantial burden of morbidity round the globe, more predominantly in less developed countries [1,2].

Protozoa parasites of the genus *Leishmania* are responsible for the leishmaniasis group of tropical infectious diseases. Although leishmaniasis is reported as the ninth largest infectious disease burden worldwide, it remains as one of the world's most neglected diseases, largely affecting the poorest equatorial areas of the globe [3,4].

Over 20 *Leishmania* species are known to be infective to humans, the most common of which are *L. donovani*, *L. infantum*, *L. siamensis*, *L. braziliensis* and *L. guyanensis*[3]. The disease is transmitted by the bite of an infected female *phlebotomine* sand fly [3]. There are four main types of leishmaniasis clinical syndromes [3]: i) visceral leishmaniasis (VL), often known as kala-azar, representing the most serious form of the disease, which has a mortality rate around 100% in the absence of appropriate treatment. The VL affects the vital organs of the body and is characterized by irregular bouts of fever, weight loss, enlargement of the spleen and liver, and anemia [3,5]; ii) cutaneous leishmaniasis (CL), the most common, causes ulcers on exposed parts of the body, leading to disfigurement, permanent scars, stigma and in some cases disability [3,6,7]; iii) mucocutaneous leishmaniasis (MCL), that is the most destructive form of the disease, causes partial or total mutilation of mucous membranes in the nose, mouth and throat [3]; iv) post kala-azar dermal leishmaniasis (PKDL), which occurs months or years after the successful treatment of VL and is a cutaneous condition characterized by a macular, depigmented eruption found mainly on the face, arms, and upper part of the trunk [3].

Leishmaniasis affects mainly agricultural areas and suburban regions in Africa, Asia, Latin America the Mediterranean Basin. However, anthroponotic CL, where humans are the major reservoir of the parasite, is predominantly urban and periurban, showing patterns of spatial clustering similar to those of anthroponotic VL in South Asia. The disease is usually characterized by large outbreaks in densely populated cities, especially in war and conflicts zones, refugee camps and in settings where there are large-scale

migration of populations [3,7]. In any case, the disease is highly associated with malnutrition, population displacement, poor housing, weak immune system and lack of resources. Leishmaniasis affects humans, livestock and pets, and the latter two can act as reservoirs for the parasites [3,8]. Until 2013 the World Health Organization (WHO) statistics shows that over 98 countries are endemic for leishmaniasis, in which 350 million people are considered at risk of contracting the disease, generating approximately 2 million new cases each year. Approximately 0.3 million of these are new VL cases, of which 0.2 million result in death [9]. More than 90% of global VL cases occur just in the six countries, i.e. Bangladesh, Brazil, Ethiopia, India, South Sudan and Sudan (Figure 1). In these particular countries 310 million people are at risk of infection, corresponding to 90% of the total population [3,6].

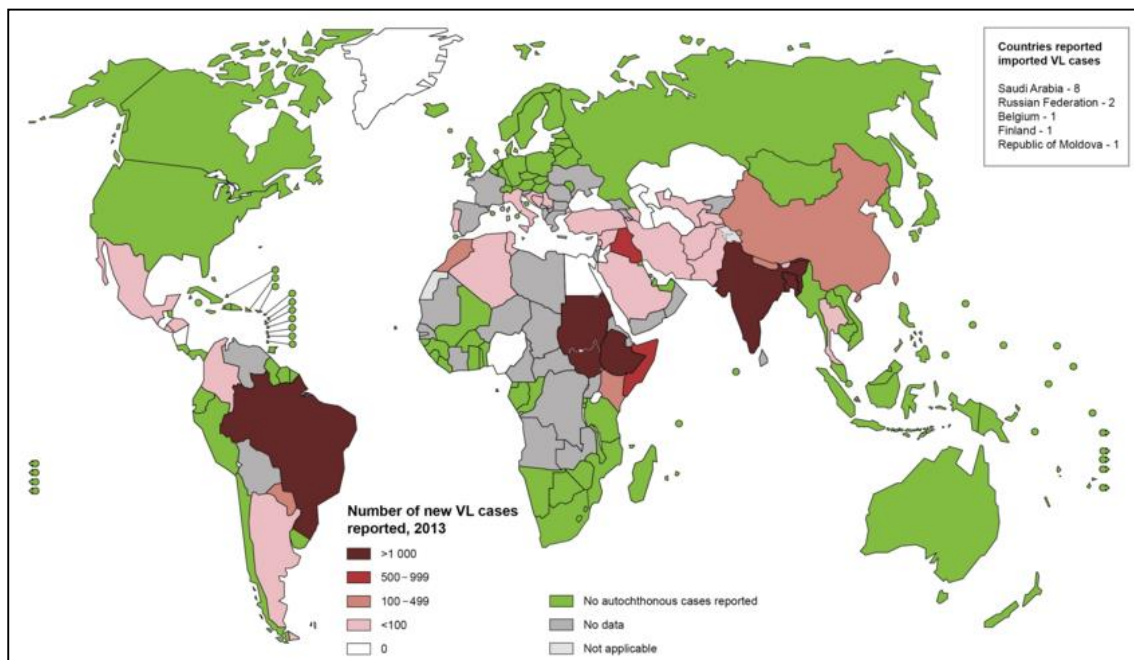


Figure 1- World map representing the status of endemicity of VL until 2013. Adapted from http://gamapserver.who.int/mapLibrary/Files/Maps/Leishmaniasis_2013 04/04/2016.

Of the several types of leishmaniasis, CL is more widely distributed, with about one-third of cases occurring in each of three epidemiological regions, the Americas, the Mediterranean basin, and Western Asia from the Middle East to Central Asia (Figure 2). In this type of leishmaniasis there are also countries with more estimated incidence (Afghanistan, Algeria, Brazil, Colombia, Costa Rica, Ethiopia, Iran, Peru, Sudan and Syria), accounting for 70 to 75% of global estimated CL incidence [3,7]. However, the

where they survive, multiply and differentiate into amastigotes within phagolysosomes, while resisting lysosomal enzymatic degradation [3,10].

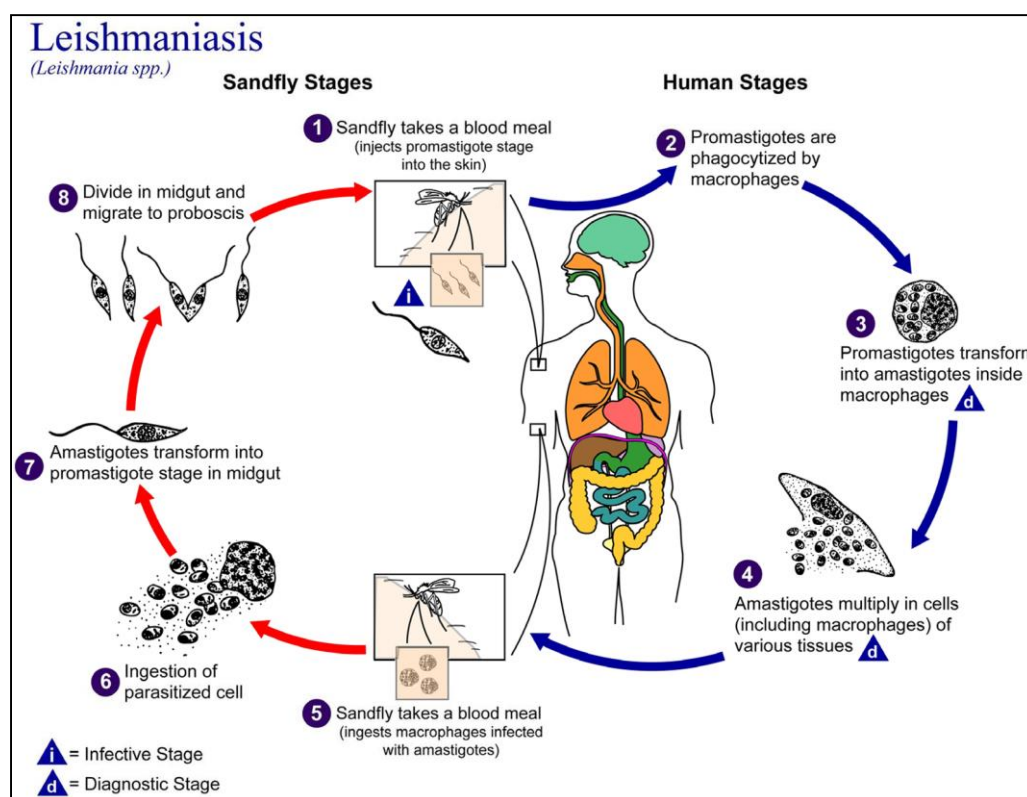


Figure 3- Life cycle of *Leishmania* parasites. Adapted from <http://www.cdc.gov/dpdx/leishmaniasis/index.html> 04/04/2016.

The uptake of promastigotes and respective transformation into amastigotes can be completed between twelve and twenty four hours [10]. After lysis of infected macrophages and dendritic cells, the amastigotes disperse via the circulatory and lymphatic system, proceeding to infect other macrophages of the mononuclear phagocytic system (MPS). Thereafter the parasite remains in the amastigote form for the whole duration of the mammalian phase of the life cycle. This phase is chronic and can last from months to years, even a lifetime, depending on the host species involved [10]. Furthermore, the duration of the infection can vary widely between individuals, as there is a strong influence of host genetics on susceptibility to infection [10]. The location of infected host cells varies with the type of leishmaniasis. In CL the amastigotes remain confined in the skin provoking papules or ulcers. In VL there may be an initial skin lesion, but usually the first explicit symptoms are the onset of fever and other clinical

evidences of visceral infection [10]. Finally the infected hosts serve as reservoirs and can infect another sand fly, beginning the sand flies stage (Figure 3, red arrows), when this insect feeds. Sand flies possess cutting mouthparts that slice into the mammalian skin and then they feed from a pool of blood that emerges from the wound. If the flies happen to feed on a cutaneous lesion they acquire parasites that cause cutaneous disease while visceral parasites are acquired from the blood itself [4,9].

The principal pathological events of VL occur in main MPS organs, the spleen and liver, where the host cells remain resident. Other sites of infection are the lymph and bone marrow. The bone marrow is a major site of hematopoiesis and blood monocytes infected with amastigotes are released into the peripheral circulation and thus made available to the sand flies. Nevertheless, in most endemic foci the acquisition of *Leishmania* parasites by individual flies is a rare event however the few infected flies are efficient vectors. Flies that acquire a *Leishmania* infection remain infected for life. Then the ingested amastigotes that can be inside of a macrophage or in its free form transform into promastigotes exclusively in the insect gut. The ultimate form of the development cycle are the mammalian infective metacycle promastigotes, which accumulate in the anterior mid gut and foregut of the sand fly, where they remain until the next cycle begins [10].

2.1. Amastigotes morphology

The amastigotes are the intracellular form of the parasite. This eukaryotic cell is smaller when compared with promastigotes, with 3-6 μm length and 1.5-3 μm in width (Figure 4). The external membrane is a conventional unit membrane under which lies a corset of microtubules, serving as a form of cytoskeleton. Although amastigotes are usually referred as a non-flagellum form, they actually have one. However it does not protrude beyond the body surface so it cannot be seen by light microscopy. This flagellum is not functional, making the amastigotes non-motile, and it can be found inside of a flagellar pocket created by an infolding of the surface membrane. The flagellar pocket is topological external to the cell although contained within it. In addition to anchoring the flagellum the main function of the pocket is to serve as a site of endocytosis and exocytosis processes, which can be explained by the presence of the Golgi complex in the vicinity of the flagellar pocket. As the amastigotes belong to the *kinetoplastea* class they

have a kinetoplast, a dense mass of mitochondrial DNA, adjacent to nucleus. They divide by longitudinal binary fission at 37°C (Figure 4) [10,11].

2.2. Promastigotes morphology

The promastigotes are the extracellular form of the *Leishmania* parasite that develops inside the gut of the invertebrate sand fly - *Phlebotomus spp.* and *Lutzomyia spp.* - where they multiply by longitudinal binary fission at 27°C. Promastigotes have an elongated 15-30 µm body and 5 mm width. These extracellular bodies are motile due to their anterior flagellum. Desmosomal plaques anchor the flagellum to the cell body as it emerges from the flagellar pocket. The structural elements of promastigotes are the same as those described for amastigotes (Figure 4) [10,11].

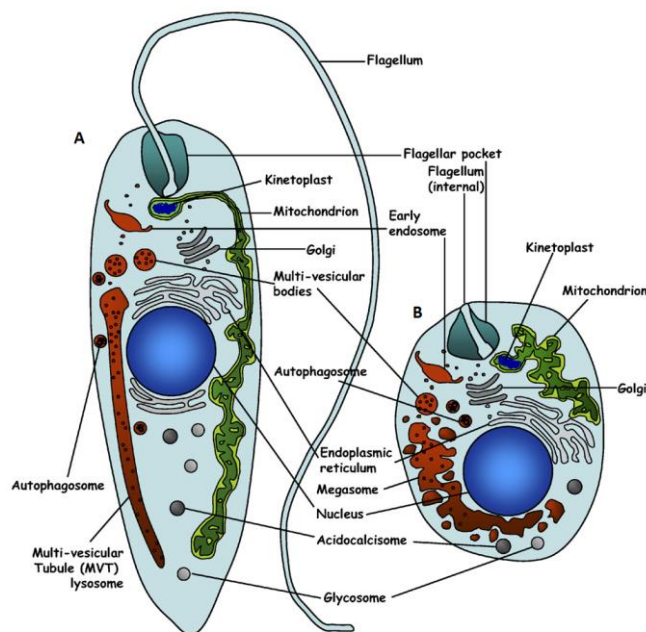


Figure 4- Illustration of promastigotes (A) and amastigotes (B) morphology with schematic representation and identification of the various cellular compartments. **Adapted from:** Protein turnover and differentiation in *Leishmania* [11].

3. Current leishmaniasis treatments

In this section we will review the drugs that are currently in use and promising approaches for the treatment of VL, which include paromomycin, pentamidine, pentavalent antimonials, miltefosine, ketoconazole, allopurinol, formulations of amphotericin B, and the more recently studied by our investigation group dinitroanilines [4,8]. Some of these drugs are also used for the treatment of CL and MCL. It is also important to notice that the treatment of VL varies from one endemic region to another not only due to the appearance of resistances or different causative species but either because of the treatment regimes recommended by WHO or the inadequate current treatment options [3,9].

3.1. Pentavalent antimonials

In 1915 Di Cristina and Carania in Italy and Rogers in India reported the first use of antimonials for the treatment of VL, however, trivalent antimonials were already used to treat CL [3]. Afterwards antimonials were found to be highly toxic and exhibited side effects such chest pain, cough and depression, although in 1925 Brahmachari made a key finding when he synthesized the pentavalent antimony compound urea stibamine (1, Figure 5), an effective chemotherapeutic agent against VL [3,13]. This breakthrough saved millions of lives in India where several villages were depopulated by VL epidemics. New advances were made in antimony therapy of VL through the synthesis of antimony gluconate (Glucantime[®], Sanofi-Aventis) (2, Figure 5) in 1937 and sodium stibogluconate (Pentostam[®], GlaxoSmithKline) (3, Figure 5) in 1945. These two drugs were the first line of treatment for more than 70 years in most endemic countries [4,9].

Both Pentostam[®] and Glucantime[®] have poor oral absorption so they are given via intramuscular injections or intravenous infusions. In addition, the treatment with these two compounds is lengthy, potentially toxic and painful. Common side effects of these specific pentavalent antimonials include prolonged QTc interval, ventricular premature beats and ventricular fibrillation. These cardiovascular conditions are often associated with fatal cardiac arrhythmias [3,14]. Arthralgia and myalgia, elevated hepatic enzymes and pancreatitis are other common adverse events [4,9].

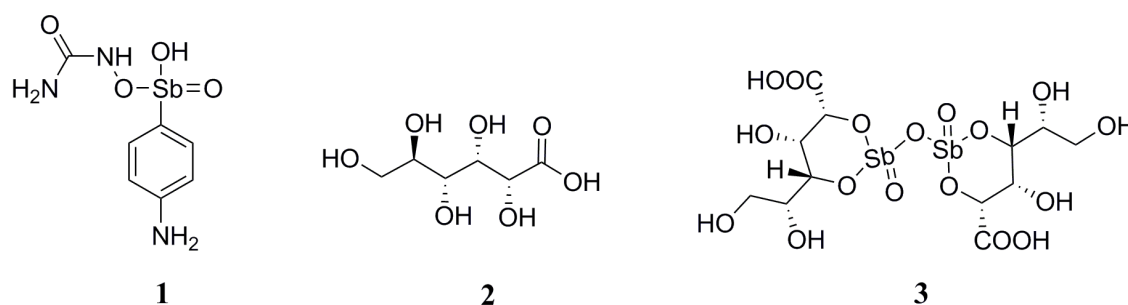


Figure 5- Structures of the most common pentavalent antimonials: **1-** urea stibamine; **2-** gluconate; **3-** stibogluconate.

Over the years treatment with pentavalent antimonials has become ineffective in parts of India and Nepal, as resistance has developed. Therefore, in 1992 the recommendation dose to treat VL in India was enlarged from 10 mg/kg to 20 mg/kg a day for 28–30 days. In the beginning of the XXI century, in some regions of India 60% of the VL cases were refractory to this treatment. This antimony resistance is apparently due to the contamination of drinking water by arsenic, which can be chelated by the pentavalent antimonials, thus decreasing the effective dose [3,13]. Even though, pentavalent antimonials continue to be efficacious in other parts of Southeast Asia, and the WHO currently recommends a combination of pentavalent antimony and paromomycin as the first line therapy options in this region [9].

Pentavalent antimonials still are the first choice for the treatment of VL in South America where the species that cause VL is the *L. infantum* rather than *L. donovani*, and so there is no evidence of resistance [14]. Likewise, in the Mediterranean countries, although it is a rare disease, VL is also caused by *L. infantum*. During the 1990s, antimonials were the first-line of treatment in most countries of this region (e.g. France, Greece, Italy, Malta, Spain, Portugal, Albania, Israel, Turkey, Morocco, Algeria, and Tunisia) with cure rates above 95%. Nevertheless, more recently, pentavalent antimonials have been replaced by AmBisome[®] (Gilead Sciences) as the first line of treatment in European countries [15].

It is important to refer as well that antimonials have also been used extensively as the primary treatment option for CL and ML with high disparity of cure rates that can balance between 20% and 100%, depending on country, genetics and parasite species [7].

Although pentavalent antimonials have a long history of use in human medicine, their molecular and cellular mechanisms of action are not yet well understood. It is not even clear whether the final active form is Sb(V) or Sb(III) [13]. The cell transporter, which

allows the entry of pentavalent antimonials is at the date unknown although speculation indicates that Sb(V) enters into the amastigote form of the parasite via a protein that recognizes a sugar moiety-like structure shared with gluconate [13]. Three main models could be proposed regarding the mechanism of action of pentavalent antimonials [13].

Prodrug Model – This model is based on the principle that Sb(V) is less active against *Leishmania* than Sb(III). According to this model Sb(V) behaves as a prodrug, which undergoes biological reduction to the much more active, but also more toxic trivalent form of antimony – Sb(III). However, the site (amastigote or macrophage) and mechanism of reduction (enzymatic or nonenzymatic) remain controversial. The likely is that the reduction occurs inside the amastigote with active participation of thiol compounds from de mammalian host and the ones of parasite origin such glutathione and trypanothione, respectively. Once the reduction happen trypanothione reductase (TR) and zinc finger proteins are both potential molecular targets of Sb(III) [13].

Intrinsic Antileishmanial Activity Model - Intrinsic antileishmanial activity of sodium stibogluconate – Sb(V), but not Sb(III), specifically inhibits type I DNA topoisomerase, thus inhibiting of unwinding and cleavage. It is believed that Sb(V) may form a complex with adenine nucleosides, which is kinetically favored in acidic biological compartments such as the inside of parasite amastigotes [13].

Host Immune Activation Model - According to this model antimonials have the ability to eliminate intracellular *Leishmania* parasites via activation of host immune system. The action of sodium antimonials is multifaceted and so they can activate both innate and adaptive immunity, thereby inducing effective antileishmanial immune response. This not only improves the existing infection but also protects from relapse [13].

3.2. Pentamidine

Pentamidine (Figure 6) is an aromatic diamidine and is formulated as a salt. It was first implemented for the treatment of human african trypanosomiasis (sleeping sickness). The first reports of pentamidine use are dated from 1949 and 1950 in India and Spain respectively. The selective accumulation of pentamidine by the parasite, rather than the

host cell, is a major reason for the pentamidine selectivity [3]. Most regimens are based on intramuscular injection or intravenous infusion of 4 mg/kg/day of pentamidine usually during 30 days (Pentacarinat[®], Sanofi-Aventis). Side effects include hypoglycemia, hypotension, fever, myocarditis and renal toxicity. When pentavalent atimonials were not effective, pentamidine was the second choice of therapy for treatment of VL, however its toxicity and rapidly emerging resistance led to its replacement by amphotericin B in the 1990s. Evidence of the emerging resistance were very notable at the time; in fact, during the early years of increased pentamidine use in India, 10 injections were sufficient to cure almost 100% of the patients, whereas about 10 years later 15 or more injections were required in order to cure only 65%-77% of patients [3]. However, in French Guiana and Suriname pentamidine is still the first line of treatment for CL caused by *L. guyanensis* with highly cure rates [16].

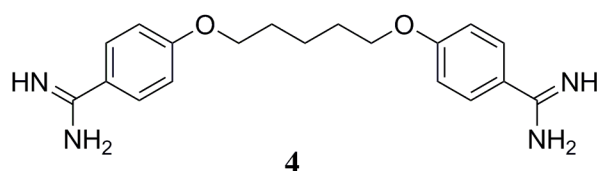


Figure 6- Structure of pentamidine.

Several mechanisms of action have been suggested but the precise manner in which pentamidine acts, and its major macromolecular targets, have not been entirely elucidated. So far it is clear that pentamidine is selectively accumulated by pathogenic protozoa through high affinity pathogen membrane transporters [14,15]

3.3. Amphotericin B

Amphotericin B (Figure 7) is a polyene antibiotic with antifungal activity, isolated from *Streptomyces nodosus* in 1953 [19]. Santos in 1960 reported for the first time *in vitro* activity of amphotericin B on *Leishmania* [3]. Three years later in Brazil the first patients with VL were treated successfully with amphotericin B [3]. The drug major advantage relies in the fact that increases membrane permeability by binding to ergosterol present in the *Leishmania* plasma membrane [16,17]. Amphotericin B is insoluble in aqueous

solutions at pH=7 and for this reason the original formulation used sodium deoxycholate in order to improve solubility, thus amphotericin B can be used in complex with deoxycholate or with lipid formulations, mainly liposomes, for intravenous infusion. It is also important to refer that amphotericin B has a very long elimination half-life, with substantial levels accumulating in the liver and spleen and to a lesser extent in the lungs and kidneys [16,17,21].

Amphotericin B deoxycholate was used largely to treat ML and the first clinical trials for the treatment of VL were performed at the beginning of the 1990s [3]. It demonstrated response rates of closely 100% as first line treatment, and cure rates above 90% in those cases where antimonials had previously failed [22]. However, the deoxycholate form of the drug has many adverse effects including infusion reactions, nephrotoxicity, hypokalemia, and myocarditis [23]. In addition to the side effects, amphotericin needs close monitoring and hospitalization for 4–5 weeks, conditions hard to keep in countries with low income settings [3].

In order to attenuate its toxicity and increase the therapeutic potential, alternative formulations of amphotericin B have been developed and incorporated into regular clinical use. The molecular structure of amphotericin B deoxycholate, has poor water solubility and excellent lipid solubility, which makes the drug an ideal candidate for incorporation into lipid-based preparations [20]. Lipid formulations of amphotericin B are in fact very effective at lower doses and have reduced toxicity, but the high cost complicates treatment of patients in the less development countries that happens to be the more affected with *Leishmania* epidemics [22].

AmBisome® (Gilead Sciences) is a liposomal formulation of amphotericin B for injection. Initially developed by NeXstar Pharmaceuticals, it was a huge step in the fight against *Leishmania* in low-income countries that have been received access to reduced-price liposomal amphotericin B through the Gilead/WHO AmBisome donation programme [24]. Attempts have been made to develop inexpensive lipid-containing amphotericin B deoxycholate, particularly by mixing it with commercially available emulsions for parenteral nutrition, while other lipid-based amphotericin B formulations have been licensed (Abelcet®, Teva Pharma) [20]. Due to the effectiveness of AmBisome® treating VL, this liposomal formulation is considered the reference drug in the Mediterranean countries and is the alternative in the low incoming countries when the first line of treatment fails [3].

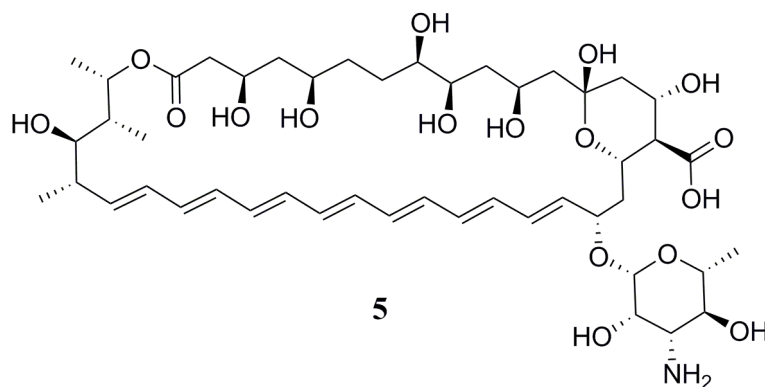


Figure 7- Structure of amphotericin B.

Liposomal amphotericin B has affinity for fungal and protozoa membrane cells, penetrating through the wall and entering into the cytoplasm due to its lipid composition [21]. The proper mechanism responsible for the membrane disruption and parasite cell death is unclear. However it is believed that when amphotericin B binds with ergosterol, a transmembrane channel is formed, causing monovalent ion (K^+ , Na^+ , H^+ and Cl^-) leakage, which is thought as the primary effect leading to cell death. Recently researchers have found new evidence that channel formation is not the only mechanism responsible for cell death [25].

3.4. Paromomycin

Paromomycin (Humatin[®], Pfizer) (Figure 8) is a broad-spectrum aminoglycoside antibiotic first isolated in the 1950s from *Streptomyces krestomuceticus* [4,23]. It is soluble in aqueous solutions and can be administered by intramuscular injection, capsule or in topical cream [27]. CL is the type of leishmaniasis that is mostly cured by paromomycin with very efficacious cure rates and the most common adverse effect is pain in the site of injection [14,25]. About 5% of patients can experience reversible ototoxicity and a rise of hepatic transaminases [29,30]. Paromomycin showed inferior cure rates when compared with amphotericin B, miltefosine and antimonials treating VL, nevertheless its affordability is the main advantage [3].

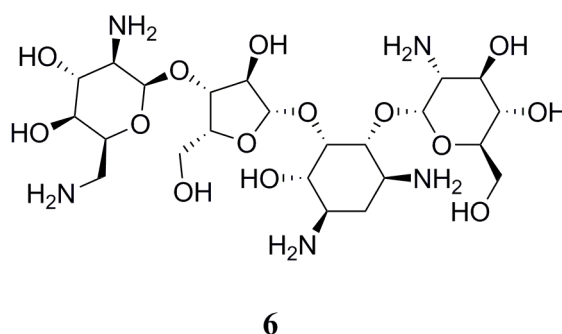


Figure 8- Structure of paromomycin.

The uptake of paromomycin by *Leishmania* cells occurs upon association with a highly negatively charged lipophosphoglycan, a major component of their cell surface. This structure is greatly reduced in amastigotes when compared with promastigotes which can be seen as a disadvantage since the main target should be the intracellular form of the parasite [31]. Moreover, paromomycin is a protein synthesis inhibitor and acts by binding to 16S ribosomal RNA and disrupting translocation of tRNA during translation in non-resistant cells [26]. This mechanism has been well studied in non-*Leishmania* parasites and bacteria but its mode of action is not well understood in *Leishmania spp.* However, it has been proposed that it might alter membrane fluidity, interact with ribosomes, interfere with the mitochondrial membrane potential and inhibit respiration [32].

3.5. Miltefosine

Miltefosine (Figure 9) was initially developed as an experimental anticancer drug (Miltex[®], Baxter) but is actually a broad-spectrum phospholipid antimicrobial drug [3]. In the 1990s several laboratories discovered that miltefosine has antileishmanial activity, and in 2002, it was approved in India as the first oral treatment of VL [3,33,34]. In 2002 a phase III trial with miltefosine in India resulted in a 94% cure rate, and thus it was selected for the VL elimination program in India, Nepal, and Bangladesh [35]. A study in 2012 suggests that miltefosine efficacy is starting to decline and the cure rate has been substantially reduced [36]. In the most affected regions of Africa miltefosine efficacy was found to be equivalent to the antimonials treatment [37]. Nowadays miltefosine is considered to be the first effective oral treatment regimen for CL, with greater accessibility and lower toxicity compared to antimonials [38]. The most common adverse

events include gastrointestinal side effects and occasional hepatotoxicity and nephrotoxicity [36]. Another miltefosine limitation is teratogenicity. There is evidence that the adverse effects are more severe in women and young children[39]. In 2014 it was approved by the FDA to treat cutaneous or mucosal leishmaniasis (Impavido[®], Paladin).

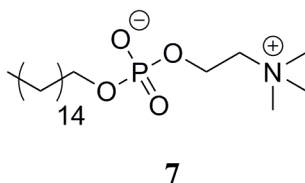


Figure 9- Structure of miltefosine.

Being first developed to act as an anticancer drug, most data about miltefosine's mechanism of action were obtained in tumor cell lines where this compound can trigger apoptosis [40]. Concerning its antileishmanial effect, the mechanism of action is only partly known and some authors have shown evidence that the promastigotes treated with miltefosine present an apoptosis-like death. How this compound can induce apoptosis is not entirely clear either in mammalian cells or parasites. It has been suggested that miltefosine inhibits the production of phosphatidyl choline, an essential molecule in the synthesis and integrity of cellular membranes and a source of signaling molecules [40].

3.6. Ketoconazole

Ketoconazole (Figure 10) is an imidazole antifungal used orally and topically. Its therapeutic potential activity against *Leishmania spp.* has been explored as an alternative to conventional first- and second-line therapy for VL and CL [41]. The efficacy of ketoconazole varies depending on species and the tests against CL resulted in a 75% cure with mild side effects in patients infected with *L. braziliensis*, and almost 90% of the patients afflicted with CL caused by *L. mexicana* [3,42]. Among the main existing imidazole antifungals - fluconazole, itraconazole, ketoconazole – only the latter was found to be consistently efficacious and is now used as the first choice for treatment of CL infections caused by *L. mexicana* [3].

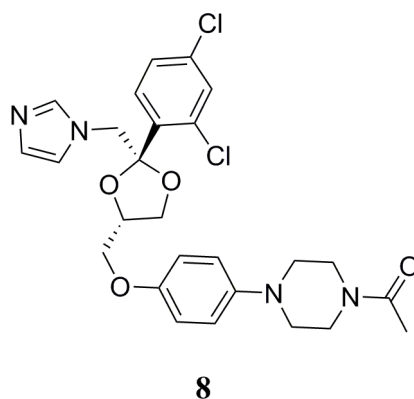


Figure 10- Structure of ketoconazole.

Azoles are oral antifungal drugs that also interfere with the fungal and protozoa synthesis of ergosterol at the lanosterol demethylase step resulting in the accumulation of 14 α -methyl sterols that are metabolized by the target of ketoconazole, the cytochrome P450 14 α -methylase [43].

3.7. *Allopurinol*

Domestic dogs are the most important urban reservoirs of *L. infantum*, for this reason is important to refer the first line of treatment against leishmaniasis for infected dogs. Pentavalent antimonials were the first line treatment for dogs in Europe since the XX century. However this treatment does not promote parasitological cure in infected dogs, leading to frequent relapses and needing continuous administration of these drugs poorly tolerated and expensive drugs [44].

Allopurinol (Figure 11) is a purine analog and its anti-leishmanial activity was first described in 1974 by Pfaller and Marr [45]. It emerged as an alternative orally active drug presenting low toxicity, low cost, lack of known resistance, effectiveness in reverting the clinical signs of canine VL, and prevents recurrence of the disease [46]. However, allopurinol is the only drug recommended by the WHO for the treatment of canine leishmaniasis, although it does not lead to complete elimination of the parasite. In veterinary medicine it is currently considered the major first line drug for long term treatment of canine leishmaniasis, often in combination with pentavalent antimonials or miltefosine for the first month and then continued alone [47].

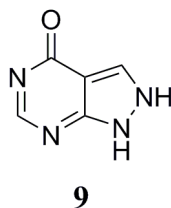


Figure 11- Structure of allopurinol.

Allopurinol's antileishmanial activity is attributed to the inhibition of the enzyme hypoxanthine-guanine phosphoribosyl transferase present in purine salvage pathway of *Leishmania* parasite. Herein allopurinol is phosphorylated and most likely incorporated into nucleic acids, leading to disrupted protein translation and selective parasite death [46].

3.8. Dinitroanilines

Dinitroanilines are derived from both aniline and dinitrobenzenes, representing a group of very promising antiparasitic agents with proven efficacy against several parasitic protozoa, such as *Trypanosoma spp.*, *Plasmodium falciparum*, *Toxoplasma gondii* and *Leishmania spp* [48,49,50,51,52].

Trifluralin and oryzalin (10 and 11, Figure 12) are the most well studied compounds belonging to this class of herbicides that are commercially available since the 1960s [53]. The recent investigation of trifluralin and oryzalin as potential antileishmania agents relies on their advantages when compared with the first line of treatment drugs. Trifluralin and related compounds are inexpensive to manufacture, their traits are well characterized, including their toxicities and shelf-lives [54]. They showed to be non-carcinogenic, non-teratogenic, and non-mutagenic [54]. Nevertheless, their use as antileishmania therapeutic agent is limited by their low water solubility and low vapor pressure associated with an *in vivo* rapid clearance, causing heterogeneous results in biological assays [12].

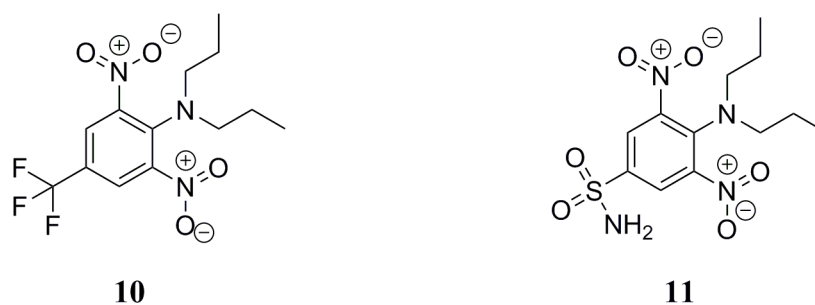


Figure 12- Structures of trifluralin and oryzalin.

Carvalho *et al.* successfully developed liposomal formulations of trifluralin which demonstrated superior antileishmanial activity when compared to the free drug either in a murine model of VL (*L. donovani*) and in the treatment of experimental canine leishmaniasis (*L. infantum*) [54,55]. These liposomal formulations showed advantages in reducing parasite loads in mice, without the need of toxic solvents in the administration step while in the treatment of canine leishmaniasis they were effective in improving the clinical condition of the dogs by reducing parasite density and immunomodulating the generation of a potential protective immune response [54,55].

Lopes *et al.* reported the incorporation of oryzalin in appropriate liposomal formulations. These formulations enabled an increase of oryzalin solubility and delivery of the drug to the main affected organs of leishmanial infection [57]. These authors also developed a solid lipid nanoparticle (SLN) formulation of tripalmitin and lecithin containing oryzalin with the aim for leishmaniasis treatment [12]. A comparative study of liposomes versus SLN both loaded with oryzalin showed that *in vitro* both systems caused a reduction of oryzalin cytotoxicity, abolished the hemolytic activity while maintaining its antileishmanial intracellular activity [58]. The same study concluded that *in vivo* the incorporation of oryzalin in liposomes and in SLN clearly improved its pharmacological performance without no significant differences between both nanoformulations, except for the preferential activity found in each target organs that is the liver for liposomes and the spleen for SLN [58].

Dinitroanilines exert their herbicide effect causing multinucleation, accumulation of cells at the metaphase, and the loss of microtubules [54]. This antimetabolic activity determined by the capacity of dinitroanilines binding to tubulin - the main structural component of microtubule - in a highly specific manner resulting in their depolymerization [49]. The nitrile group of dinitroanilines binds to amino acid residues, generally, lysine or arginine, located between tubulin subunits preventing further cell division [59]. This interaction is

specific in a way that these compounds efficiently just bind to the tubulins of plants and protozoa parasites and not employ any to the animal tubulins despite an extremely high level of similarity between their sequences [48].

Table 1- Overview of existing drugs for VL treatment.

Drug	Efficacy	Advantages	Limitations	Cost
Pentavalent Antimonials	35-95%	Low cost Effective against <i>L. infantum</i> Can be co-administered FDA approved	Drug resistance for <i>L. donovani</i> in India Fatal cardiac arrhythmias Depression	50-70\$
Pentamidine	70-80%	Potential use in combinatorial therapy Also effective against CL FDA approved	Fever Renal toxicity Drug resistance High cost	100\$
Liposomal amphoterecin B (Ambisome)	≈100%	Effective with low toxicity profile No evidence of resistance Selectivity for parasite membrane FDA approved	High half-life High cost Renal toxicity Fever and rigor during infusion	280\$
Paramomycin	45-95%	Low cost FDA approved	Inferior cure rates Pain at injection site	10\$
Miltefosine	95%	Highly potent First oral treatment for CL and VL FDA approved	Highly toxic Evidence of resistance Renal toxicity	70\$

4. *Leishmania* iron

Once the infection is established, the parasites replicate as amastigotes within acidic phagolysosomes of macrophages, creating a harsh acidic environment [60]. Most microorganisms are destroyed in this hostile acidic environment, but the intracellular stages of *Leishmania* have a plant-like adaptive mechanism that allow them to survive and acquire essential nutrients and minerals from the host cell [8]. One of such essential nutrients is iron that can be obtained within the phagolysosomes as inorganic iron or in the form of iron-containing porphyrins such as the heme [8]. It is the iron that allows triggering the mechanism of action of the tetraoxanes specifically designed for this work. It is known that *Leishmania* has the ability to express specialized membrane proteins in the acquisition of iron or heme from the host, even though iron can be toxic in high amounts due to its redox potential [61]. Recent studies have been made with the purpose of determining how *Leishmania* acquires and utilizes iron but so far these processes remain unclear.

Inorganic iron is available as the ferric insoluble (Fe^{3+}) form at physiological pH in the host cells. Mammalian hosts control the free iron levels in biological fluids, and transport it using the carrier protein transferrin. When binding to transferrin receptors, the iron-containing protein is internalized by the host cell via endocytosis. At this point, iron (III) is released when it reaches an acidified intracellular compartment. In order to cross the parasite membranes iron (III) must be first reduced to the highly reactive and toxic iron (II). Being extremely harmful for cells, iron (II) transport must be tightly controlled. Therefore the majority of iron (III) that enters in cells complexed to transferrin is reduced to iron (II) by a host ferric reductase (LFR1/FRO2) and then translocated to the cytosol by the ferrous iron transporter LIT1/IRT1 (Figure 13). However, a small amount of transferrin can keep moving deeper into the endocytic pathway and reach *Leishmania* phagolysosomes, where iron (II) becomes available for acquisition by the parasites [8,61,62].

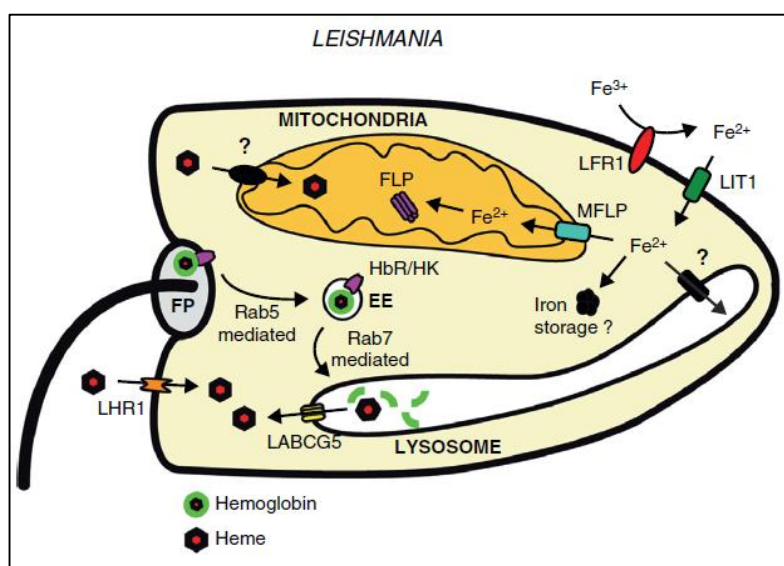


Figure 13- Schematic representation of iron acquisition pathways in *Leishmania*. *Leishmania* utilizes a ferric reductase (LFR1/FRO2) to reduce iron and a ferrous iron transporter (LIT1/IRT1) to transport it into the cytosol. In *Leishmania*, there are no identified iron transporters in the lysosome, but a mitoferrin-like protein (MFLP) may transport iron into the mitochondria for storage in association with a frataxin-like protein (FLP). Iron-containing heme can be acquired by *Leishmania* in two ways. Hemoglobin may bind to a hexokinase (HbR/HK) and traffic to the parasite's lysosome, where it is degraded releasing heme which is translocated to the cytosol by the ABC transporter, LABC5. Heme is also transported directly into the cytosol by the heme transporter, LHR1. **Adapted from:** Pathways of iron acquisition and utilization in *Leishmania* [8].

These findings were very important for the purpose of the present work on the account that our group has ongoing investigation studies with tetraoxane compounds with potential activity against the malaria parasite and specifically designed to be activated by malaria iron. Thus we designed specific tetraoxanes with potential activity against *Leishmania*, which also present a structure able to be activated by iron (II) that enters *Leishmania* phagolysosomes.

5. Tetraoxanes

The discovery of antimalarial properties of artemisinin (12, Figure 14) and the identification of its pharmacophore, the 1,2,4-trioxane (13, Figure 14,) allowed the exploration of new approaches for combating the disease [64]. Thus, in the past 50 years several synthetic and semisynthetic peroxide compounds intended as antimalarials have been developed. Some of the most promising compounds that emerged from these studies were 1,2,4,5-tetraoxanes (14, Figure 14) [63,64,65].

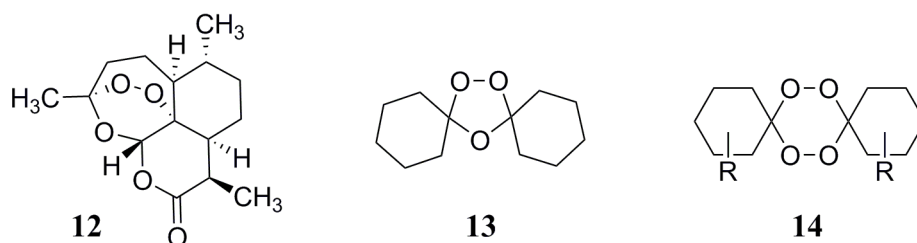


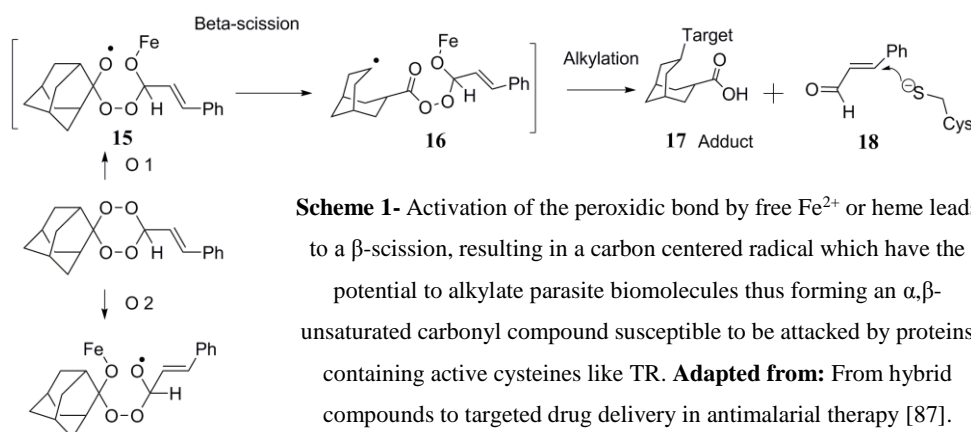
Figure 14- Chemical structure of **12-** Artemisinin; **13-** 1,2,4-trioxane; **14-** 1,2,4,5-tetraoxane.

To the best of our knowledge there are no studies reporting to tetraoxanes with the purpose of assessing their potential antileishmanial activity, so there is no information concerning structure-activity relationship. However, it is established that high steric hindrance tetraoxanes prevent the activation by iron radicals by inhibition of electron transfer from the heme or other species of iron and for this reason the activity decreases [63,64]. Docking studies suggest that the proximity between iron (II) atom and tetraoxane's oxygen favors the activity of such compounds, and therefore supports the electron transfer of the peroxidic bond, which is crucial to trigger the mechanism of action [67].

Subsequent studies revealed that functional groups such as alkenes, alkynes and ethers allow more potent tetraoxanes since such functions help to stabilize the radical formed after rupture of the peroxidic bond [64]. The adamantane group seems to employ higher stability peroxidic bond, because it is metabolically stable [63,65].

5.1. Mechanism of action

Tetraoxanes are activated by the iron or heme present inside the parasite by scission of the peroxidic bond [67]. The iron coordinates with the less steric hindrance oxygen of the peroxidic bond (15, Scheme 1) which leads to the formation of oxy radicals that undergo a rearrangement - β -scission - resulting in carbon-centered radicals (16, Scheme 1) [65,67]. This intermediate decomposes into two fairly toxic molecules for the parasite: 17 and 18, the product of the specific design of the synthesized tetraoxanes in this work. The critical step of tetraoxane decomposition is the alkylation of parasite biomolecules. This structure, with the radical positioned in the carbon, is highly reactive and may alkylate the parasite biomolecules essential for his survival, and simultaneously contributes to increase oxidative stress (Scheme 1). The increase of oxidative stress creates a quite harmful environment that makes very difficult for *Leishmania spp.* to survive [4]. With this new approach another molecule is formed, an α,β -unsaturated carbonyl, a potential inhibitor of the enzyme TR (18, Scheme 1). The sulfur atom of cysteine present in the active center of TR act as a nucleophile capable of reacting with the α,β -unsaturated carbonyl formed before [69]. Being the sulfur molecules usually soft nucleophiles they react preferentially at the β carbon, hence the importance of the specific utilization of an α,β -unsaturated carbonyl as reagent in the synthesis process.



Scheme 1- Activation of the peroxidic bond by free Fe^{2+} or heme leads to a β -scission, resulting in a carbon centered radical which have the potential to alkylate parasite biomolecules thus forming an α,β -unsaturated carbonyl compound susceptible to be attacked by proteins containing active cysteines like TR. **Adapted from:** From hybrid compounds to targeted drug delivery in antimalarial therapy [87].

6. Trypanothione reductase

All living organisms contain high levels of two classes of low-molecular weight compounds: aliphatic nitrogenous bases, known as polyamines, and thiol-containing compounds, of which glutathione is the most ubiquitous [70].

In mammals, the major intracellular thiol-protecting agent is indeed glutathione. This substrate of glutathione reductase (GR) plays an important role in cell defenses against oxidative stress induced by oxygen and nitrogen derived reactive species [71].

Leishmania contains an unusual form of this antioxidant compound consisting of two molecules of glutathione joined by a spermidine linker, forming trypanothione [71,72].

Trypanothione was discovered as a result of studies on an apparently unusual glutathione reductase activity in the African trypanosome, *Trypanosoma brucei brucei*. This discovery was performed by Alan Fairlamb in 1985 and the compound was named trypanothione because it was uniquely found in parasitic protozoans of the suborder Trypanosomatina [73,72].

The trypanothione biosynthesis reaction is catalyzed by glutathionyl spermidine/trypanothione synthetase with consumption of ATP [75]. *Leishmania spp.* contains high concentrations of trypanothione for maintenance of an intracellular reducing environment and here lies trypanothione's major function, i.e. protection against oxidative stress of the Kinetoplastida class of parasites where the presence of this thiol is exclusive [75].

Like other organisms living in an aerobic environment, *Leishmania* parasites are exposed to reactive oxygen intermediates such as superoxide anion, hydrogen peroxide and hydroxyl radical. These compounds are generated internally and externally by the host's immune defense system. Reactive oxygen species can then cause lethal damage by reacting with cellular components such as DNA and membrane lipids. At this point no enzymatic removal is possible, so the low molecular-weight radical scavengers, such as trypanothione and glutathione, become extremely important by trapping the reactive species. These mechanisms of trapping hydroxyl radical and other free radicals can be regarded as the last line of defense since the general cellular strategy is to minimize hydroxyl radical formation by keeping the levels of their precursors as low as possible by enzymatic means [73].

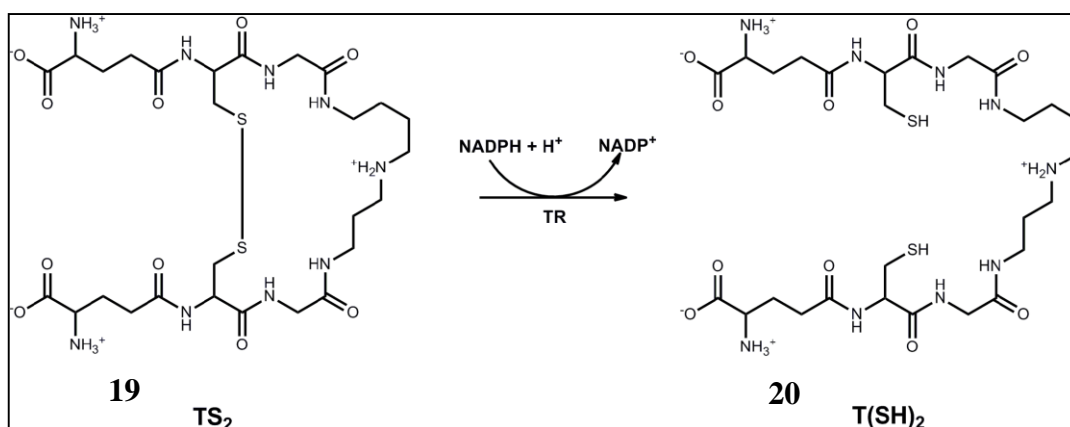


Figure 15- TR-catalyzed reduction of trypanothione disulfide (TS₂) (19) to the dithiol trypanothione (T(SH)₂) (20).

Adapted from: Trypanothione Reductase: A Target Protein for a Combined *In Vitro* and *In Silico* Screening Approach [70].

Figure 15 shows the structure of trypanothione disulfide (T[S]₂) and its two-electron reduced form, dihydrotrypanothione (T[SH]₂). At physiological pH values, both forms are zwitterions with a net charge of +1 – resulting from three positive amines and the two negative carboxylic acids. In contrast, glutathione (GSH) and glutathione disulfide (GSSG) have a net charge of -2 (Figure 16). This may be one of the main reasons for the substrate-discriminatory properties of TR and human GR discussed below [73].

The characterization of *Leishmania* metabolism has suggested biochemical pathways sufficiently different from human metabolic pathways where chemical intervention might prove a viable route to control the infection. One such pathway uses TR, the enzyme that regulates an intracellular reducing environmental.

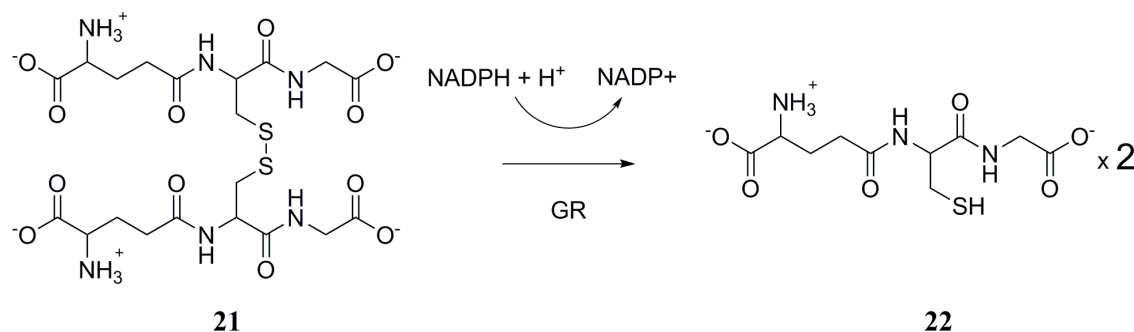


Figure 16- GR-catalyzed reduction of (21) glutathione disulfide - GSSH - to two (22) thiol glutathione -GSH.

TR mediates the elimination of various reactive species, like GR in mammalian, via electron transfer cascade which contains other enzymes such trypanredoxin and trypanredoxin peroxidase [73].

The low molecular mass thiols such trypanothione and redox enzymes protect the parasites from reactive derivatives and facilitate adaptation to various aerobic metabolisms and environmental conditions. In the course of this protective role TR reduces trypanothione with the transfer of the hydrogen from NADPH reducing trypanothione [75].

TR and GR are closely related enzymes. They are both homodimeric and belong to the FAD-dependent NADPH oxidoreductase family, with a subunit molecular weight of approximately 52 kDa [72]. They catalyze the transfer of electrons from NADPH to their specific substrates via a FAD prosthetic group and a redox active cysteine disulfide [73].

Trypanothione reductase shares close structural similarities with glutathione reductase, lipoamide dehydrogenase and eukaryotic thioredoxin reductase. Although TR's and mammalian GR's share approximately 40% sequence identity and the residues involved in catalysis are conserved, the enzymes are mutually exclusive with respect to disulfide substrate specificity which makes TR a key drug target enzyme [69,72].

TR of *Leishmania donovani* was first purified and characterized in 1995 by Mark Cunningham and Alan Fairlamb, however there is no available crystalline structure in the Protein Data Bank for TR of this *Leishmania* species [62]. Structural features and crystal structures of TR from *trypanosomatids* – *brucei* and *cruzi* (A, Figure 17), *Crithidia fasciculata* and *L. infantum* were solved.

This enzyme has in its active center a highly preserved active cysteine which promotes the catalysis - Cys52 and Cys57 in *L. infantum*, Cys53 and Cys58 in *Trypanosoma cruzi* (B, Figure 17) and *Crithidia fasciculata* [68,72].

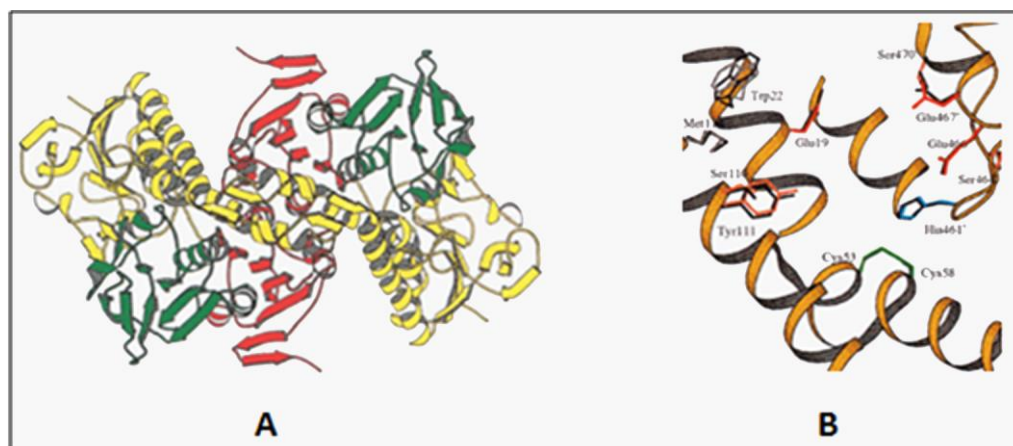


Figure 17- Ribbon drawing of the trypanothione reductase dimer. Elements of secondary structure are shown as spirals for α -helices, arrows for β -strands. Domains are colored as follows: yellow, FAD-binding domain; green, NADPH-binding domain; red, interface domain – **A**; View into the disulfide substrate binding site and catalytic center. Residues implicated in binding of substrate or involved in catalysis are shown and labeled - **B**. **Adapted from:** The crystal structure of TR from the human pathogen *Trypanosoma cruzi* at 2.3 Å resolution [69].

The importance of the gene that codes for TR was studied by knocking it out in *Leishmania donovani* and *major*. In the absence of such gene the parasites showed a decreased capacity to survive inside host macrophages, growth arrest, loss of viability and virulence. These works indicate that TR is an essential enzyme for parasite survival and thus a very promising target for new drug development for treating leishmaniasis [72,76].

Thereby the absence of trypanothione in mammalian metabolisms makes TR an attractive target for novel drug candidates thus enabling almost exclusive therapeutic selectivity.

7. Nanoparticulate Drug Carriers

Particulate drug carriers have been a topic widely investigated for many years because of the advantageous characteristics of such transporters systems. These drug carriers include oil-in-water emulsions, liposomes, microparticles and nanoparticles based on synthetic or natural polymers, or natural molecules such as lipids [78].

They can be tailored to incorporate lipophilic drugs with poor oral distribution or reduce systemic exposure of molecules that are easily degradable. These systems are also commonly used for controlling the drug release and carry it to the site of action [78].

There are several examples of studies that can show the impact of particulate drug carriers. The oil in water (o/w) emulsions have been introduced successfully to the clinic

for parenteral nutrition in the fifties and it was based on these o/w emulsions that formulations containing diazepam and etomidate were developed [79]. The main purpose of these emulsions was to reduce drug side effects, pain of injection and inflammation at the injection site, however such carriers are thermodynamically unstable and therefore, emulsions often tend to agglomerate or even break, rapidly releasing the drug as soon as they reach the blood stream [79].

Another example are the well established and extensively investigated liposomes discovered in 1965 by Alec Bangham. This particulate carrier system consists of one or more phospholipid bilayers separated by internal aqueous compartments [80]. The attractiveness in the application of liposomes resides on the compatibility of their constituent components with the body system, thereby presenting low inherent toxicity and therefore, liposomes have been successfully employed for the controlled release and site specific drug delivery [78].

Liposomes were first found their way to the cosmetic market, in 1983, incorporating the anti-aging product Capture[®] (Dior) which smoothed the way for liposome-based pharmaceutical products. Then in the eighties and beginning of the nineties new pharmaceutical products with this delivery system came to the market and include the synthetic lung surfactant Alveofact[®] (Dr Karl Thomae GmbH/Biberach, Germany) for pulmonary instillation; Epi-Pevaryl[®] (Janssen-Cilag), a topical product for antimycotic therapy; and other products for intravenous injection, such as the above mentioned amphotericin-containing Ambisome[®], and doxorubicin-containing Doxil[®] (Janssen Products) and Daunoxome[®] (Galen US, Inc) [79]. However, the total number of products on the market is still limited and the main reason for this is the non-availability of a 'cheap' pharmaceutical liposomal formulation [79].

Finally we reach the second generation of colloidal carriers that deserve a highlight in this work: the solid lipid nanoparticles (Figure 18).

Since the beginning of the nineties, when R.H. Muller and M.R. Gasco, by two different methods, first described SLN, attention from various research groups have focused on this efficient and non-toxic alternative lipophilic colloidal drug carrier prepared either with physiological lipids or lipid molecules used as common pharmaceutical excipients [64,65]. The two main production techniques for SLN were independently established by Muller and Gasco: the high pressure homogenization and the microemulsion-based technique respectively [78]. SLN production methods do not necessarily need to employ organic solvents thus minimizing the toxicological risk [78].

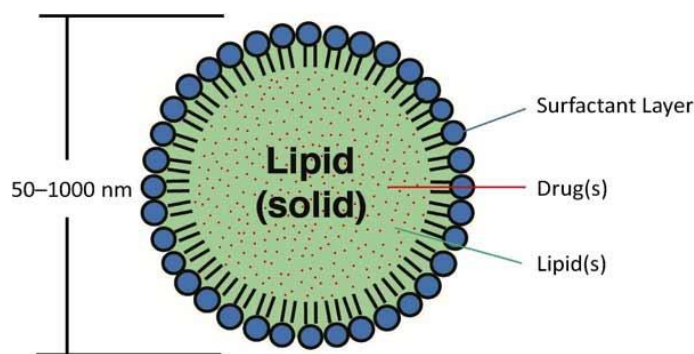


Figure 18- Solid lipid nanoparticle general structure with the main components highlighted. **Adapted from:** Recent Techniques and Patents on Solid Lipid Nanoparticles as Novel Carrier for Drug Delivery [88].

Their colloidal nature and the controlled release behavior enable drug protection and administration by parenteral and non-parenteral routes thus emphasizing the versatility of this nanoparticulate carrier [78].

The SLNs combine the advantage of polymeric nanoparticles, fat emulsions, and liposomes in one pharmaceutical technology. These advantages emerge mainly due to SLN better stability profile, ease of scalability and commercialization, easy to sterilize and relative cost effective [64,65]. The nano-scale size, relatively narrow size distribution, particulate nature and inherent structure SLNs provide unique biological opportunities for site-specific drug delivery along with controlled release of active drug over a long period, especially in the treatment of parasitic infections such leishmaniasis since the SLN are rapidly cleared by the mononuclear phagocyte system (MPS) leading to passive targeting to liver and spleen which are the critical affected organs by *Leishmania* amastigotes [12,57].

In order to overcome the drawbacks of SLN, the nanostructured lipid carriers (NLC) have been introduced at end of the nineties. NLC are composed of blends of solid and liquid lipids thus improving drug loading and firmly retaining the drug during storage [81]. NLC matrix shows a melting point depression when compared to the original solid lipid but the matrix remains solid at body temperature. By giving the lipid matrix a less ordered nanostructure, the drug loading is enhanced while the expulsion phenomenon during storage is limited by preventing the formation of perfect crystals [82].

Notwithstanding liposomes are still used more frequently used on parasitic diseases, the value of SLN has been increasing in this research field by the incorporation of known

antileishmaniasis and antimalaria agents as demonstrated by the following studies using amphotericin B [80,81], artemether [85], miltefosin [52] and curcuminoids [86].

8. Work's aim

Currently there are several alternatives for the treatment of leishmaniasis. However, due to the appearance of resistance, host genetics, globe region and specific infective specie, lack of conditions for the suitable treatment process or/and the high cost of efficacious drugs for countries with low incoming settings, the treatment and elimination of the disease namely VL seems to fail over the years.

Efforts have been made in order to discover new alternatives or reducing side effects and toxicity of the existing approved drugs by combined them with polymeric or lipid-based particulate drug carriers, such as liposomes or nanoparticles.

To the best of our knowledge the strategy we want to employ in this work is innovative and aims at designing and synthesizing three completely new tetraoxane molecules (Figure 19) intended for encapsulation in tripalmitin nanoparticles.

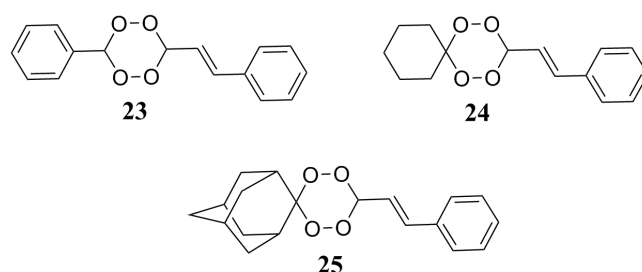


Figure 19- Tetraoxanes specific designed for the purpose of this work. **23-** (*E*)-3-phenyl-6-styryl-1,2,4,5-tetraoxane; **24-** (*E*)-3-styryl-1,2,4,5-tetraoxaspiro [5.5] undecane; **25-** (1*r*,5*R*,7*S*)-4'-((*E*)-styryl)spiro[adamantane-2,1'-cyclohexane]

A possible drawback of these tetraoxanes may be related to some toxicity due to the α,β -unsaturation in the starting material *trans*-cinnamaldehyde. Therefore they may be potentially mutagenic and carcinogenic for their susceptibility to be attacked by DNA and other biomolecules at the β carbon. These compounds are also not soluble in water. Therefore the encapsulation of such compounds seems to be the right approach to increase their efficacy, specificity, tolerability and therapeutic index. With the

encapsulation of this hybrid compounds in SLN we aim to obtain high selectivity and less toxicity since SLN are rapidly cleared by the MPS – as mentioned before - leading to passive targeting to liver and spleen which are the critically affected organs by *Leishmania* amastigotes.

These tetraoxanes were design to act against *Leishmania* in two different ways: the original molecule is activated by *Leishmania* iron, and then decomposes into two compounds with different but supportive roles inside the parasite: the structure with the carbon center radical will contribute to increase the oxidative stress and will alkylate the parasite biomolecules, whereas the α,β -unsaturated aldehyde will act as inhibitor of TR.

Shortly, our goal was to synthesize and characterize three tetraoxane compounds followed by their encapsulation into tripalmitin SLN and all the associated processes of optimization and characterization. The studies included physicochemical stability evaluation and *in vitro* assays in order to assess the activity of the tetraoxanes encapsulated in SLN against *Leishmania* parasites within infected macrophages.

9. References

- [1] K. Krämer, Alexander; Kretzschmar, Mirjam; Krickeberg, “Modern Infectious Disease Epidemiology”, in *Public Health, Statistics*, 23, 2010.
- [2] A. Cavalli and M. L. Bolognesi, “Neglected tropical diseases: Multi-target-directed ligands in the search for novel lead candidates against Trypanosoma and Leishmania” *J. Med. Chem.*, 52(23), 7339–7359, 2009.
- [3] A. S. Nagle, S. Khare, A. B. Kumar, F. Supek, A. Buchynskyy, C. J. N. Mathison, N. K. Chennamaneni, N. Pendem, F. S. Buckner, M. H. Gelb, and V. Molteni, “Recent Developments in Drug Discovery for Leishmaniasis and Human African Trypanosomiasis” *Chem. Rev.*, 114(22), 11305–47, 2014.
- [4] S. S. Chauhan, S. Pandey, R. Shivahare, K. Ramalingam, S. Krishna, P. Vishwakarma, M. I. Siddiqi, S. Gupta, N. Goyal, and P. M. S. Chauhan, “Novel β -carboline–quinazolinone hybrid as an inhibitor of Leishmania donovani trypanothione reductase: Synthesis, molecular docking and bioevaluation”, *Med. Chem. Commun.*, 6(2), 351–356, 2015.
- [5] F. Chappuis, S. Sundar, A. Hailu, H. Ghalib, S. Rijal, R. W. Peeling, J. Alvar, and M. Boelaert, “Visceral leishmaniasis: what are the needs for diagnosis, treatment and control?”, *Nat.Rev.Microbiol.*, 5, 873–882, 2007.
- [6] Iowa State University/College of Veterinary Medicine, “Leishmaniasis (Cutaneous and Visceral)”, *Iowa State Univ.*, 1–11, 2009.
- [7] P. Minodier and P. Parola, “Cutaneous leishmaniasis treatment”, *Travel Med. Infect. Dis.*, 5(3), 150–158, 2007.
- [8] A. R. Flannery, R. L. Renberg, and N. W. Andrews, “Pathways of iron acquisition and utilization in Leishmania”, *Curr. Opin. Microbiol.*, 16(6), 716–721, 2013.
- [9] W.H.Organization, “http://www.who.int/gho/neglected_diseases/leishmaniasis/en/”, *Leishmaniasis*, 04-04-2016.
- [10] R. W. A. and P. A. Bates, “Chapter 12; Leishmaniasis in the old world; Microbiology and Microbial Infections” in *Volume 5; Parasitology*, Ninth Edit., F. E. C. J. P. K. D. Wakelin, Ed. Topley and Wilson’s, 1998, pp. 215–225.
- [11] S. Besteiro, R. A. M. Williams, G. H. Coombs, and J. C. Mottram, “Protein turnover and differentiation in Leishmania”, *Int. J. Parasitol.*, 37(10), 1063–1075, 2007.
- [12] R. Lopes, C. V. Eleutério, L. M. D. Gonçalves, M. E. M. Cruz, and a. J. Almeida,

- “Lipid nanoparticles containing oryzalin for the treatment of leishmaniasis”, *Eur. J. Pharm. Sci.*, 45(4), 442–450, 2012.
- [13] A. K. Haldar, P. Sen, and S. Roy, “Use of antimony in the treatment of leishmaniasis: current status and future directions”, *Mol. Biol. Int.*, 2011, 571242, 2011.
- [14] Y. M. Brustoloni, R. V. Cunha, L. Z. Cônsolo, A. L. L. Oliveira, M. E. C. Dorval, and E. T. Oshiro, “Treatment of visceral leishmaniasis in children in the Central-West Region of Brazil”, *Infection*, 38(4), 261–267, 2010.
- [15] E. Rosenthal, P. Delaunay, P. Y. Jeandel, H. Haas, C. Pomares-Estran, and P. Marty, “Le traitement de la leishmaniose viscérale en Europe en 2009. Place de l’amphotéricine B liposomale”, *Med. Mal. Infect.*, 39(10), 741–744, 2009.
- [16] M. Roussel, M. Nacher, G. Fremont, B. Rotureau, E. Clyti, D. Sainte-Marie, B. Carme, R. Pradinaud, and P. Couppie, “Comparison between one and two injections of pentamidine isethionate, at 7 mg/kg in each injection, in the treatment of cutaneous leishmaniasis in French Guiana”, *Ann. Trop. Med. Parasitol.*, 100(4), 307–314, 2006.
- [17] Y. Zhang, Z. Li, D. S. Pilch, and M. J. Leibowitz, “Pentamidine inhibits catalytic activity of group I intron Ca.LSU by altering RNA folding”, *Nucleic Acids Res.*, 30(13), 2961–71, 2002.
- [18] T. Sun and Y. Zhang, “Pentamidine binds to tRNA through non-specific hydrophobic interactions and inhibits aminoacylation and translation”, *Nucleic Acids Res.*, 36(5), 1654–1664, 2008.
- [19] D. Slain, “Lipid-based amphotericin B for the treatment of fungal infections”, *Pharmacotherapy*, 19, 306–323, 1999.
- [20] R. J. Hamill, “Amphotericin B formulations: A comparative review of efficacy and toxicity”, *Drugs*, 73(9), 919–934, 2013.
- [21] J. Adler-Moore and R. T. Proffitt, “AmBisome: liposomal formulation, structure, mechanism of action and pre-clinical experience”, *J. Antimicrob. Chemother.*, 49(1), 21–30, 2002.
- [22] C. J. Baginski M, “Recent advances in development of amphotericin B formulations for the treatment of visceral leishmaniasis”, *Curr Drug Metab.*, 10(5), 459–69.
- [23] C. J. Baginski M, “Nephrotoxicity of different formulations of amphotericin B: Summarizing evidence by network meta-analysis”, *Curr Drug Metab.*, 10(5), 459-69, 2013.
- [24] W.H.Organisation, “<http://www.who.int/neglected->

diseases/Gilead_donation_2011/en/”, *Leishmaniasis*, 04-04-2016.

[25] C. J. Baginski M, “Amphotericin B and its new derivatives - mode of action”, *Curr Drug Metab*, 10(5), 459–69.

[26] B. Chawla, A. Jhingran, A. Panigrahi, K. D. Stuart, and R. Madhubala, “Paromomycin affects translation and vesicle-mediated trafficking as revealed by proteomics of paromomycin -susceptible -resistant leishmania donovani”, *PLoS One* 6(10), 2011.

[27] A. Ben Salah, N. Ben Messaoud, E. Guedri, A. Zaatour, N. Ben Alaya, J. Bettaieb, A. Gharbi, N. Belhadj Hamida, A. Boukthir, S. Chlif, K. Abdelhamid, Z. El Ahmadi, H. Louzir, M. Mokni, G. Morizot, P. Buffet, P. L. Smith, K. M. Kopydlowski, M. Kreishman-Deitrick, K. S. Smith, C. J. Nielsen, D. R. Ullman, J. a Norwood, G. D. Thorne, W. F. McCarthy, R. C. Adams, R. M. Rice, D. Tang, J. Berman, J. Ransom, A. J. Magill, and M. Grogl, “Topical paromomycin with or without gentamicin for cutaneous leishmaniasis”, *N. Engl. J. Med.*, 368(6), 524–32, 2013.

[28] B. A. Arana, C. E. Mendoza, N. R. Rizzo, and A. Kroeger, “Randomized, controlled, double-blind trial of topical treatment of cutaneous leishmaniasis with paromomycin plus methylbenzethonium chloride ointment in Guatemala”, *Am. J. Trop. Med. Hyg.*, 65(5), 466–470, 2001.

[29] M. M. Gaspar, S. Calado, J. Pereira, H. Ferronha, I. Correia, H. Castro, A. M. Tomás, and M. E. M. Cruz, “Targeted delivery of paromomycin in murine infectious diseases through association to nano lipid systems”, *Nanomedicine Nanotechnology, Biol. Med.*, 11(7), 1851–1860, 2015.

[30] Santosh K. Bhargava, C. H. D. Fall, and C. Osmond, “Injectable Paromomycin for Visceral Leishmaniasis in India”, *N. Engl. J. Med.*, vol. 350(25), 865–875, 2004.

[31] A. Jhingran, B. Chawla, S. Saxena, M. P. Barrett, and R. Madhubala, “Paromomycin: Uptake and resistance in *Leishmania donovani*”, *Mol. Biochem. Parasitol.*, 164(2), 111–117, 2009.

[32] M. M. Fernández, E. L. Malchiodi, and I. D. Algranati, “Differential effects of paromomycin on ribosomes of *Leishmania Mexicana* and mammalian cells”, *Antimicrob. Agents Chemother*, 55(1), 86–93, 2011.

[33] Y. V Croft SL, Snowdon D, “The activities of four anti-cancer alkyl-lysophospholipids against *Leishmania donovani*, *Trypanosoma cruzi* and *Trypanosoma brucei*”, *J Antimicro Chemo*, 38, 1041–7, 1996.

[34] T. P. C. Dorlo, M. Balasegaram, J. H. Beijnen, and P. J. de vries, “Miltefosine: A

review of its pharmacology and therapeutic efficacy in the treatment of leishmaniasis”, *J. Antimicrob. Chemother.*, 67(11), 2576–2597, 2012.

[35] Shyam Sundar, T.K. Jha, CP Thakur, Juergen Engel, Herbert Sindermann, Christina Fischer, Klaus Junge, Anthony Bryceson, Jonathan Berman, “Oral Miltefosine for Indian Visceral Leishmaniasis”, *Society*, 347(22), 1081–1090, 2002.

[36] S. Sundar, A. Singh, M. Rai, V. K. Prajapati, A. K. Singh, B. Ostyn, M. Boelaert, J. C. Dujardin, and J. Chakravarty, “Efficacy of miltefosine in the treatment of visceral leishmaniasis in India after a decade of use”, *Clin. Infect. Dis.*, 55(4), 543–550, 2012.

[37] K. Ritmeijer, A. Dejenie, Y. Assefa, T. B. Hundie, J. Mesure, G. Boots, M. den Boer, and R. N. Davidson, “A comparison of miltefosine and sodium stibogluconate for treatment of visceral leishmaniasis in an Ethiopian population with high prevalence of HIV infection”, *Clin. Infect. Dis.*, 43(3), 357–364, 2006.

[38] P. R. Machado, J. Ampuero, L. H. Guimarães, L. Villasboas, A. T. Rocha, A. Schriefer, R. S. Sousa, A. Talhari, G. Penna, and E. M. Carvalho, “Miltefosine in the treatment of cutaneous leishmaniasis caused by *leishmania braziliensis* in Brazil: A randomized and controlled trial”, *PLoS Negl. Trop. Dis.*, 4(12), 1–6, 2010.

[39] H. Sindermann and J. Engel, “Development of miltefosine as an oral treatment for leishmaniasis”, *Trans. R. Soc. Trop. Med. Hyg.*, 100(1), 2–5, 2006.

[40] S. Sundar and P. L. Olliaro, “Miltefosine in the treatment of leishmaniasis: Clinical evidence for informed clinical risk management”, *Ther. Clin. Risk Manag.*, 3(5), 733–740, 2007.

[41] D. P. Eiras, L. A. Kirkman, and H. W. Murray, “Cutaneous Leishmaniasis: Current Treatment Practices in the USA for Returning Travelers”, *Curr. Treat. Options Infect. Dis.*, 7(1), 52–62, 2015.

[42] B. J. Saenz RE, Paz H, “Efficacy of ketoconazole against *Leishmania braziliensis panamensis* cutaneous leishmaniasis”, *Am J Med.*, 89(2), 147–55.

[43] Jeanne Hawkins Van Tyle, “Mechanism of Action, Spectrum of Activity, Pharmacokinetics, Drug Interactions, Adverse Reactions and Therapeutic Use”, *Drugs in perspective*, 4, 334–337, 1987.

[44] S. M. Da Silva, I. F. G. Amorim, R. R. Ribeiro, E. G. Azevedo, C. Demicheli, M. N. Melo, W. L. Tafuri, N. F. Gontijo, M. S. M. Michalick, and F. Frézard, “Efficacy of combined therapy with liposome-encapsulated meglumine antimoniate and allopurinol in treatment of canine visceral leishmaniasis”, *Antimicrob. Agents Chemother.*, 56(6), 2858–2867, 2012.

- [45] M. A. Pfaller and J. J. Marr, “Antileishmanial effect of allopurinol”, *Antimicrob. Agents Chemother.*, 5(5), 496–472, 1974.
- [46] D. Yasur-Landau, C. L. Jaffe, L. David, and G. Baneth, “Allopurinol Resistance in *Leishmania infantum* from Dogs with Disease Relapse”, *PLoS Negl. Trop. Dis.*, 10(1), 1–13, 2016.
- [47] L. Manna, R. Corso, G. Galiero, A. Cerrone, P. Muzj, and A. E. Gravino, “Long-term follow-up of dogs with leishmaniosis treated with meglumine antimoniate plus allopurinol versus miltefosine plus allopurinol,” *Parasit. Vectors*, 8, 289, 2015.
- [48] Y. M. Traub-Cseko, J. M. Ramalho-Ortigão, A. P. Dantas, S. L. De Castro, H. S. Barbosa, and K. H. Downing, “Dinitroaniline herbicides against protozoan parasites: The case of *Trypanosoma cruzi*”, *Trends Parasitol.*, 17(3), 136–141, 2001.
- [49] B. J. Fennell, J. A. Naughton, E. Dempsey, and A. Bell, “Cellular and molecular actions of dinitroaniline and phosphorothioamidate herbicides on *Plasmodium falciparum*: Tubulin as a specific antimalarial target,” *Mol. Biochem. Parasitol.*, 145(2), 226–238, 2006.
- [50] T. J. Stokkermans, J. D. Schwartzman, K. Keenan, N. S. Morrissette, L. G. Tilney, and D. S. Roos, “Inhibition of *Toxoplasma gondii* replication by dinitroaniline herbicides”, *Exp. Parasitol.*, 84(3), 355–370, 1996.
- [51] A. Armson, S. W. Kamau, F. Grimm, J. A. Reynoldson, W. M. Best, L. M. MacDonald, and R. C. A. Thompson, “A comparison of the effects of a benzimidazole and the dinitroanilines against *Leishmania infantum*”, *Acta Trop.*, 73(3), 303–311, 1999.
- [52] A. Estella-Hermoso de Mendoza, M. Rayo, F. Mollinedo, and M. J. Blanco-Prieto, “Lipid nanoparticles for alkyl lysophospholipid edelfosine encapsulation: Development and in vitro characterization”, *Eur. J. Pharm. Biopharm.*, 68(2), 207–213, 2008.
- [53] A. Analysis and T. Note, “Dinitroanilines”, *Agrochemicals Analysis Technical Note*, March, 2–4, 2014.
- [54] M. M. Y. Chan, J. Tzeng, T. J. Emge, C. T. Ho, and D. Fong, “Structure-function analysis of antimicrotubule dinitroanilines against promastigotes of the parasitic protozoan *Leishmania mexicana*”, *Antimicrob. Agents Chemother.*, 37(9), 1909–1913, 1993.
- [55] M. Carvalheiro, J. Jorge, C. Eleutério, A. F. Pinhal, A. C. Sousa, J. G. Morais, and M. E. M. Cruz, “Trifluralin liposomal formulations active against *Leishmania donovani* infections” *Eur. J. Pharm. Biopharm.*, 71(2), 292–296, 2009.
- [56] C. Marques, M. Carvalheiro, M. A. Pereira, J. Jorge, M. E. M. Cruz, and G. M.

Santos-Gomes, “Efficacy of the liposome trifluralin in the treatment of experimental canine leishmaniosis”, *Vet. J.*, 178(1), 133–137, 2008.

[57] R. M. Lopes, M. L. Corvo, C. V. Eleutério, M. C. Carvalheiro, E. Scoulica, and M. E. M. Cruz, “Formulation of oryzalin (ORZ) liposomes: In vitro studies and in vivo fate”, *Eur. J. Pharm. Biopharm.*, 82(2), 281–290, 2012.

[58] R. M. Lopes, M. M. Gaspar, J. Pereira, C. V. Eleutério, M. Carvalheiro, A. J. Almeida, and M. E. M. Cruz, “Liposomes versus lipid nanoparticles: comparative study of lipid-based systems as oryzalin carriers for the treatment of leishmaniasis”, *J. Biomed. Nanotechnol.*, 10(12), 3647–3657, 2014.

[59] A. Y. Nyporko, A. I. Yemets, V. N. Brytsun, M. O. Lozinsky, and Y. B. Blume, “Structural and biological characterization of the tubulin interaction with dinitroanilines”, *Cytol. Genet.*, 43(4), 267–282, 2009.

[60] J. C. Antoine, E. Prina, T. Lang, and N. Courret, “The biogenesis and properties of the parasitophorous vacuoles that harbour *Leishmania* in murine macrophages”, *Trends Microbiol.*, 6(10), 392–401, 1998.

[61] C. S. Voyiatzaki and K. P. Soteriadou, “Identification and isolation of the *Leishmania* transferrin receptor”, *J. Biol. Chem.*, 267(13), 9112–9117, 1992.

[62] M. E. Wilson, T. S. Lewis, M. A. Miller, M. L. McCormick, and B. E. Britigan, “*Leishmania chagasi*: Uptake of iron bound to lactoferrin or transferrin requires an iron reductase”, *Exp. Parasitol.*, 100(3), 196–207, 2002.

[63] A. R. Flannery, C. Huynh, B. Mitra, R. A. Mortara, and N. W. Andrews, “LFR1 ferric iron reductase of *Leishmania amazonensis* is essential for the generation of infective parasite forms”, *J. Biol. Chem.*, 286(26), 23266–23279, 2011.

[64] F. Harris and L. Pierpoint, “Photodynamic Therapy Based on 5-Aminolevulinic Acid and Its Use as an Antimicrobial Agent” *Med. Res. Rev.*, 29(6), 1292–1327, 2012.

[65] K. Borstnik, I. H. Paik, T. A. Shapiro, and G. H. Posner, “Antimalarial chemotherapeutic peroxides: Artemisinin, yingzhaosu A and related compounds” *Int. J. Parasitol.*, 32(13), 1661–1667, 2002.

[66] D. M. Opsenica and B. A. Šolaja, “Antimalarial peroxides”, *Journal of Serbian Chemical Society*, 74(11), 1155–1193, 2009.

[67] I. Opsenica, N. Terzić, D. Opsenica, G. Angelovski, M. Lehnig, P. Eilbracht, B. Tinant, Z. Juranić, K. S. Smith, Y. S. Yang, D. S. Diaz, P. L. Smith, W. K. Milhous, D. Doković, and B. A. Šolaja, “Tetraoxane antimalarials and their reaction with Fe(II)”, *J. Med. Chem.*, 49(13), 3790–3799, 2006.

- [68] F. Bousejra-El Garah, M. H. L. Wong, R. K. Amewu, S. Muangnoicharoen, J. L. Maggs, J. L. Stigliani, B. K. Park, J. Chadwick, S. A. Ward, and P. M. O'Neill, "Comparison of the reactivity of antimalarial 1,2,4,5-tetraoxanes with 1,2,4-trioxolanes in the presence of ferrous iron salts, heme, and ferrous iron salts/phosphatidylcholine", *J. Med. Chem.*, 54(19), 6443–6455, 2011.
- [69] Y. Zhang, C. S. Bond, S. Bailey, M. L. Cunningham, A. H. Fairlamb, and W. N. Hunter, "The crystal structure of trypanothione reductase from the human pathogen *Trypanosoma cruzi* at 2.3 Å resolution", *Protein Sci.*, 5(1), 52–61, 1996.
- [70] M. Beig, F. Oellien, L. Garoff, S. Noack, R. L. Krauth-Siegel, and P. M. Selzer, "Trypanothione Reductase: A Target Protein for a Combined In Vitro and In Silico Screening Approach", *PLoS Negl. Trop. Dis.*, 9(6), 2015.
- [71] M. Deponte, "Glutathione catalysis and the reaction mechanisms of glutathione-dependent enzymes," *Biochim. Biophys. Acta - Gen. Subj.*, 1830(5), 3217–3266, 2013.
- [72] O. Mutlu, "Molecular modeling, structural analysis and identification of ligand binding sites of trypanothione reductase from", *J. Vector Borne Dis.*, 50(1), 38–44, 2013.
- [73] H. Fairlamb and A. Cerami, "Metabolism and functions of trypanothione in the Kinetoplastida", *Annu. Rev. Microbiol.*, 46, 695–729, 1992.
- [74] A. Fairlamb, P. Blackburn, P. Ulrich, B. Chait, and A. Cerami, "Trypanothione: a novel bis (glutathionyl) spermidine cofactor for glutathione reductase in trypanosomatids", *Science*, vol. 227(4693), 1485–7, 1985.
- [75] L. R. Krauth-siegel and M. A. Comini, "The Trypanothione System", Chapter 11; Peroxiredoxin Systems, *L. Flohé and J. R. Harris*, 231–251, 2007.
- [76] M. L. Cunningham and A. H. Fairlamb, "Trypanothione reductase from *Leishmania donovani* - Purification, characterisation and inhibition by trivalent antimonials", *Eur. J. Biochem.*, 230(2), 460–468, 1995.
- [77] J. Tovar, S. Wilkinson, J. C. Mottram, and A. H. Fairlamb, "Evidence that trypanothione reductase is an essential enzyme in *Leishmania* by targeted replacement of the tryA gene locus", *Mol. Microbiol.*, 29(2), 653–660, 1998.
- [78] A. J. Almeida and E. Souto, "Solid lipid nanoparticles as a drug delivery system for peptides and proteins", *Adv. Drug Deliv. Rev.*, 59(6), 478–490, 2007.
- [79] R. H. Muller, K. Mader, and S. Gohla, "Solid lipid nanoparticles (SLN) for controlled drug delivery - A review of the state of the art," *Eur. J. Pharm. Biopharm.*, 50(1), 161–177, 2000.
- [80] R. Gaurav and S. Tejal, "Liposomal Drug Delivery System: An Overview," *Int. J.*

Pharm. Biol. Arch. 2(6), 1575–1580, 2011.

[81] E. B. Souto, A. J. Almeida, and R. H. Muller, “Lipid nanoparticles (SLN[®], NLC[®]) for cutaneous drug delivery: Structure, protection and skin effects”, *J. Biomed. Nanotechnol.*, 3(4), 317–331, 2007.

[82] M. Fathi, M. R. Mozafari, and M. Mohebbi, “Nanoencapsulation of food ingredients using lipid based delivery systems”, *Trends Food Sci. Technol.*, 23(1), 13–27, 2012.

[83] K. O. Lemke A, Kiderlen AF, “Amphotericin B”, *Appl Microbiol Biotechnol.*, 68, (2), 151–62.

[84] V. Jain, A. Gupta, V. K. Pawar, S. Asthana, A. K. Jaiswal, A. Dube, and M. K. Chourasia, “Chitosan-Assisted Immunotherapy for Intervention of Experimental Leishmaniasis via Amphotericin B-Loaded Solid Lipid Nanoparticles”, *Appl. Biochem. Biotechnol.*, 174(4), 1309–1330, 2014.

[85] N. P. Aditya, S. Patankar, B. Madhusudhan, R. S. R. Murthy, and E. B. Souto, “Arthemeter-loaded lipid nanoparticles produced by modified thin-film hydration: Pharmacokinetics, toxicological and in vivo anti-malarial activity”, *Eur. J. Pharm. Sci.*, 40(5), 448–455, 2010.

[86] A. P. Nayak, W. Tiyaboonchai, S. Patankar, B. Madhusudhan, and E. B. Souto, “Curcuminoids-loaded lipid nanoparticles: Novel approach towards malaria treatment”, *Colloids Surfaces B Biointerfaces*, 81(1), 263–273, 2010.

[87] R. Oliveira, D. Miranda, J. Magalhães, R. Capela, M. J. Perry, P. M. O’Neill, R. Moreira, and F. Lopes, “From hybrid compounds to targeted drug delivery in antimalarial therapy”, *Bioorganic Med. Chem.*, 23(16), 5120–5130, 2015.

[88] H. D. S. Khatak, “Recent Techniques and Patents on Solid Lipid Nanoparticles as Novel Carrier for Drug Delivery”, *Recent Pat. Nanotechnol.*, 9, 150–177, 2015.

Chapter 2

Synthesis and characterization of 1,2,4,5-tetraoxanes derived from *trans*- cinnamaldehyde

Chapter 2 – Synthesis and characterization of 1,2,4,5-tetraoxanes derived from *trans*-cinnamaldehyde

1. Introduction

As referred in chapter 1, the discovery of artemisinin as a potent antimalarial agent and the identification of its peroxidic pharmacophore led to the synthesis and posterior biological assays of numerous compounds with a peroxide group as part of their structure [1,2]. One of the most promising class which emerges from these studies was 1,2,4,5-tetraoxane [3,4,5,6]. The peroxide core is reductively activated by iron (II) to form carbon-centered radicals and reactive oxygen species (ROS). Our lab have shown that 1,2,4,5-tetraoxane degrade to carbonyl species in tandem with free radical production [7]. Our goal is to translate this proved model from the malaria parasite to the *Leishmania* parasite, since *Leishmania spp*, acquire their iron from host cells, and are dependent on TR as protection against oxidative stress. TR is a flavoenzyme which defends the *Leishmania* parasite against oxidative stress, by neutralizing hydrogen peroxide produced by macrophages during infection [8].

Thus, our innovative compounds have the potential to disrupt the redox balance through two different, but synergistic mechanisms leading to ROS production and, ultimately, to parasite's death by inhibition of TR [7,8].

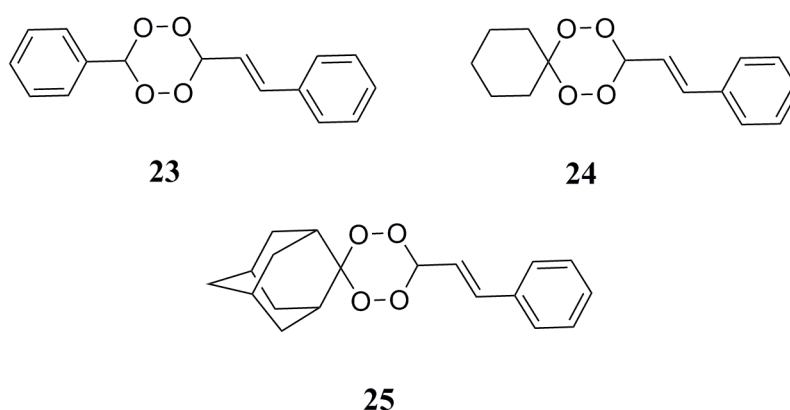


Figure 1- Tetraoxanes compounds designed for this study. **23-** (*E*)-3-phenyl-6-styryl-1,2,4,5-tetraoxane; **24-** (*E*)-3-styryl-1,2,4,5-tetraoxaspiro [5.5] undecane; **25-** (1*r*,5*R*,7*S*)-4'-((*E*)-styryl)spiro[adamantane-2,1'-cyclohexane]

In this chapter our aim is to develop new tetraoxane-based compounds (figure 1) that can be selectively activated inside the parasite using a Fe (II) -based triggering mechanism in order to increase the concentrations of ROS in *Leishmania* parasites and suppress the antioxidant defense mechanism of the parasite by inhibiting TR.

These compounds have the particularity of having *trans*-cinnamaldehyde that can act as TR inhibitor.

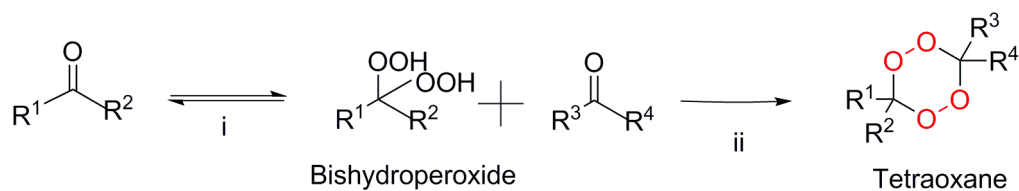
The phenyl, cyclohexane and adamantyl groups contribute to increase lipophilicity of the final tetraoxanes, which is an important physical property to account, once these compounds were synthesized with the purpose of lipid nanoencapsulation. Therefore, a higher log P means better tetraoxane-lipid interaction – table 1.

Table 1- Theoretical Log P calculated by software <http://www.molinspiration.com/services/logp.html>.

Compound	cLog P
23	3.955
24	4.349
25	5.214

Figure 2 illustrates the retrosynthetic analysis of the three selected tetraoxanes and the scheme 1 represents the synthetic route followed.

In addition to *trans*-cinnamaldehyde, the other three starting reagents were selected taking into consideration their contribution to stability, lipophilicity and more importantly antiparasitic activity. Benzaldehyde, cyclohexanone and 2-adamantanone, figure 2, are all lipophilic molecules, which is an important property when exploring the nanoencapsulation route.



Scheme 1- Synthetic procedure used to obtain the Tetraoxanes compounds. **Reagents and conditions:** i) HCO_2H , CH_3CN , H_2O_2 50%, r.t.; ii) Re_2O_7 , CH_2Cl_2 , 0°C . R^1 , R^2 , R^3 and R^4 are representing aldehydes or ketones.

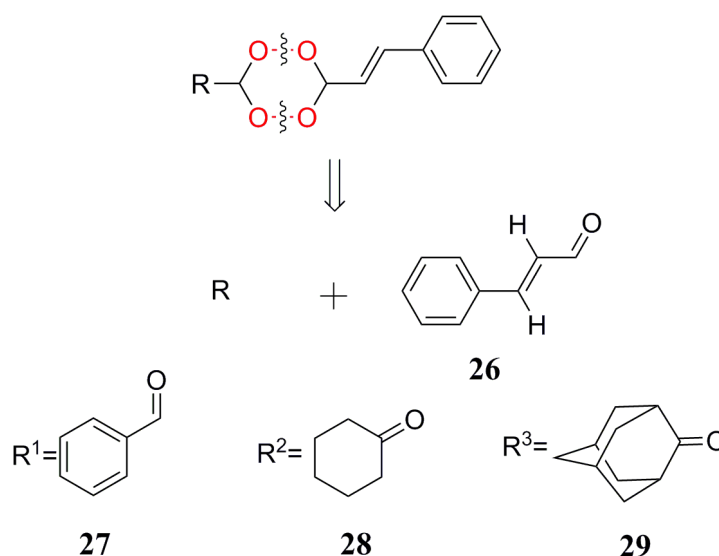


Figure 2- Tetraoxanes retrosynthetic scheme. **26-** *trans*-cinnamaldehyde; **27-** benzaldehyde; **28-** cyclohexanone; **29-** 2-adamantanone.

According to Kumar *et al* tetraoxanes derived from cycloalkanones were the first to show antimalarial activity similar to the one found in artemisinin. Therefore, we selected cyclohexanone to be one of the moieties of our tetraoxanes [3]. Kim *et al* reported antimalarial activity of 3,6-disubstituted tetraoxanes, where phenyl ring was part of the active pharmacophore. However, some of the compounds showed poor antimalarial activity. This activity was significantly lower than the tetraoxanes derived from cycloalkanones [10,11]. The major advantage of choosing benzaldehyde when compared to cyclohexanone is the opportunity to have structural diversity, since this class of compounds is easier to functionalize than cyclic ketones. Thus a tetraoxane derived from the non-substituted benzaldehyde was also synthesized.

Finally, the synthesis of a tetraoxane derived from 2-adamantanone was tried because reports from antimalarial studies showed that the introduction of this group not only increases the stability of tetraoxane group but also improves its activity extensively and provides protection from metabolization [13].

2. Materials and methods

2.1. Reagents

All the reagents used during the experimental synthesis section were provided by Sigma-Aldrich, Alfa Aesar, and Merck.

2.2. Solvents

Analytical grade solvents were used in the synthesis of all compounds.

Dichloromethane (DCM) and acetonitrile (ACN) were distilled at atmospheric pressure in the presence of sodium carbonate.

Ethyl acetate and hexane, used for compounds purification, were also distilled in the presence of sodium carbonate.

CDCl₃ - Merck, with a degree of purity higher than 95%, was used for NMR analysis.

2.3. Chromatography

All chromatography columns were prepared with silica gel 60 M, 0.040-0.063 mm (Merck). The thin layer chromatographies were carried out on silica gel plates - Merck Kieselgel F254, 0.25 mm thickness - and revealed using a CAMAG UV lamp at a wavelength of 254 nm, or alternatively, using *N,N*-dimethyl-*p*-diphenylenediamine or *p*-anisaldehyde.

2.4. Equipment

Melting points were determined on a Kofler Bock Monoscop M. camera by the Ph. Eur. 2.2.16. instantaneous method.

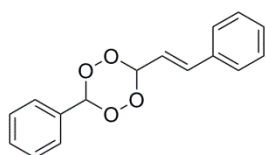
Infrared spectra (IR) were performed on a Nicolet Impact 400 FTIR spectrophotometer using potassium bromide tablets.

The $^1\text{H-NMR}$, $^{13}\text{C-NMR}$ and 2D-NMR spectra were recorded on a Bruker 300 Ultra Shield. The chemical shift values δ_{H} and δ_{C} are reported in ppm relative to d_3 -chloroform and coupling constants (J) are in Hz. The spectra analysis were done at the software MestReNova, version: 6.0.2-5475 from © 2009 Mestrelab Research S.L.

2.5. General procedures for the synthesis of the tetraoxanes

2.5.1. (E)-3-phenyl-6-styryl-1,2,4,5-tetraoxane (23)

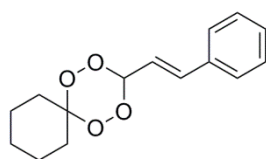
To a stirring solution of benzaldehyde (1.89 mmol) in dry acetonitrile (ACN) (2.60 mL) and formic acid (2.60 mL) at 0°C, was added hydrogen peroxide 50% (1.30 mL). After about 2-3 h of stirring at room temperature, it was added a new refill of hydrogen peroxide 50% and then the bishydroperoxide was extracted with DCM (3 x 15 mL). If at the moment of the extraction the two separation phases were not clear, it was added brine solution. The organic phases were combined, dried with anhydrous sodium sulfate, filtered and concentrated under reduced pressure. The concentrated bishydroperoxide was added to a solution of *trans*-cinnamaldehyde (3.78 mmol) in dry DCM (3.20 mL) with rhenium (VII) oxide (0.05 mmol) at 0°C. The formation of product was followed by TLC and after about 2-3 h the reaction mixture was filtered with a plug of silica and the solvent evaporated. Purification was carried out by column chromatography on silica using ethyl acetate:n-hexane (3:97) as eluent.



Yield: 71%; white crystal; **m.p** 132-135°C; **vmax/cm⁻¹** 997.24 (-O-O-), 1066.68 (-O-O-). **¹H NMR (300 MHz, CDCl₃):** δ_H/ppm 7.51-7.34 (m, 10H, Ar), 7.03 (d, J=16.3 Hz, 1H), 6.81 (s, 1H), 6.59 (dd, J=6.3, 0.6Hz, 1H), 6.02 (dd, J=16.3, 6.3 Hz, 1H). **¹³C NMR (75 MHz, CDCl₃):** δC/ppm 140.64 and 116.76 (CH=CH), 131.46-127.43 (Ar(CH)), 134.86 and 131.13 (Ar(C)), 108.19 and 107.32 (CH-O-O-CH). **Elemental Analysis:** calcd- C, 71.1 %; H, 5.2 %; O, 23.7 %; Found- C, 71.6 %; H, 5.2 %; O, 23.2 %.

2.5.2. (E)-3-styryl-1,2,4,5-tetraoxaspiro [5.5] undecane (24)

To a stirring solution of cyclohexanone (2.04 mmol) in dry ACN (2.80 mL) and formic acid as catalyst (2.80 mL) at 0°C, was added hydrogen peroxide 50% (1.40 mL). After about 2-3 h of stirring at room temperature, it was added a new refill of hydrogen peroxide 50% and then the bishydroperoxide was extracted with DCM (3 x 15 mL). If necessary it was added brine solution. The organic phases were combined, dried with anhydrous sodium sulfate, filtered and concentrated under reduced pressure. The concentrated bishydroperoxide was added to a solution of *trans*-cinnamaldehyde (3.27 mmol) in dry DCM (3.50 mL) with rhenium (VII) oxide (0.05 mmol) at 0°C. The formation of product was followed by TLC and after about 2-3 h the reaction mixture was filtered with a plug of silica and the solvent evaporated. Purification was carried out by column chromatography on silica using ethyl acetate:n-hexane (2.5:97.5) as eluent.



Yield: 47%; white crystal; **m.p** 96-100°C; **vmax/cm⁻¹** 974.09 (-O-O-), 1060.89 (-O-O-). **¹H NMR (300 MHz, CDCl₃):** δ_H/ppm 7.43-7.32 (m, 5H), 6.93 (d, J=16.3 Hz, 1H), 6.33 (d, J=6.2 Hz, 1H), 5.97 (dd, J=16.3, 6.1 Hz, 1H), 2.36 (t, 2H), 1.7-1.49 (m, 8H). **¹³C NMR (75 MHz, CDCl₃):** δC/ppm 139.84 and 117.46 (CH=CH), 135.00 (Ar(C)), 127.35-129.54 (Ar(CH)), 108.78 (CyHex(C)), 107.01 (O-CH-O), 32.03-22.01 (CyHex(CH)). **Elemental Analysis:** calcd- C, 68.7 %; H, 6.9 %; O, 24.4 %; Found- C, 68.7 %; H, 7.2 %; O, 24.1 %.

2.5.3. Attempt to synthesize (1r,5R,7S)-4'-((E)-styryl)spiro[adamantane-2,1'-cyclohexane] (25)

Method A- To a stirring solution of *trans*-cinnamaldehyde (0.33 mmol) in dry ACN (1.00 mL) and rhenium (VII) oxide (0.02 mmol) as catalyst at 0°C, was added hydrogen peroxide 50% (0.26 mL). After about 2-3 h of stirring at 0°C, it was added a new refill of hydrogen peroxide 50 % and then the bishydroperoxide was extracted with DCM (3 x 7.5 mL). If necessary it was added brine solution. The organic phases were combined, dried with anhydrous sodium sulfate, filtered and concentrated under reduced pressure. The concentrated bishydroperoxide was added to a solution of 2-adamantanone (0.57 mmol), in dry DCM (1.50 mL) with rhenium (VII) oxide (0.007 mmol) as catalyst at 0°C. The formation of product was followed by TLC and after about 2-3 h the reaction mixture was filtered with a plug of silica and the solvent evaporated. Purification was carried out by column chromatography on silica using ethyl acetate:n-hexane (2:98) as eluent. The compound was not synthesized by this procedure. A complex mixture without the desired compound was obtained.

Method B- To a stirring solution of 2-adamantanone (0.33 mmol) in dry ACN (1.00 mL) and rhenium (VII) oxide (0.02 mmol) as catalyst at 0°C, was added hydrogen peroxide 50% (0.26 mL). The remaining protocol is equal to method A but in the second step it was added *trans*-cinnamaldehyde (0.54 mmol). The compound was not synthesized by this procedure. A complex mixture without the desired compound was obtained.

Method C- Equal to method A but the first catalyst was formic acid (1.00 mL) and the second was phosphomolybdic acid (PMA) (0.038 mmol) and (MgSO₄). Both reactions occurred at room temperature. The compound was not synthesized by this procedure. A complex mixture without the desired compound was obtained.

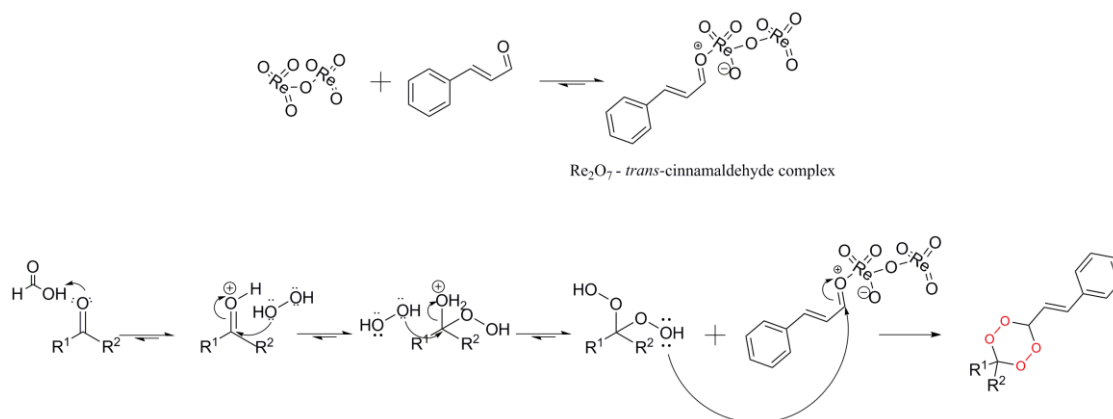
Method D- Equal to method C but the first catalyst was PMA (0.0076 mmol) and the first solvent was ethylic ether (1.00 mL). The compound was not synthesized by this procedure. A complex mixture without the desired compound was obtained.

Method E- Equal to method C but the second reaction occurred at room temperature. The compound was not synthesized by this procedure. A complex mixture without the desired compound was obtained.

3. Results and discussion

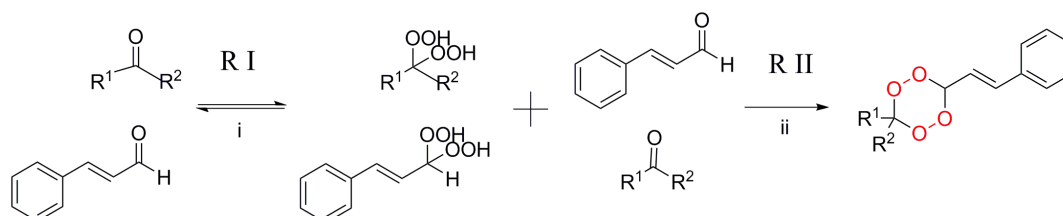
3.1. Synthesis methodology

Bishydroperoxides are the intermediates derived from aldehydes and ketones with a major role in the synthesis of several classes of peroxides where tetraoxanes are included. From the different methodologies described in literature to synthesize the tetraoxanes, a method described by O'Neill and optimized in our research group was used in this work [14]. In the first step a carbonyl compound is oxidized with hydrogen peroxide resorting to acidic catalysis, followed by cyclization of the bishydroperoxide with another carbonilic compound using Re_2O_7 catalysis, thus forming the tetraoxane (Mechanism 1).



Mechanism 1- Proposed reaction mechanism for the synthesis of the desired tetraoxanes.

The bishydroperoxide intermediate was produced starting with *trans*-cinnamaldehyde or, alternatively, with benzaldehyde, cyclohexanone or 2-adamantanone (table 2 and scheme 2).

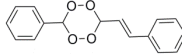
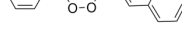
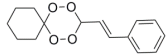
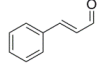
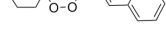
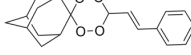
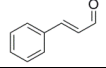


Scheme 2- Schematic illustration of the approach used for the synthesis reactions of the desired tetraoxanes. R I and R II represent the order of reagent addition. i) HCO_2H , CH_3CN , H_2O_2 50%, r.t.; ii) Re_2O_7 , CH_2Cl_2 , 0°C . R^1 and R^2 are representing aldehydes or ketones.

It was observed that the formation of bishydroperoxide intermediate was not favored using *trans*-cinnamaldehyde as starting material because the reaction led to several secondary products and low yield of the final product. In contrast, when the bishydroperoxide intermediate was synthesized from benzaldehyde or cyclohexanone the final tetraoxanes were obtained in good yields, and were easily purified.

Tetraoxane **25** was not obtained either forming the intermediate from 2-adamantanone or in *trans*-cinnamaldehyde. Both tetraoxanes **23** and **24** were purified by column chromatography with final yields of 71% and 47% respectively – table 2.

Table 2- Summary of the synthesis reactions where R I (Reagent 1) and R II (Reagent 2) are the reaction 1 and reaction 2 in scheme 2 respectively.

R I	R II	Product	Yield (%)
			71
			7
			47
			20
			-
			-

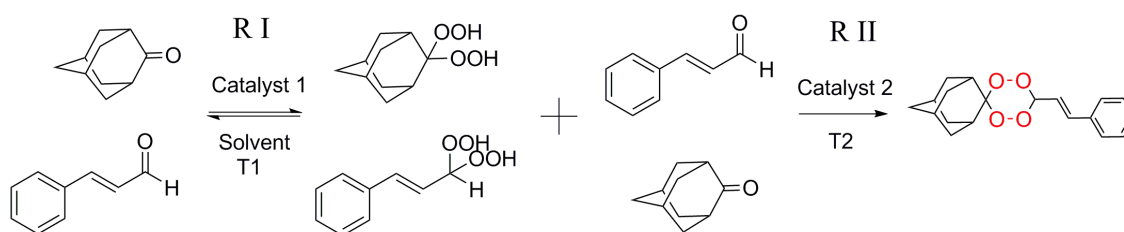
All compounds were characterized by $^1\text{H-NMR}$, $^{13}\text{C-NMR}$, 2D-NMR, infrared spectroscopy, elemental analysis and melting point. The methodology with better reaction yield was selected to scale-up, in order to proceed to the nanoencapsulation studies.

3.1.1. Optimization of adamantane-tetraoxane synthesis

From experience in our research group and from literature it is known that forming the bishydroperoxide from 2-adamantanone is a very difficult process. Therefore, in order to

synthesize the tetraoxane with the adamantyl group, the reaction was performed using *trans*-cinnamaldehyde as starting material to form the corresponding bishydroperoxide intermediate.

When the reaction was performed starting with *trans*-cinnamaldehyde (Reagent I, table 2), despite the low yield for tetraoxanes **23** and **24**, the desired compounds were obtained (table 2). However, in this case there was no final tetraoxane at all. It can be rationalized that the bishydroperoxide is formed from *trans*-cinnamaldehyde with a final low yield and, therefore the non formation of adamantane tetraoxane is most likely being affected in the second step (i.e. when used as Reagent II, table 2). Thus to optimize the adamantane tetraoxane synthesis reaction it was assumed that would be more correct if *trans*-cinnamaldehyde was the RI since the first step of the reaction which involves the formation of the bishydroperoxide intermediate in the *trans*-cinnamaldehyde carbonyl could be followed by thin-layer chromatography by rf comparison with the other synthesis. There was no evidence that the bishydroperoxide intermediate may be formed in 2-adamantanone. All significant changes are explicit in table 3 and the followed reaction is summarized in scheme 3.



Scheme 3- Schematic illustration of the approach used to optimize the synthesis reactions of the adamantane-tetraoxane. RI and RII represent the order of reagent addition.

Table 3- Conditions used for the different reactions with the aim of synthesized the adamantane-tetraoxane. **R I-** Reagent 1; **R II-** Reagent 2; **T1-** temperature in the first step; **T2-** temperature in the second step; **r.t.-** room temperature.

RI	RII	Catalyst 1	Catalyst 2	Solvent	T 1 (°C)	T 2 (°C)
		Re ₂ O ₇	Re ₂ O ₇	ACN	0	0
		Re ₂ O ₇	Re ₂ O ₇	ACN	0	0
		HCO ₂ H	PMA(MgSO ₄)	ACN	r.t.	r.t.
		PMA	PMA(MgSO ₄)	Et ₂ O	r.t.	r.t.
		HCO ₂ H	PMA(MgSO ₄)	ACN	r.t.	r.t.

Once again, the synthesis of the adamantane tetraoxane was not succeeded and therefore the nanoencapsulation studies were performed only for molecules **23** and **24**.

3.2. Benzaldehyde-tetraoxane (23) characterization

The aromatic protons display a rather complex pattern of signals between 7.35 and 7.50 ppm, corresponding to both phenyl groups. The two vinylic protons represented in red and blue in figure 3 appear as a duplet and the double duplet at 7.05 and 6.02 ppm respectively. The signal at 7.05 ppm is more deshielded because is the nearest to the phenyl group.

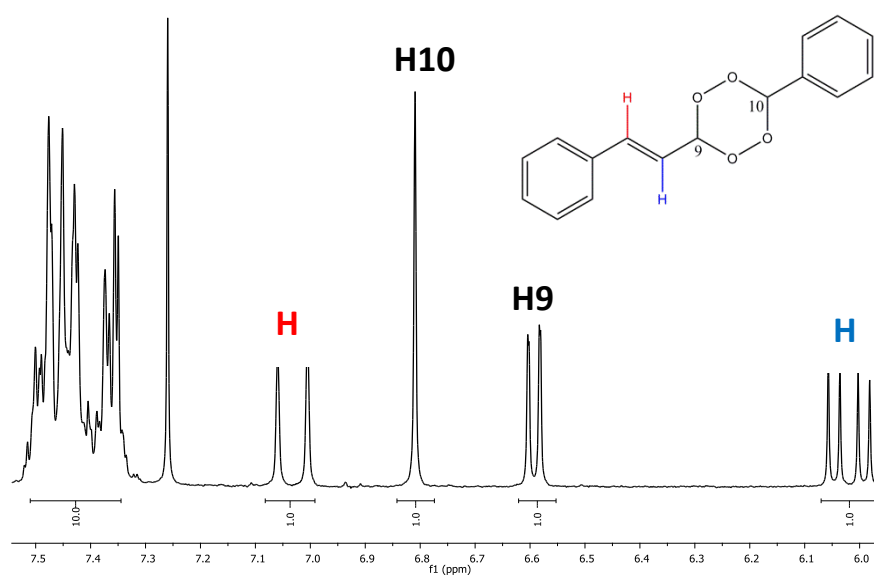


Figure 3- Benzaldehyde-tetraoxane (**23**) ^1H -NMR spectra.

These protons also have the same couple constant of 16.3 Hz, which is a characteristic value of the *trans* configuration. The singlet at 6.81 ppm corresponds to H9 and the duplet at 6.59 ppm is from H8 (see COSY spectrum in annex 1). All signals have adequate integrals to fit the 14 protons of tetraoxane **23**.

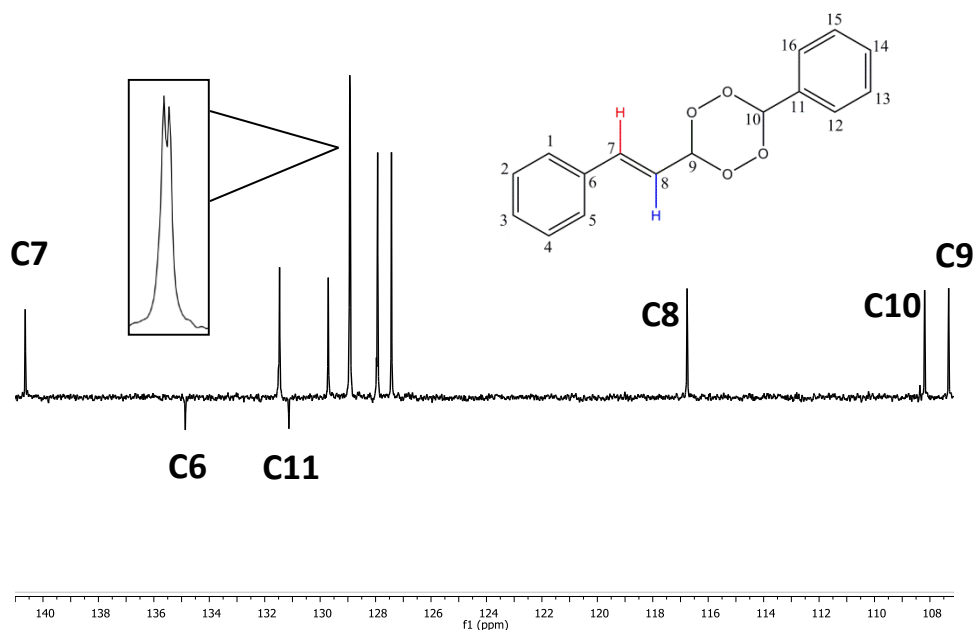


Figure 4- Benzaldehyde-tetraoxane (**23**) ^{13}C -NMR spectra.

Tetraoxane **23** has 16 carbons in total but in the ^{13}C -RMN spectra only 12 signals are expected since the pairs C1-C5, C2-C4, C12-C16 and C13-C15 are equivalent and belonging to both aromatic rings. There was indeed 12 signals in the ^{13}C -NMR even though two of them are overlapped (figure 4, enlargement). In order to attribute all the carbons in tetraoxane **23** there was performed 2D heteronuclear correlation NMR spectrums (HMQC and HMBC, figure 5 and annex 2).

Secondary and quaternary carbons are the signals pointed down in the spectra and the primary and tertiary carbons are the signals pointed up. Tetraoxane **23** only has quaternary and tertiary carbons so the two quaternary carbons in the spectra are from C6 (134.86 ppm) and C11 (131.13 ppm). At 107.32 ppm is the C9 signal and at 108.19 ppm C10 signal. The two vinyl carbons also can be identified by HMQC, at 140.64 ppm appears C7 signal and at 116.76 ppm is the signal corresponding to C8.

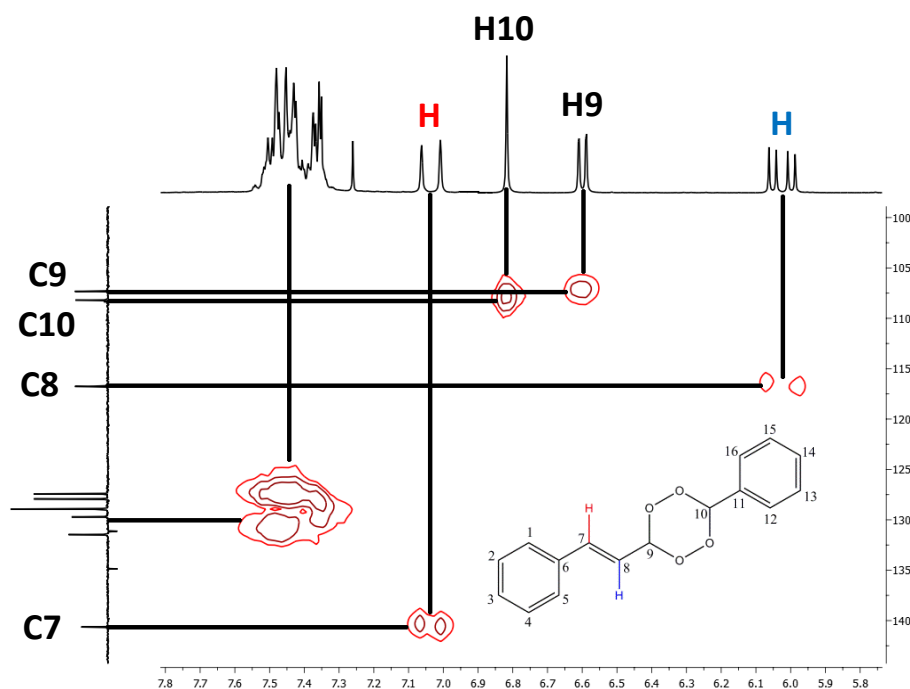


Figure 5- Benzaldehyde-tetraoxane (**23**) HMQC spectra.

Resorting to HMBC (annex 2) it was possible to assign the two quaternary carbons. C11 is coupled at 2 bounds distance with the nearest aromatic protons and with H10, while C6 is also coupled at 2 bounds distance with the nearest aromatic protons and with the closest vinyl proton (red hydrogen, figure 5).

The bands in the infrared spectrum at 997.24 cm^{-1} and 1066.68 cm^{-1} confirm the presence of the peroxidic bonds in the structure of tetraoxane **23** (annex 3). The elemental analysis is in agreement with the calculated values.

3.3. Cyclohexane-Tetraoxane (**24**) characterization

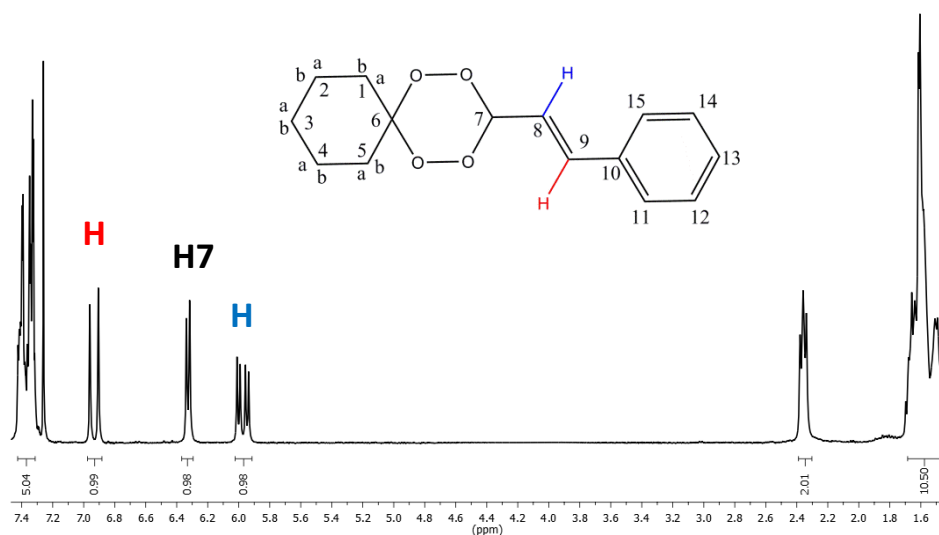


Figure 6- Cyclohexane-tetraoxane (**24**) ^1H -NMR spectra.

Figure 6 illustrates the tetraoxane **24** ^1H -NMR spectra where we can identify six different types of protons. At high field two signals belonging to the cyclohexane protons. The most deshielded signal (triplet at 2.35 ppm) may correspond to the equatorial protons 1 and 5. The signal of these two protons is more deshielded probably due to the conformation of the cyclohexane ring, which approaches them to the nearest oxygen atoms of the peroxidic bond.

The double duplet at 5.97 ppm and the duplet 6.94 ppm are from *trans*-vinylic protons (blue proton and red proton respectively in figure 6). The coupling constant is according to the characteristic *trans* configuration and is 16.3 Hz for both of these protons.

The complex signal between 7.30 ppm and 7.43 ppm results from the five aromatic protons.

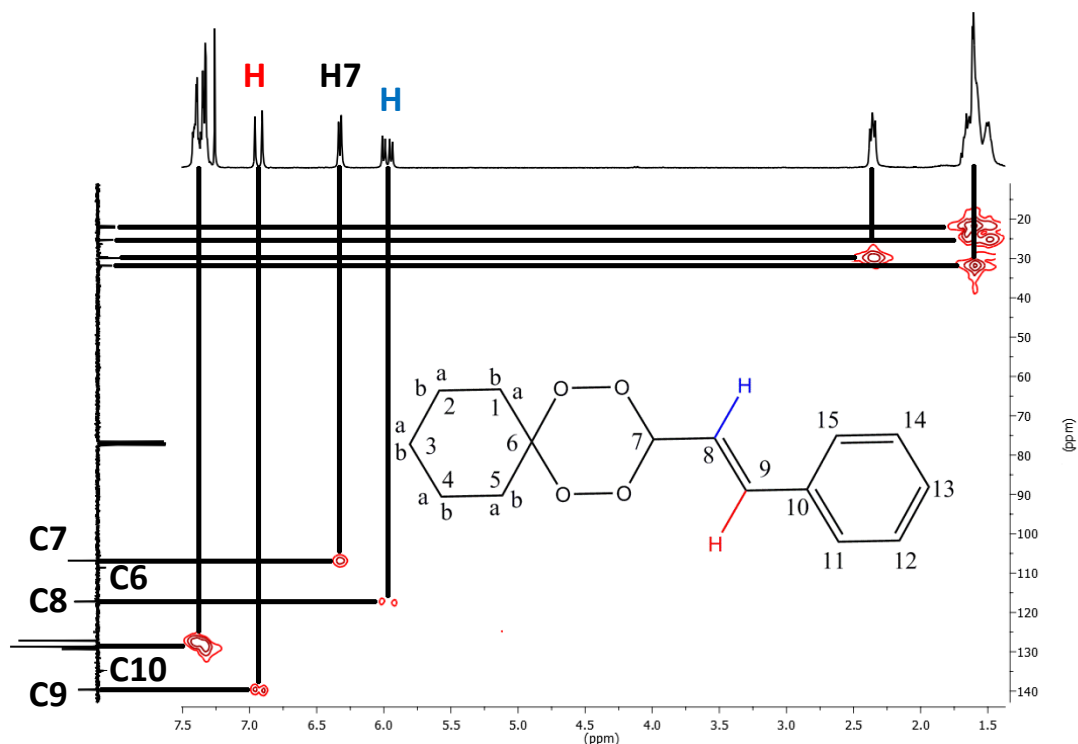


Figure 7- Cyclohexane-tetraoxane (**24**) HMQC spectra.

Resorting to HMQC spectra, the carbons in tetraoxane **24** can be identified via H-C coupling. C1 and C5 should intercept two signals being the first interception at 2.35 which correspond to the equatorial protons and then a second interception at 1.60, in the multiplet zone, for the axial protons. Thus following this argument, there were expected five signals corresponding to the cyclohexane's carbons (C1; C2 and C4; C3; C5 and C6). C6 is clearly suffering the electronegativity effect of oxygen atoms belonging to the peroxidic bond, therefore, this signal should be more deshielded when compared with the other cyclohexane's carbons and for this reason it will appear at low field.

Regarding the HMQC analysis of the tetraoxane **24** (figure 7), the carbon at 107.01 ppm is coupled with the duplet corresponding to the H7, so this signal is from C7. At 117.46 ppm the carbon is coupled with the double duplet from H8, and therefore it corresponds to C8. The most deshielded carbon at 139.84 ppm is the closest to the phenyl group and corresponds to C9 that is coupled with the duplet corresponding to the red proton. The other four signals are from the aromatic carbon atoms. The quaternary carbon of the phenyl group, C10, is at 135 ppm. The remaining three signals are from C11, C12, C13,

Chapter 2

C14 and C15. Because of the molecule's symmetry the pairs C11-C15 and C12-C14 correspond to two signals and C13 to one.

In order to prove the anterior assessment which refers that C6 signal will appear at low field an HMBC experience was performed. Looking at HBMC spectra – annex 5 - at 108.78 ppm one of the quaternary carbons is coupling with the most deshielded cyclohexane's proton. This signal corresponds to C6.

The infrared spectrum bands at 974.09 cm^{-1} and 1060.89 cm^{-1} confirm the presence of the peroxidic bonds in the structure of tetraoxane **24** (annex 6). The elemental analysis is according with the calculated values.

4. References

- [1] N. Yadav, C. Sharma, and S. K. Awasthi, "Diversification in the synthesis of antimalarial trioxane and tetraoxane analogs" *RSC Adv.*, 4(11), 5469, 2014.
- [2] K. Borstnik, I. H. Paik, T. A. Shapiro, and G. H. Posner, "Antimalarial chemotherapeutic peroxides: Artemisinin, yingzhaosu A and related compounds", *Int. J. Parasitol.*, 32(3), 1661–1667, 2002.
- [3] F. Harris and L. Pierpoint, "Photodynamic Therapy Based on 5-Aminolevulinic Acid and Its Use as an Antimicrobial Agent", *Med. Res. Rev.*, 29(6), 1292–1327, 2012.
- [4] E. Pires, M. Rosa, J. Gut, P. J. Rosenthal, and M. Prude, "Tetraoxane – Pyrimidine Nitrile Hybrids as Dual Stage Antimalarials," *J. Med. Chem.*, 57, 4916–4923, 2014.
- [5] R. Amewu, A. V Stachulski, S. a Ward, N. G. Berry, P. G. Bray, J. Davies, G. Labat, L. Vivas, and P. M. O'Neill, "Design and synthesis of orally active dispiro 1,2,4,5-tetraoxanes; synthetic antimalarials with superior activity to artemisinin", *Org. Biomol. Chem.*, 4(24), 4431–4436, 2006.
- [6] F. Marti, J. Chadwick, R. K. Amewu, H. Burrell-Saward, A. Srivastava, S. a. Ward, R. Sharma, N. Berry, and P. M. O'Neill, "Second generation analogues of RKA182: synthetic tetraoxanes with outstanding in vitro and in vivo antimalarial activities", *Medchemcomm*, 2(7), 661, 2011.
- [7] R. Oliveira, A. S. Newton, R. C. Guedes, D. Miranda, R. K. Amewu, A. Srivastava, J. Gut, P. J. Rosenthal, P. M. O'Neill, S. a. Ward, F. Lopes, and R. Moreira, "An endoperoxide-based hybrid approach to deliver falcipain inhibitors inside malaria parasites". *ChemMedChem*, 8(9), 1528–1536, 2013.
- [8] J. Tovar, M. L. Cunningham, A. C. Smith, S. L. Croft, and A. H. Fairlamb, "Down-regulation of *Leishmania donovani* trypanothione reductase by heterologous expression of a trans-dominant mutant homologue: Effect on parasite intracellular survival", *Microbiology*, 95, 5311–5316, 1998.
- [9] I. Opsenica, N. Terzić, D. Opsenica, G. Angelovski, M. Lehnig, P. Eilbracht, B. Tinant, Z. Juranić, K. S. Smith, Y. S. Yang, D. S. Diaz, P. L. Smith, W. K. Milhous, D. Doković, and B. A. Šolaja, "Tetraoxane antimalarials and their reaction with Fe(II)", *J. Med. Chem.*, 49(13), 3790–3799, 2006.
- [10] A. R. Flannery, R. L. Renberg, and N. W. Andrews, "Pathways of iron acquisition

and utilization in Leishmania”, *Curr. Opin. Microbiol.*, 16(6), 716–721, 2013.

[11] H. S. Kim, Y. Shibata, Y. Wataya, K. Tsuchiya, A. Masuyama, and M. Nojima, “Synthesis and antimalarial activity of cyclic peroxides, 1,2,4,5,7- pentoxocanes and 1,2,4,5-tetroxanes”, *J. Med. Chem.*, 42(14), 2604–2609, 1999.

[12] R. Leung-toung, T. F. Tam, Y. Zhao, C. D. Simpson, W. Li, D. Desilets, and K. Karimian, “Synthetic methods for unsymmetrically-substituted 1,2,4,5-tetroxanes and of 1,2,4,5,7-pentoxocanes Hye-Sook”, 31(10), 6230–6241, 2005.

[13] G. L. Ellis, R. Amewu, S. Sabbani, P. A. Stocks, A. Shone, D. Stanford, P. Gibbons, J. Davies, L. Vivas, S. Charnaud, E. Bongard, C. Hall, K. Rimmer, S. Lozanom, M. Jesús, D. Gargallo, S. A. Ward, and P. M. O’Neill, “Two-step synthesis of achiral dispiro-1,2,4,5-tetraoxanes with outstanding antimalarial activity, low toxicity, and high-stability profiles” *J. Med. Chem.*, 51(7), 2170–2177, 2008.

[14] P. M. O’Neill, R. K. Amewu, G. L. Nixon, F. B. ElGarah, M. Mungthin, J. Chadwick, A. E. Shone, L. Vivas, H. Lander, V. Barton, S. Muangnoicharoen, P. G. Bray, J. Davies, B. K. Park, S. Wittlin, R. Brun, M. Preschel, K. Zhang, and S. A. Ward, “Identification of a 1,2,4,5-tetraoxane antimalarial drug-development candidate (RKA 182) with superior properties to the semisynthetic artemisinins” *Angew. Chemie - Int. Ed.*, 49(33), 5693–5697, 2010.

Chapter 3

Lipid nanoparticles containing tetraoxanes for the treatment of leishmaniasis

Chapter 3 - Lipid nanoparticles containing tetraoxanes for the treatment of leishmaniasis

1. Introduction

Infectious diseases caused by viruses, parasites and bacteria are the second cause of mortality around the globe, more predominantly in the developing countries. They impose a substantial burden of morbidity, which is particularly serious for a group of 15 parasitic and bacterial diseases classified by the WHO as neglected diseases, including, among others, leishmaniasis [1].

For more than 70 years, the first-line of treatment in most affected countries has been injectable pentavalent antimonials - Pentostam® and Glucantime®. The treatment is painful, potentially toxic, very lengthy, and has become ineffective in some regions of India and Nepal, as resistance has developed. Second-line drugs include pentamidine, paromomycin and amphotericin B, but their use is limited due to toxicity and also due to the emergence of resistance [2]. A very high therapeutic index, short treatment courses and the absence of side effects make lipid formulations of amphotericin B - AmBisome® - the most attractive existing treatment for VL. However, AmBisome® is currently too expensive and, therefore, inaccessible for most endemic and low income countries [3]. In addition, the first effective oral drug for VL treatment - miltefosine - is associated with teratogenicity and haemolytic activity, while its long half-life time also might encourage the emergence of resistance [4]. For these reasons, and in the absence of an effective and cheap vaccine, there is an urgent need of new antileishmanial drugs [5].

One of the strategies currently being used to overcome these drawbacks is to take advantage of the existing and well studied pharmacophores that already are efficient against other parasites, which cause the 'neglected diseases' and transpose them to other parasite targets with similar metabolism. In this context, the present work studies the use of the tetraoxanes trigger mechanism by iron and their known antiparasitic activity, combined with the advantages of using SLN, with the purpose to develop a new efficient antileishmanial oral formulation.

In recent years it has become evident that the development of new active substances is often not enough to secure new pharmacological therapies. One of the most promising strategies, which allow overcoming this problem, is to find suitable vehicles to carry and

protect the drugs up to their site of action. In the beginning of the 90's several research groups started to study alternative drug carriers such as SLN [6]. As mentioned in chapter 1, SLN formulations combine the advantage of polymeric nanoparticles, fat emulsions, and liposomes in a single nanoparticulate entity [7]. The SLN provide unique biological opportunities for site-specific drug delivery along with controlled release of active drug over a long period, especially in the treatment of parasitic infections, such as leishmaniasis, since they are rapidly cleared by the MPS. This leads to passive targeting to liver and spleen, which are the critically organs affected by *Leishmania* amastigotes [8]. Although SLN production and scale up are fairly simple, relatively cheap and reproducible [7], there are some obstacles preventing the widespread use of SLN: the low encapsulation efficiency, resulting from the transformation of polymorphic lipid matrix, which can cause the expulsion of drug molecules from the SLN matrix [9], and; physical instability of SLN due to aggregation and fusion, as well as chemical instability, which can include hydrolysis reactions, surfactants oxidation, premature drug release and reactivity during storage [10]. These parameters can be improved by lyophilization, which eliminates the aqueous phase in which the SLN are suspended, enabling furtherhandling of colloidal systems and ensuring their long-term stability. The process usually involves the use of crioprotectants to preserve drug stability, drug loading and prevent particle aggregation. Nevertheless, lyophilized nanoparticles should maintain unchanged the main physical and chemical characteristics [11]. Sterilization is also an important step in SLN production especially when the formulation is intended for parenteral administration. The sterilization process step must not change the formulation physicochemical and pharmaceutical properties like average particle diameter and zeta potential. In this context, the proper selection of surfactants agents, is crucial to reduce temperature-induced modifications [12]. Although high temperatures affect the mobility and hydrophilicity of surfactants it has been proved that natural surfactants such as lecithin are suitable stabilizing SLN formulations intended for moist heat sterilization [8]. The main goal of this chapter was to optimize the encapsulation of the tetraoxanes **23** and **24** in SLN using either the hot high-shear homogenization or the emulsion-solvent evaporation methods. This study also involves the evaluation of relevant parameters such as the encapsulation efficiency, average particle diameter, polydispersity index (PdI), and zeta potential. The stability of the SLN was also studied using dynamic light scattering (DLS), differential scanning calorimetry (DSC) and transmission electron microscopy

(TEM). Studies also included the effect of moist heat sterilization and *in vitro* release studies in physiological and acidic medium. Finally cytotoxicity was studied using THP-1 cell viability testing while *in vitro* activity assessment studies were performed using THP-1 cells infected with *L. infantum* promastigotes.

2. Materials and methods

2.1. Reagents

Tetraoxanes **23** and **24** were synthesized in our laboratories, as part of this work, as described in Chapter 1. Glycerol tripalmitate (tripalmitin, purity $\geq 85\%$, melting point 66°C), sodium deoxycholate and polyoxyethylenesorbitan monolaurate (Tween[®] 20) were obtained from Sigma–Aldrich (Spain) and soya lecithin (Lipoid S100) from Lipoid (Ludwigshafen, Germany). Glycerol bibehenate (Compritol[®] 888 ATO; m.p. 70°C) and glycerol palmitostearate (Precirol[®] 5 ATO; m.p. 56°C) were a kind gift from Gatefossé (Lyon, France). Distilled water was of Milli-Q quality (Millipore, Bedford, MD, USA). All other reagents were of analytical grade and were used without further purification.

2.2. Solubility of tetraoxanes in the lipid matrix

A preliminary solubility study of tetraoxanes **23** and **24** in molten tripalmitin, Compritol[®] 888 ATO or Precirol[®] 5 ATO was performed following a procedure described elsewhere, with slight modifications [13]. Briefly, the tetraoxanes were melted at a temperature 10°C above their respective melting point in a controlled temperature water bath. Small amounts of the solid lipids were then successively added until the tetraoxanes were completely dissolved in the lipid. Each determination was carried out in triplicate ($n=3$).

2.3. Preparation of SLN

The SLN were prepared by emulsion solvent evaporation method using tripalmitin as the lipid component and sodium deoxycholate, Tween[®] 20 and soya lecithin as cosurfactants [8]. Briefly, tripalmitin and lecithin were dissolved in dichloromethane - organic phase (1 mL) - and then added to the aqueous phase (5 mL) containing the Tween[®] 20 and sodium deoxycholate. The dispersion step was performed during a 3 min period of sonication (Branson Sonifier 250, Danbury, USA). Afterwards, this dispersion was homogenized for 5 min at 125,000 rpm using a Silverson HighSpeedMixer L4RT (Silverson Machines, Chesham, UK). The nanoparticles dispersion was then kept under stirring for overnight at room temperature until complete evaporation of the dichloromethane. Tetraoxanes **23** (3 and 5 mg) and **24** (3 and 5 mg) were incorporated to the organic phase.

2.4. SLN characterization

2.4.1. Measurement of particle size and zeta potential

SLN mean diameter (\emptyset) and polydispersity index (PdI) were determined by quasi-elastic laser light scattering in a Malvern Zetasizer 2000 (Malvern Instruments; UK). The surface charge (zeta potential, ζ) was determined by laser Doppler anemometry in a Zetasizer 2000 (Malvern Instruments, UK). All samples were measured with $n=3$. Samples were diluted appropriately with purified water for the measurements. The data was recorded and analyzed using the Zetasizer Software, 7.11 (Copyright[®] 2002-2014 Malvern Instruments Ltd.).

2.4.2. Determination of tetraoxanes encapsulated in SLN

The amount of tetraoxanes encapsulated in SLN was dosing by UV/Vis spectrophotometry (FLUOstar Omega, BMG Labtech). The analysis was performed by UV detection at a fixed wavelength of 262 and 260 nm for tetraoxanes **23** and **24**

respectively. For both tetraoxanes standard curves were constructed with five different concentrations (see examples in figure 1)

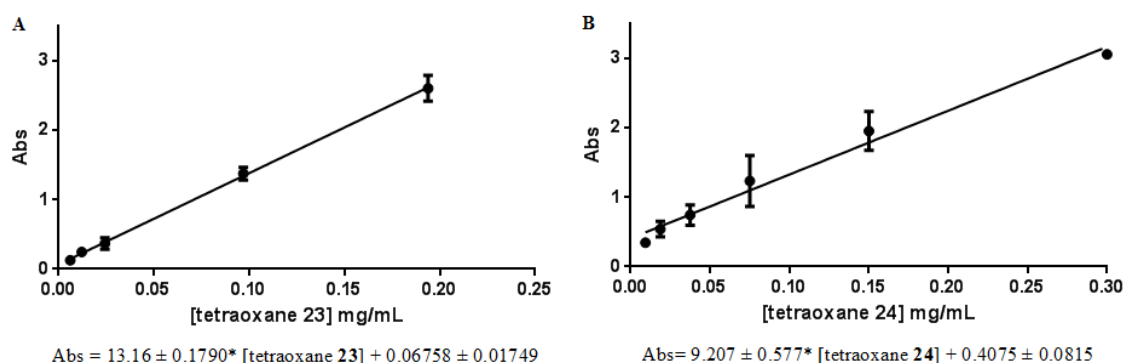


Figure 1- (A) Calibration curve for the estimation of tetraoxane **23** by UV/Vis spectrophotometry at 262 nm ($n=3$). (B) Calibration curve for the estimation of tetraoxane **24** by UV/Vis spectrophotometry at 260 nm ($n=3$).

2.4.3. Encapsulation efficiency and drug loading

After preparation, non-incorporated tetraoxanes were separated from the SLN dispersion by size exclusion chromatography in a PD-10 column (Bio-Rad Laboratories, California, USA) and the amount of incorporated tetraoxanes inside the SLN was quantified by ultraviolet/visible spectrophotometry (UV/Vis), using the method described above (section 2.4.2.). The encapsulation efficacy (EE) and drug loading capacity (DL) were determined using the following equations:

$$EE (\%) = \frac{\text{Amount of Tetraoxane encapsulated in SLN}}{\text{Initial amount of Tetraoxane}} \times 100$$

$$DL (\%) = \frac{\text{Amount of Tetraoxane encapsulated in SLN}}{\text{Amount of Tripalmitin}} \times 100$$

2.5. Stability studies

Stability of SLN suspensions was evaluated in different conditions: at $4\pm 3^{\circ}\text{C}$ and after sterilization in autoclave (121°C , 15 min).

2.5.1. Stability in suspension

The SLN suspensions were stored at 4°C for at least 20 days and mean particle diameter, PDI and zeta potential were determined. Stability evaluation was also performed in terms of drug loading after separation of non-incorporated tetraoxanes by size exclusion chromatography (please refer to section 2.4.3.).

2.5.2. Effect of sterilization

The SLN formulations were divided into two aliquots of equal volume after preparation. One aliquot was autoclaved at 121°C for 15 min while the other one (reference) was kept at 4°C for comparative evaluation of physical properties (particle diameter, PDI, zeta potential and DL).

2.6. Differential scanning calorimetry (DSC) studies

Measurements were performed on a calorimeter DSC Q200 (TA Instruments, DE, USA). Amounts between 3 and 15 mg of SLN dispersions and bulk materials (tripalmitin, lecithin, tetraoxanes, Tween[®] 20 and sodium desoxycholate) were weighted into aluminium pans, which were hermetically sealed and then measured against an empty reference pan. The pan was heated and the thermograms were recorded at temperature range from -20 to 250°C at a heating rate of $10^{\circ}\text{C}/\text{min}$. The heat flow was measured.

2.7. Dynamic light scattering (DLS) studies

The influence of temperature on the physical stability of SLN suspensions was assessed using DLS (Zetasizer Nano S; Malvern Instruments, UK). Samples were appropriately diluted with purified water in a quartz cell and particle size analysis was performed while heating the sample from 25°C up to 90°C at a rate of 0.5°C/min and subsequently followed by cooling from 90°C to 25°C at a rate of 0.5°C/min. Particle size measurements were made every 0.5°C. For each sample, measurements were carried out in triplicate ($n=3$).

2.8. Transmission electron microscopy (TEM)

SLN morphology analysis was made by transmission electron microscopy using a Hitachi H-8100 (Japan) microscope equipped with a energy dispersive spectroscopy X-ray (EDS) microanalysis system with light elements detector - ThermoNoran (USA). An aliquot of the SLN suspension was applied on a copper grid and dried at room temperature. Analyses of TEM were held at Instituto Superior Técnico of Lisbon University.

2.9. In vitro Release Study

A 50 μL aliquot of purified SLN was dispersed in 950 μL phosphate-buffered saline (PBS) buffer, pH 7.4, and a 100 μL aliquot of purified SLN was dispersed in 900 μL of hydrochloric acid (HCL) buffer, pH 1.0. Three samples in individual Eppendorf tubes were used for each time point studied – 0.0 h, 0.5 h, 1.0 h, 1.5 h and 2.0 h. Empty SLN was the assay reference. The tubes were kept in an incubator with stirring at a temperature of 37°C. At the predetermined time points, the solutions were centrifuged at 18000 rpm at 4°C. The supernatant was removed and the loaded SLN in the pellet were lysed with 500 μL of ACN. The amount of non-released tetraoxane compounds was quantified by the method described in section 2.4.2. This amount was subtracted to the initial known loaded amount in order to calculate the real released tetraoxane.

2.10. Cell viability study

Cell viability was assessed after 24 h and 48 h incubation of THP-1 cells (human acute monocytic leukaemia cell line) with different concentrations of free tetraoxanes (0.03–500 µg/mL) in RPMI medium with 2% of dimethyl sulfoxide (DMSO). After incubation time at 37°C, with 5% CO₂, cells were exposed to a 20 µL of 3-(4,5-dimethylthiazol-2-yl)-5-(3-carboxymethoxyphenyl)-2-(4-sulfophenyl)-2H-tetrazolium (MTS) + phenazine methosulfate (PMS) solution for 3 h at 37°C. The MTS is converted, by living cells, into a dark, water insoluble, blue formazan product. The plates were transferred to the microplate reader (Tecan infinit N200, Tecan, Austria) to measure the absorbance of the solution, at 630 nm and 490 nm. Cell viability (%) was calculated and compared with the untreated control.

2.11. In vitro activity studies

The *in vitro* activity studies were performed according to the method described by Babu LT *et al.* [14]. Both the free tetraoxanes and their respective SLN formulations were incubated for 48 h with *L. infantum* infected THP-1 cells at different concentrations – 1.6-25 µg/mL. As positive control was used Triton 1%. After the incubation time, cells were exposed to a 20 µL of MTS + PMS solution for 3 h at 37°C. The MTS is converted, by living cells, into a dark, water insoluble, blue formazan product. The plates were transferred to the microplate reader (Tecan infinit N200, Tecan, Austria) to measure the absorbance of the solution, at 630 nm and 490 nm. Parasite viability (%) was calculated and compared with the untreated control.

3. Results and discussion

3.1. Development of SLN formulations as carriers for tetraoxanes 23 and 24

Although several methodologies, for SLN preparation, could be applied to tetraoxane nanoencapsulation, the emulsion-solvent evaporation technique was selected. This method involves the utilization of an organic solvent, which is of major relevance not only in terms of the rising importance of “green chemistry”, but mainly because organic solvents should be avoided for safety concerns. This choice was mainly due to the solubility testing of the tetraoxanes **23** and **24** in three solid lipids previously studied in our research group (tripalmitin, Compritol® 888 ATO and Precirol® 5 ATO), which revealed that only tetraoxane **24** was soluble in tripalmitin (≤ 0.32 w/w), while compound **23** was not soluble in the lipids tested. At this point the potentially more suitable method (hot high-shear homogenization) was excluded because it involves, as a critical step, the dissolution of the tetraoxanes in the lipid, at high temperatures, for subsequent emulsification.

As this could not be performed, the emulsion-solvent evaporation method was used as an alternative. As mentioned above, tripalmitin and the tetraoxanes were dissolved in dichloromethane and the resulting mixture was emulsified in an aqueous solution of the surfactants. Dichloromethane is a good solvent for both the tetraoxanes and the lipids. Particles were formed upon dichloromethane evaporation. Although the process has the advantage of being performed at room temperature, dichloromethane is a class 2 solvent for which the maximum residual concentration allowed in final medicinal products is 600 ppm [15]. Nevertheless, previous NMR studies confirmed that the final dichloromethane residues in nanoparticles are well below 600 ppm [16].

So, the SLN formulations were prepared using the emulsion solvent evaporation method with tripalmitin as the lipid component. For this method there were fewer restrictions concerning the choice of the lipid, but tripalmitin appeared as the right choice because tetraoxane **24** can be dissolved in this well studied lipid in SLN formulations [8].

The protocol was carefully optimized before the present study because the selection of the surfactant system is of great importance for the preparation of SLN in order to maintain the colloidal state of the formulation during storage and upon administration [17].

Previous works showed that Tween[®] 20 - non-ionic surfactant - alone or in combination with lecithin does not provide the desired particle size and PdI ranges [14,17]. Therefore, the inclusion of sodium deoxycholate - ionic co-surfactant – is essential for particle stabilization and preparation of SLN with a low particle size of about 100–130 nm and a narrow PdI of about 0.2. Tween[®] 20 should contribute for the reduction of the surface tension, which enables the internal phase dispersion during the emulsification step and participates in the coverage and stabilization of newly formed surfaces [14,17]. The inclusion of lecithin enables concentration-dependent particle size reduction. Increasing the amount of lecithin is also an important factor for the stabilization process and thus preventing particle aggregation due to uncovered lipid surfaces. Lecithin's influence on particle size was already described in the literature [8,15,17]. However, the amount of surfactant available may be not sufficient to cover and stabilize all particle surfaces if the concentration in tripalmitin is extremely high, because this would lead to an increase of surface area due to an increase in the number of particles. In this case higher amounts of surfactants would be necessary to stabilize the SLN or larger particles and more heterogeneous particle populations will be formed.

3.2. Characterization of SLN formulations

For the preparation of tetraoxane-containing SLN all the parameters studied were compared with empty-SLN. The qualitative composition of **SLN 23** and **SLN 24** formulations are showed in Table 1.

Table 1- Composition of **SLN 23** and **SLN 24** formulations

Formulation	Tetraoxane (mg)		Lipid (mg)		Surfactants (% , v/v)	
	23	24	Tripalmitin	Lecithin	Sodium deoxycholate	Tween [®] 20
1	5	5	50	3.6	0.6	0.5
2	3	3	50	3.6	0.6	0.5

Both tetraoxanes were successfully incorporated in the SLN with an EE \geq 44% (w/w). The characterization of formulation 1 is showed in table 2 for **SLN 22** and **SLN 24**.

Table 2- Characterization of formulation 1 for SLN 23 and SLN 24 (mean \pm SD, $n=3$). **EE-** encapsulation efficacy; **DL-** loading capacity; **Ø-** mean particle diameter; **PdI-** polydispersity index; **ζ-** zeta potential.

Formulation	EE (%)	DL (%)	Ø (nm)	PdI	ζ (mV)
Empty SLN	-	-	123 \pm 1	0.28 \pm 0.01	-23 \pm 1
SLN 23	58 \pm 4	6.17 \pm 0.38	113 \pm 2	0.25 \pm 0.01	-16 \pm 1
SLN 24	44 \pm 5	5.09 \pm 0.54	144 \pm 1	0.46 \pm 0.01	-18 \pm 1

Although EE for both molecules was lower than expected for lipophilic drugs (logP = 3.96 for compound **23** and 4.35 for compound **24**) the formulations presented particle mean diameters and PdI within the values described in the literature for this lipid matrix and preparation method [8], except for **SLN 24**, which presented a PdI higher than desired (Table 2). Concerning zeta potential, the magnitude of the surface charge decreased when the tetraoxanes were introduced in the formulation, suggesting the drugs may be at least partially located at the SLN surface. These values (ca. -16 and -18 mV) are below the ideal threshold to ensure the physical stability of colloidal dispersions, and may be responsible for some aggregation, thus resulting in higher PdI values (0.46 for the **SLN 24**). A minimum zeta potential of \geq -60 mV is required for excellent and \geq -30 mV for a good physical stability [9]. Nevertheless, in combination with a steric stabilizing effect of Tween[®] 20, the obtained values may still be enough for ensuring physical stability and desirable for macrophage targeting [9,16,21,22].

As an attempt to improve the EE of both compounds a new SLN formulation (formulation 2) was developed with lower amounts of each tetraoxane for the same quantity of tripalmitin, i.e. the initial drug:lipid ratio was changed from 3.0:10 to 1.6:10 for both compounds **23** and **24**. Taking into consideration the low EE of the previous formulations (EE <44%), these modifications intended to reduce drug waste. This alteration improved EE to values \geq 87% (w/w), thus yielding DL values similar to those of obtained with the previous formulations (Table 3). The new composition resulted in similar physical characteristics, including a slightly higher mean particle diameter for **SLN 23** and a lower

PdI. In both cases the surface charge resulted in more negative values, more compatible with stable colloidal dispersions, and more desirable for macrophage targeting (Table 3).

Table 3- Characterization of formulation 2 for **SLN 23** and **SLN 24** (mean \pm SD, $n=3$). **EE**- encapsulation efficacy; **DL**- loading capacity; **\emptyset** - mean particle diameter; **PdI**- polydispersity index; **ζ** - zeta potential.

Formulation	EE (%)	DL (%)	\emptyset (nm)	PdI	ζ (mV)
Empty SLN	-	-	123 \pm 1	0.28 \pm 0.01	-23 \pm 1
SLN 23	87 \pm 3	5.22 \pm 0.18	118 \pm 1	0.25 \pm 0.01	-21 \pm 1
SLN 24	88 \pm 3	5.31 \pm 0.20	125 \pm 2	0.26 \pm 0.01	-23 \pm 1

The mean particle diameter of **SLN 23** was consistently lower with those of empty SLN and **SLN 24**, which is in agreement with the fact that this tetraoxane is not soluble in tripalmitin, recrystallizing upon solvent evaporation and staying mainly entrapped within the lipid matrix. It should be noticed that tripalmitin presents a purity degree of only 85%, thus forming less perfect crystals, with many imperfections that allow to accommodate tetraoxane **23** crystals [21,22].

In the case of **SLN 24**, the tetraoxane is soluble in tripalmitin. Therefore, the presence of certain amount of drug in the lipid matrix will produce an increase in particle size compared to empty SLN.

These SLN formulations containing ca. 6% (w/w) of drug were then submitted to further characterization studies using techniques such as DLS, DSC, TEM, *in vitro* release studies and cell viability and *in vitro* activity studies with THP-1 cells.

3.3. TEM study

In order to get information about the morphology of the SLN and also confirm the particle size distribution, the SLN were analyzed by TEM (Figure 2). The images demonstrate that both SLN formulations consist of spherical nanoparticles. The diameter average particle slightly decreased which is normal due to the dry process before the analysis. **SLN 24** seems to have tendency to aggregate while **SLN 23** are apparently widely dispersed.

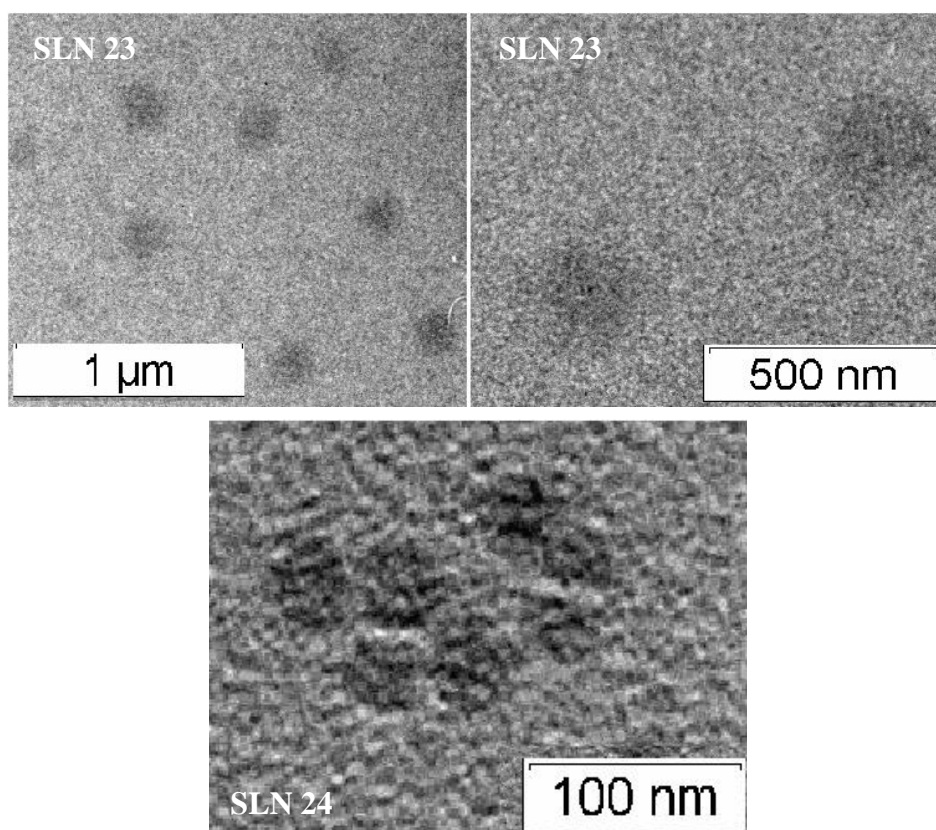


Figure 2- SLN formulations photos obtained by TEM.

3.4. DSC study

Thermograms were set between -20°C and 240°C . Figure 3 shows 0°C as starting temperature because data between -20°C and 0°C was thought irrelevant for the analysis. The thermogram of pure tripalmitin showed a melting peak of 63°C . Similarly, the thermogram of pure tetraoxane **23** shows a distinguished peak at about 135°C , whereas tetraoxane **24** showed a sharp melting endotherm at approximately 100°C (Figure 3). Both endotherm peaks are in agreement with the melting points reported in chapter 2.

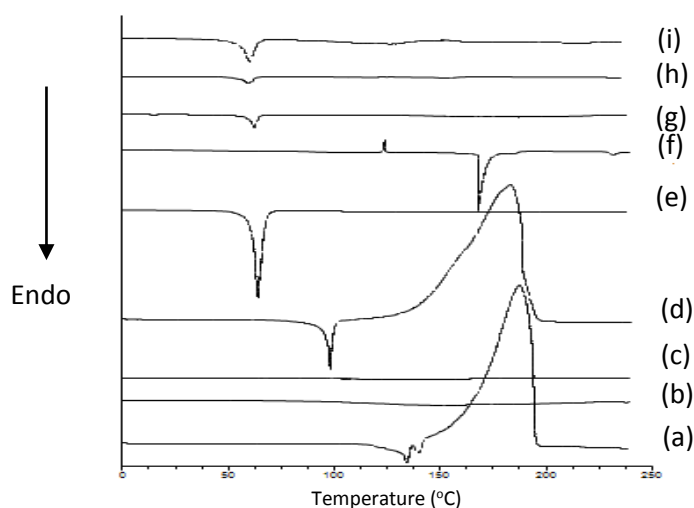


Figure 3- DSC thermograms of bulk samples. (a) free tetraoxane **23**; (b) lecithin; (c) Tween[®] 20; (d) free tetraoxane **24**; (e) tripalmitin; (f) sodium deoxycholate; (g) empty SLN; (h) **SLN 24** and (i) **SLN 23**.

However, thermograms of both freeze-dried **SLN 23** and **SLN 24** preparations did not show the melting peak of their respective tetraoxanes, but only that of the lipid. The absence of tetraoxanes melting in the SLN thermograms can be assigned to the amorphous or molecularly dispersed structure of both tetraoxanes in the lipid matrix. It may also be due to the low drug:lipid ratio of the formulations. In all formulations, the melting point of tripalmitin was depressed (61.5°C for empty SLN; 60.7°C for **SLN 23**; 61.0°C for **SLN 24**) when compared to the melting point of the bulk lipid (64.0°C).

To understand this effect it is important to recognize that for less ordered crystals or amorphous solids, the melting of the substance requires much less energy than crystalline substances that need to overcome lattice forces. This same effect was reported before by Lopes *et al.* [8] and was attributed to the creation of lattice defects onto the lipid matrices following a decrease in crystallinity in comparison to their bulk counterparts. Another explanation for this phenomenon of melting point depression might also be related to the small particle size - nano scale – which means that their surface area or the presence of surfactants significantly increases [24,22,26]. Therefore and in spite of the observed reduction on tripalmitin's melting point in the SLN, no significant effect was observed on lipid matrix thermal behaviour pattern after tetraoxane's incorporation.

3.5. Physical stability

The ability of the SLN to retain the incorporated tetraoxanes and to keep their physicochemical properties during storage was assessed at 4°C during 20 days. The stability of SLN **23** and SLN **24** was evaluated in terms of particle mean diameter, PDI and surface charge (Table 4).

Table 4- Characterization of formulation 2 for SLN **23** and SLN **24** after 20 days at 4°C (mean±SD, n=3). Ø-mean particle diameter; PDI- polydispersity index; ζ- zeta potential.

Formulation	Ø (nm)	PDI	ζ (mV)
Empty SLN	121±1	0.27±0.01	-23±1
SLN 23	122±3	0.26±0.01	-21±2
SLN 24	124±4	0.26±0.03	-20±1

No relevant changes were observed on mean particle diameter, PDI and surface charge for empty SLN or for SLN **23** and SLN **24**. The SLN dispersions were physically stable during 20 days at 4°C.

However, it is important to assess whether the preparations may stand further harsh pharmaceutical processing involving drastic conditions such as high temperatures and pressures. Therefore, SLN **23**, SLN **24** and empty SLN were submitted to autoclaving at 121°C/15 min, i.e., the most common moist heat terminal sterilization process, and the effects on mean particle diameter and PDI, surface charge and DL were assessed (Table 5).

Table 5- Characterization of formulation 2 for SLN **23** and SLN **24** after sterilization by autoclaving (mean±SD, n=3). DL- loading capacity; Ø- mean particle diameter; PDI- polydispersity index; ζ- zeta potential.

Formulation	DL (%)	Ø (nm)	PDI	ζ (mV)
Empty SLN	-	80±1	0.24±0.01	-27±1
SLN 23	0.39±0.04	91±1	0.24±0.01	-20±1
SLN 24	1.96±0.98	92±2	0.24±0.01	-21±1

After sterilization by autoclaving the mean particle diameter decreased slightly, thus confirming the results of the DLS studies (section 3.6.). PDI and surface charge remain unchanged. However the DL decreased more than 90% for **SLN 23** and almost 65% for **SLN 24**. Tripalmitin presents a melting point of about 66°C, so the SLN lipid core will melt during the autoclaving and will recrystallize during cooling. This phenomenon is responsible for the significant reduction of DL, mainly in the case of **SLN 23**, where the tetraoxane is not soluble in tripalmitin. So when the lipid core melts the majority of tetraoxane **23** disperses because this compound never truly mixes with tripalmitin and at the time of lipid recrystallization the absence of DCM prevents the formation of an emulsion. Therefore, the drug tends to partition into, or even precipitate in the aqueous phase. Concerning tetraoxane **24**, the DL also decreases in spite of its solubility in tripalmitin, probably due to drug to partition of the drug into the aqueous phase. Both formulations did not stand sterilization by autoclaving, showing their instability by the significantly decrease of DL. For this reason, these formulations are only suitable for oral administration.

Throughout this process, particle stability is highly dependent on the composition of the SLN formulation, particularly the stabilizing surfactants that surround the lipid core [19, 20].

3.6. DLS study

The effect of temperature on the mean particle diameter was evaluated by DLS (Figure 4). **SLN 23** shows an initial increase in particle size, about 20 nm in the first 5°C of heating reaching a maximum of 146 nm. The mean particle diameter remains stable until it decreased at the melting point of tripalmitin.

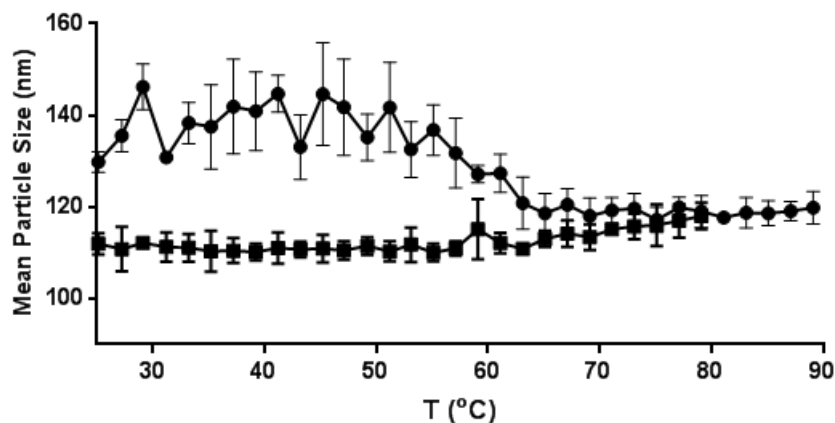


Figure 4- Variation of the average diameter of **SLN 23** formulation: (●) 25-90°C and (■) 90-25°C (mean±SD, $n=3$).

This is the same phenomenon during sterilization by autoclaving. The melting of tripalmitin enabled the loss of tetraoxane **23**, reducing the SLN size. Another baseline was observed from the melting temperature of tripalmitin up to 90°C. In the cooling phase, the mean particle diameter suffers a slight variance, but never recovered the original starting mean particle diameter because of the losses of tetraoxane compound during the melting of tripalmitin and its recrystallization.

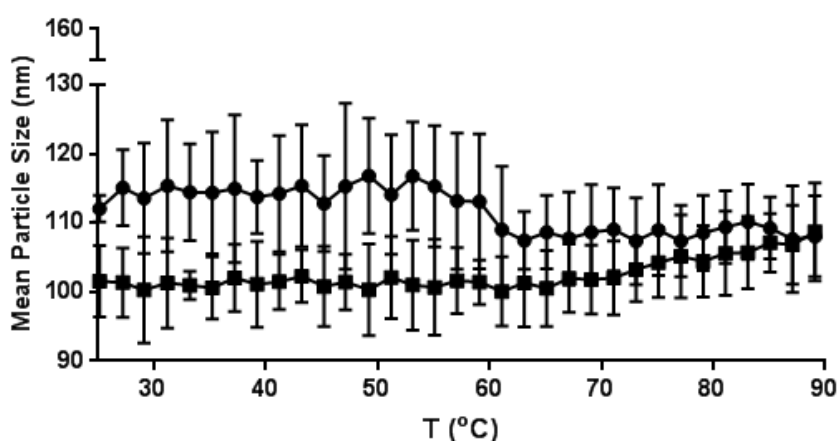


Figure 5- Variation of the average diameter of **SLN 24** formulation: (●) 25-90°C and (■) 90-25°C (mean±SD, $n=3$).

Although the SLN 24 formulation has shown a similar behavior, when compared to **SLN 23**, the initial mean particle diameter increase was almost insignificant, reaching a maximum of 125 nm (Figure 5). There was also a decrease due to with the melting of

tripalmitin. In the cooling phase the initial particle size was not recovered, although it was less evident than that observed with **SLN 23**, because tetraoxane **24** is soluble in tripalmitin. So when this lipid recrystallizes, a larger amount of compound **24** stays within the nanoparticle. As expected this formulation was thermally more stable, with mild changes of the mean particle diameter.

3.7. *In vitro* Release study

Since the major objective of the SLN preparation was to achieve optimal formulations for future oral administration, drug release was study, as well as formulation stability under physiological pH and stomach pH. As the formulations have as their major targets both the spleen and the liver macrophages, release studies were carried out in order to assess whether the two synthesized tetraoxanes remained inside the SLN between the time of administration and the organs referred before. As both tetraoxanes are hydrophobic molecules, a diffusional release profile was thought as improbable, so most of the drugs would remain inside the SLN as their affinity for the lipophilic tripalmitin matrix was theoretically higher.

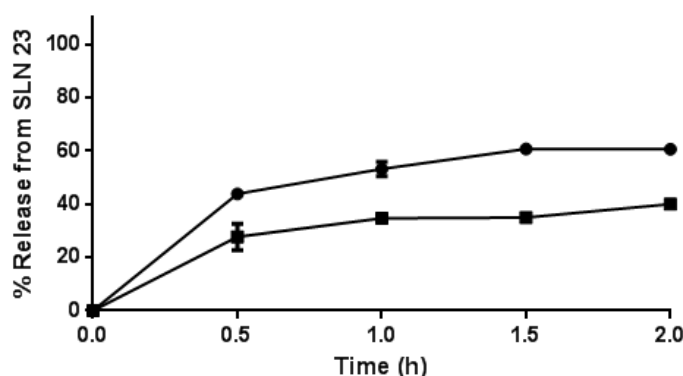


Figure 6- Release studies of **SLN 23** dispersed in aqueous buffers of different pH: (●) release at pH 7.4 and (■) release at pH 1.0 (mean±SD, n=3).

The release profiles of tetraoxane **23** from the SLN formulation at both pH values presented the same trend (Figure 6). However, at pH 1.0 the **SLN 23** is apparently more stable, releasing about 15% less than at neutral pH. In this case drug release reaches a maximum of 40%, while at pH 7.4 about 60% of drug were released. Drug release is slow

in both media, with no burst effect. Nevertheless, release acidic medium shows that **SLN 23** is not gastroresistant, an important feature if the formulation is intended for oral administration. This release study also shows that although not being soluble in tripalmitin, tetraoxane **23** remains entrapped inside the lipid matrix because of its hydrophobic chemical structure. However, there is room for formulation improvement if these SLN are intended for oral administration.

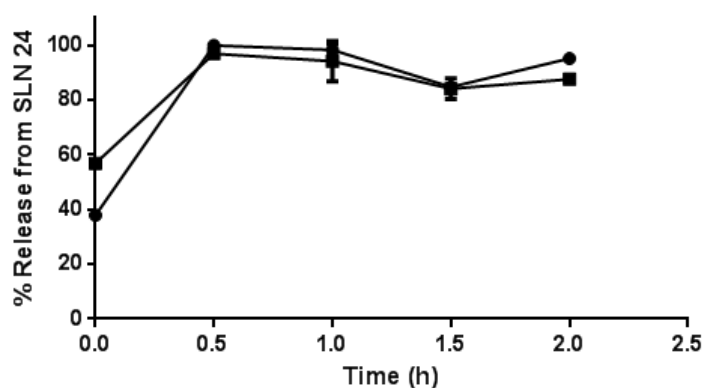


Figure 7- Release studies of **SLN 24** dispersed in aqueous buffers of different pH: (●) release at pH 7.4 and (■) release at pH 1.0 (mean±SD, $n=3$).

On the other hand, the release profile (Figure 7) of tetraoxane **24** is quite different that of **23**. In this case, a burst release of about 50% was observed in both media and after 30 min all drug was released from the SLN. So the **SLN 24** seemed to be much less stable than the **SLN 23** at the pH values herein studied. This was unexpected because their different solubility in tripalmitin would predict that the majority of compound **24** would remain entrapped inside the nanoparticle matrix. As for compound **23** this formulation is not gastroresistant, requiring further optimization towards stability in aqueous media in order to maintain the initial drug loading upon oral administration.

Briefly, after the administration, almost entirely the content of the compound **24** inside the SLN vehicle is lost before it reaches the spleen and/or liver macrophages.

3.8. Cell viability studies

In vitro cell viability studies are essential in the development of suitable formulations, particularly considering they will submit to *in vivo* studies by the oral route in a suitable therapeutic animal model of leishmaniasis. Since human-monocyte transformed macrophages are one of the most widely used models for testing drugs against leishmaniasis, the cytotoxicity of the synthesized tetraoxanes **23** and **24** was evaluated against THP-1 cells - human acute monocytic leukaemia cell line. The cytotoxicity of empty SLN as well as **SLN 23** and **SLN 24** were not tested since recently Lopes *et al.* [8] studied the effect of similar SLN formulations on the viability of THP-1 cells. The empty SLN and drug-loaded SLN used in that study had the same lipid and surfactant composition as those SLN presented in this work. These authors concluded that both empty SLN and drug-loaded SLN were non-cytotoxicity, demonstrating a rather protective role of SLN formulations to the mammalian cells. Therefore, in the present work cell viability studies were performed only with both tetraoxanes, since empty SLN have already been proved as non-cytotoxic towards THP-1 cells at the concentrations herein tested. Figure 8 shows the survival percentage of THP-1 cells at 24 h after treatment with different concentrations of both tetraoxanes **23** and **24**.

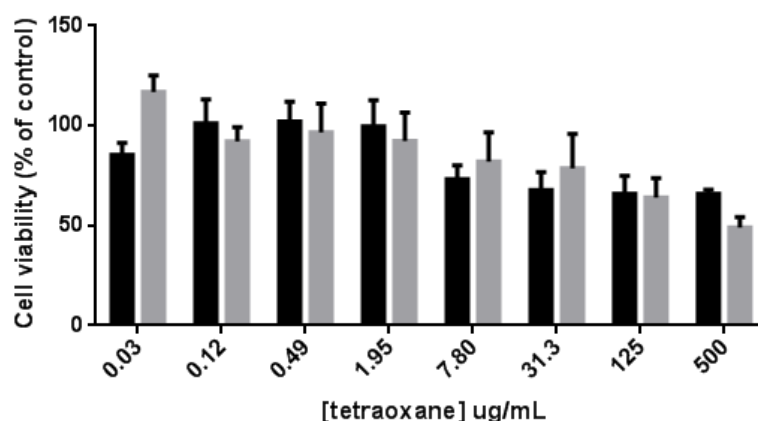


Figure 8- Cellular viability of THP-1 cells after 24 h of incubation with different concentrations of both free compounds **23** and **24**: (■) tetraoxane **23** and (▒) tetraoxane **24** (mean±SD, n=3).

Both compounds are non-toxic for THP-1 cells at tested concentrations when incubated for 24 h. In both cases the cell viability is always above 50% which corresponds to $EC_{50} >$

500 $\mu\text{g/mL}$. Nevertheless the two compounds seem to start decrease cell viability consistently at 7.80 $\mu\text{g/mL}$.

The survival percentage of THP-1 cells was also evaluated at 48 h after treatment with the tetraoxanes in study at the same range of concentrations as the previous assay (Figure 9).

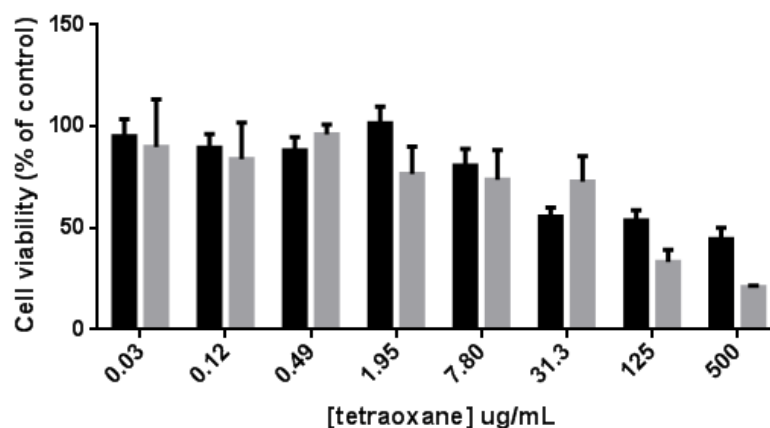


Figure 9- Cellular viability of THP-1 cells after 48 h of incubation with different concentrations of both free compounds **23** and **24**: (■) tetraoxane **23** and (▒) tetraoxane **24** (mean \pm SD, $n=3$).

After 48 h of incubation tetraoxane **24** appears to be more toxic when compared with compound **23**. Both compound showed be toxic to THP-1 cells at 125 $\mu\text{g/mL}$ where the cell viability is for the first time below 50%. Similarly to the effect at 24 h, THP-1 cell viability starts to decrease above 7.80 $\mu\text{g/mL}$. At 48 h compounds **23** and **24** had EC_{50} values of 73.0 $\mu\text{g/mL}$ and 65.0 $\mu\text{g/mL}$, respectively. The EC_{50} values are summarized in Table 6.

Table 6- Cellular toxicity of free tetraoxanes **23** and **24** at different incubation times.

Compound	Incubation time (h)	EC_{50} ($\mu\text{g/mL}$)
23	24	> 500
	48	73.0
24	24	> 500
	48	65.0

3.9. *In vitro* activity studies

Tetraoxane-loaded SLN and free-tetraoxanes were evaluated *in vitro* for their antileishmanial activity, against the *L. infantum* intracellular form, using infected macrophages. The results were compared to the standard antileishmanial drug miltefosine. As positive control (lysis of all cells) Triton-X-100 (1%) was used, and as negative control were used non-treated infected THP-1 cells with *L. infantum* parasites. The insoluble free tetraoxanes were solubilized using DMSO as a co-solvent to avoid precipitation in the cell medium. The SLN formulations were incubated without any co-solvent which is a considerable advantage when we want to maintain the cell assays as real as possible and without the interference of organic solvents.

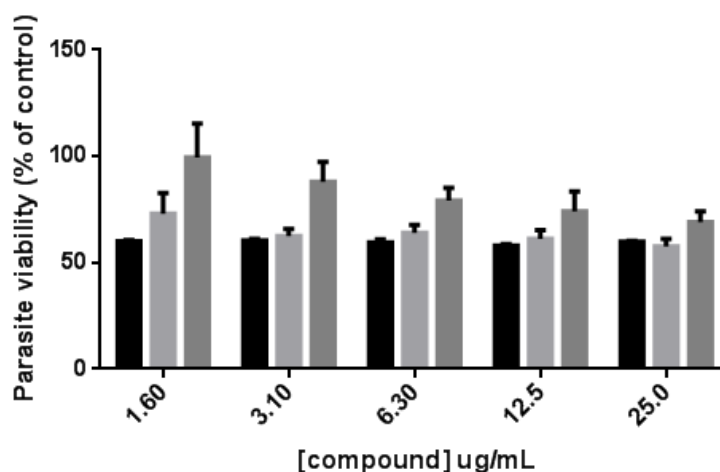


Figure 10- Activity against *L. infantum* parasite of the free tetraoxanes **23** and **24** when compared with miltefosine after 48 h of incubation: (■) miltefosine; (▨) tetraoxane **23** and (▩) tetraoxane **24** (mean±SD, n=3).

Figure 10 shows the activity of the synthesized tetraoxanes against the *L. infantum* parasite and the comparison with miltefosine. At the studied concentrations miltefosine kills always about 60% of the parasites. Tetraoxane **23** has an initial activity a little less potent than miltefosine but above 3.10 $\mu\text{g/mL}$, its activity is about 60%, i.e. the same activity of the standard antileishmanial drug miltefosine, thus showing a very promising *in vitro* activity against *L. infantum* parasite.

The free form of compound **24** demonstrated less potency for the tested concentrations when compared with both tetraoxane **23** and miltefosine. Its activity is still increasing

throughout the concentration range tested, which means that it did not yet reach a plateau. Therefore, higher concentrations of this compound could be even more potent than its counterpart and miltefosine.

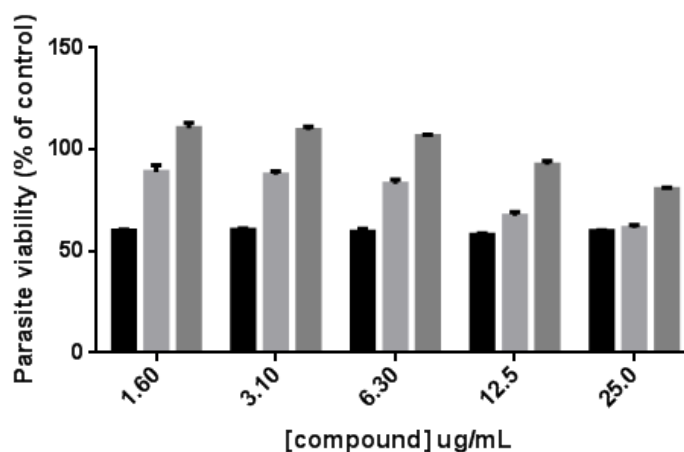


Figure 11- Activity against *L. infantum* parasite of SLN 23 and SLN 24 when compared with miltefosine after 48 h of incubation: (■) miltefosine; (▨) SLN 23 and (▩) SLN 24 (mean±SD, n=3).

Figure 11 shows the activity against *L. infantum* parasite of the nanoencapsulated tetraoxanes **23** and **24**. Neither of SLN formulations stabilized into a baseline for tested concentrations, demonstrating they can be even more potent than the free form compounds if further concentrations had been tested.

For the same concentrations both formulations showed to be less potent than the respective free drugs. Compound **23** killed about 60% of the parasites at 3.10 µg/mL while a dose of 25.0 µg/mL was needed to achieve the same results for the SLN formulation. However, a 25 µg/mL dose of free tetraoxane only killed more 4% of the parasites, when compared with the same dosage of SLN 23, and more 2% when compared with miltefosine, which means that at the highest concentration tested (25 µg/mL) either the free compound **23** and SLN 23 have almost the same activity as an approved antileishmanial.

Formulation SLN 24 followed the same tendency of its free form, but was much less potent within the concentrations herein tested. At 25 µg/mL the parasite viability was about 80%, i.e. more 10% when compared to its free form, and more 30% compared with miltefosine.

SLN 23 showed a very good activity against *L. infantum* parasites being in fact the better formulation of the two. At 25 µg/mL this formulation has the same activity of the already approved drug miltefosine. The advantages when compared with its free form are the theoretical better targeting of the macrophages employed by the tripalmitin's nanosystems and the non-utilization of DMSO as co-solvent for solubilization because the two tetraoxanes compounds are hydrophobic and not suitable for any kind of administration by its free form. Additionally for incubation times longer than 24 h, when both free forms of the tetraoxanes are already cytotoxic, the SLN act as protective vehicles preventing cellular death and delivering the compounds to the site of action of the parasites.

Summing up, these are two very promising compounds with similar activity as antileishmanial when compared to miltefosine. **SLN 23** showed to be more potent at studied concentrations and its free form is also less toxic when incubated for longer than 24 h.

4. References

- [1] A. S. Nagle, S. Khare, A. B. Kumar, F. Supek, A. Buchynskyy, C. J. N. Mathison, N. K. Chennamaneni, N. Pendem, F. S. Buckner, M. H. Gelb, and V. Molteni, “Recent Developments in Drug Discovery for Leishmaniasis and Human African Trypanosomiasis”, *Chem. Rev.*, 114(22), 11305–47, 2014.
- [2] L. Monzote, “Current Treatment of Leishmaniasis:”, 1, 9-19, 2009.
- [3] V. Vanlerberghe, G. Diap, P. J. Guerin, F. Meheus, S. Gerstl, P. V. D. Stuyft, and M. Boelaert, “Drug policy for visceral leishmaniasis: A cost-effectiveness analysis”, *Trop. Med. Int. Heal.*, 12(2), 274–283, 2007.
- [4] T. P. C. Dorlo, M. Balasegaram, J. H. Beijnen, and P. J. de vries, “Miltefosine: A review of its pharmacology and therapeutic efficacy in the treatment of leishmaniasis”, *J. Antimicrob. Chemother.*, 67(11), 2576–2597, 2012.
- [5] F. Modabber, “Leishmaniasis vaccines: Past, present and future”, *Int. J. Antimicrob. Agents*, 36(1), 58–61, 2010.
- [6] R. H. Muller, K. Mader, and S. Gohla, “Solid lipid nanoparticles (SLN) for controlled drug delivery - A review of the state of the art”, *Eur. J. Pharm. Biopharm.*, 50(1), 161–177, 2000.
- [7] A. J. Almeida and E. Souto, “Solid lipid nanoparticles as a drug delivery system for peptides and proteins”, *Adv. Drug Deliv. Rev.*, 59(6), 478–490, 2007.
- [8] R. Lopes, C. V. Eleutério, L. M. D. Goncalves, M. E. M. Cruz, and A. J. Almeida, “Lipid nanoparticles containing oryzalin for the treatment of leishmaniasis”, *Eur. J. Pharm. Sci.*, 45(4), 442–450, 2012.
- [9] C. Freitas and R. H. Müller, “Effect of light and temperature on zeta potential and physical stability in solid lipid nanoparticle (SLN[®]) dispersions”, *Int. J. Pharm.*, 168(2), 221–229, 1998.
- [10] C. Freitas and R. H. Müller, “Correlation between long-term stability of solid lipid nanoparticles (SLNTM) and crystallinity of the lipid phase”, *Eur. J. Pharm. Biopharm.*, 47(2), 125–132, 1999.
- [11] W. Abdelwahed, G. Degobert, and H. Fessi, “Investigation of nanocapsules stabilization by amorphous excipients during freeze-drying and storage,” *Eur. J. Pharm. Biopharm.*, vol. 63, no. 2, pp. 87–94, 2006.
- [12] R. Cavalli, O. Caputo, M. E. Carlotti, M. Trotta, C. Scarnecchia, and M. R. Gasco, “Sterilization and freeze-drying of drug-free and drug-loaded solid lipid nanoparticles”,

Int. J. Pharm., 148(1), 47–54, 1997.

[13] D. P. Gaspar, V. Faria, L. M. D. Gonçalves, P. Taboada, C. Remuñán-López, and A. J. Almeida, “Rifabutin-loaded solid lipid nanoparticles for inhaled antitubercular therapy: Physicochemical and in vitro studies”, *Int. J. Pharm.*, vol. 497(1–2), 199–209, 2016.

[14] S. K. Jain, R. Sahu, L. a Walker, and B. L. Tekwani, “A parasite rescue and transformation assay for antileishmanial screening against intracellular *Leishmania donovani* amastigotes in THP1 human acute monocytic leukemia cell line”, *J. Vis. Exp.*, 70, 1–14, 2012.

[15] E. M. A. (EMA), “Note for guidance on impurities: residual solvents”, *EMA London, CPMP/ICH*, 283, 95, 2006.

[16] H. F. Florindo, S. Pandit, L. M. D. Gonçalves, H. O. Alpar, and A. J. Almeida, “Surface modified polymeric nanoparticles for immunisation against equine strangles”, *Int. J. Pharm.*, 390(1), 25–31, 2010.

[17] A. A. Mancini G, Lopes R, Clemente P, Raposo S, Gonçalves LMD, Bica A, Ribeiro HM, “Lecithin and parabens play a crucial role in tripalmitin-based lipid nanoparticle stabilization throughout moist heat sterilization and freeze-drying”, *Eur. J. Lipid Sci. Technol.*, 117, 1947–1959, 2015.

[18] H. Bunjes, M. H. J. Koch, and K. Westesen, “Influence of emulsifiers on the crystallization of solid lipid nanoparticles,” *J. Pharm. Sci.*, 92(7) 1509–1520, 2003.

[19] M. A. Schubert and C. C. Muller-Goymann, “Characterisation of surface-modified solid lipid nanoparticles (SLN): Influence of lecithin and nonionic emulsifier”, *Eur. J. Pharm. Biopharm.*, 61(1–2), 77–86, 2005.

[20] M. Üner and G. Yener, “Importance of solid lipid nanoparticles (SLN) in various administration routes and future perspective,” *Int. J. Nanomedicine*, 2(3), 289–300, 2007.

[21] B. Palla and D. Shah, “Stabilization of High Ionic Strength Slurries Using the Synergistic Effects of a Mixed Surfactant System”, 223(1), 102–111, 2000.

[22] D. K. Chou, R. Krishnamurthy, T. W. Randolph, J. F. Carpenter, and M. C. Manning, “Effects of Tween 20® and Tween 80® on the stability of Albutropin during agitation”, *J. Pharm. Sci.*, 94(6), 1368–1381, 2005.

[23] U. Ruktanonchai, U. Sakulkhu, P. Bejrappa, P. Opanasopit, N. Bunyapraphatsara, V. Junyaprasert, and S. Puttipipatkachorn, “Effect of lipid types on physicochemical characteristics, stability and antioxidant activity of gamma-oryzanol-loaded lipid

- nanoparticles”, *J. Microencapsul. Micro Nano Carriers*, 26, (7) 614–626, 2009.
- [24] K. Vivek, H. Reddy, and R. S. R. Murthy, “Investigations of the effect of the lipid matrix on drug entrapment, in vitro release, and physical stability of olanzapine-loaded solid lipid nanoparticles” *AAPS PharmSciTech*, 8(4), 83, 2007.
- [25] R. M. Lopes, M. L. Corvo, C. V. Eleutério, M. C. Carvalheiro, E. Scoulica, and M. E. M. Cruz, “Formulation of oryzalin (ORZ) liposomes: In vitro studies and in vivo fate”, *Eur. J. Pharm. Biopharm.*, 82(2), 281–290, 2012.
- [26] H. Bunjes and M. H. J. Koch, “Saturated phospholipids promote crystallization but slow down polymorphic transitions in triglyceride nanoparticles” *J. Control. Release*, 107(2), 229–243, 2005.
- [27] A. zur Mühlen, C. Schwarz, and W. Mehnert, “Solid lipid nanoparticles (SLN) for controlled drug delivery--drug release and release mechanism” *Eur. J. Pharm. Biopharm.*, 45(2), 149–155, 1998.
- [28] M. A. Schubert, B. C. Schicke, and C. C. Muller-Goymann, “Thermal analysis of the crystallization and melting behavior of lipid matrices and lipid nanoparticles containing high amounts of lecithin”, *Int. J. Pharm.*, 298(1), 242–254, 2005.

Chapter 4



Concluding remark and future work

Chapter 4 - Concluding remark and future work

1. Concluding remarks

Summarizing the chemical synthesis research work developed in this thesis, there are some concluding remarks to be noted. The two final compounds **23** and **24** were successfully synthesized and characterized by infrared spectroscopy, unidimensional – ¹H-NMR, ¹³C-NMR - and bidimensional NMR – COSY, HMBC, HMQC. Thereby, it was possible to identify all characteristic protons from the two tetraoxane compounds, such as the *trans*-vynilic protons, the aromatic protons as well as the protons of the tetraoxane ring. The elemental analysis study was in agreement with the calculated values and the melting points determined using two different techniques (the Ph. Eur. 2.2.16. instantaneous method and DSC) were similar.

Concerning the formulation research work, a proven stable SLN formulation was used, based on tripalmitin as the lipid component and three surfactants acceptable for administration - Tween[®] 20, soya lecithin and sodium desoxycholate. Either **SLN 23** or **SLN 24** presented suitable physicochemical properties (diameter, surface charge and polydispersity index) as well as high encapsulation efficiencies. Preliminary stability studies showed that SLNs could be stored at 4°C for at least 20 days without any change of their properties. The DSC analysis showed that both tetraoxanes are entrapped in the lipid matrix of the SLN. However, **SLN 24** is more stable under the effect of temperature, although but both formulations suffer recrystallization upon cooling below the melting point of tripalmitin, leading to a marked decrease in DL, as observed throughout autoclaving. Irrespective of the release medium tested, tetraoxane **24** is released at a faster rate and higher amount than tetraoxane **23**, probably due to the different structure of the lipid matrix resulting from the differences in solubility between both drugs. Finally, both tetraoxanes may be considered as non cytotoxic, while **SLN 23** showed a good *in vitro* activity against leishmania infected THP-1 cells, when compared with the standard antileishmanial drug miltefosine.

Overall, this strategy allowed achieving new compounds-loaded SLN that are promising candidates as antileishmaniasis agents.

2. Future work

As this work is a completely novel approach, with the introduction of tetraoxane compounds as potential dual acting agents in the treatment of leishmaniasis, including their nanoencapsulation in solid lipid particles, the upcoming work is still of great importance.

The introduction of other groups in the tetraoxane skeleton seems to be the next logical step in order to obtain structure variability and possible new interactions moieties with TR. This step will normally lead to the structure-activity relationship studies that must be made in order to understand which functions are essential to, or are able to improve the activity as TR inhibitor. After the tetraoxane activation (referred in chapter 1) the final α,β -unsaturated molecule, which acts as TR inhibitor, is the *trans*-cinnamaldehyde, therefore, is essential to assess the activity and cytotoxicity of this compound. It also can be performed docking studies in order to understand the interactions between the compounds and the enzyme.

The tetraoxane derived from the 2-adamantanone still needs to be synthesized because the literature refers that the adamantyl group gives stability to the final tetraoxane. It is important to explore new methodologies that enable the formation of the bishydroperoxide intermediate either in the 2-adamantanone or in the *trans*-cinnamaldehyde with a higher yield in the first step of the reaction.

A stable and promising antileishmaniasis SLN formulation of compound **23** was achieved. However, further optimizations are needed to increase drug loading, the stability under harsh formulation procedures and modulate drug release at both studied pH values while maintaining its physicochemical properties. Although **SLN 24** formulation is even more stable under temperature variations and after throughout autoclaving when compared with **SLN 23**, after 30 min tetraoxane **24** is completely released, indicating the need to improve this formulation towards gastroresistance. The optimization of all these crucial parameters may certainly involve the inclusion of different triacylglycerols and the investigation of liophilisation as a stabilizing technique that will allow increasing storage time of such formulations.

The next logical step in this area will be the *in vivo* studies to determine whether the SLN formulations remain active against *Leishmania* parasite or not, and if they act as vehicles through passive targeting, as they should carry and protect the tetraoxanes to the MPS. The

cell localization *in vitro* and *in vivo* can be confirmed using probes with fluorescent tags synthesized by the uprising bioorthogonal chemistry.

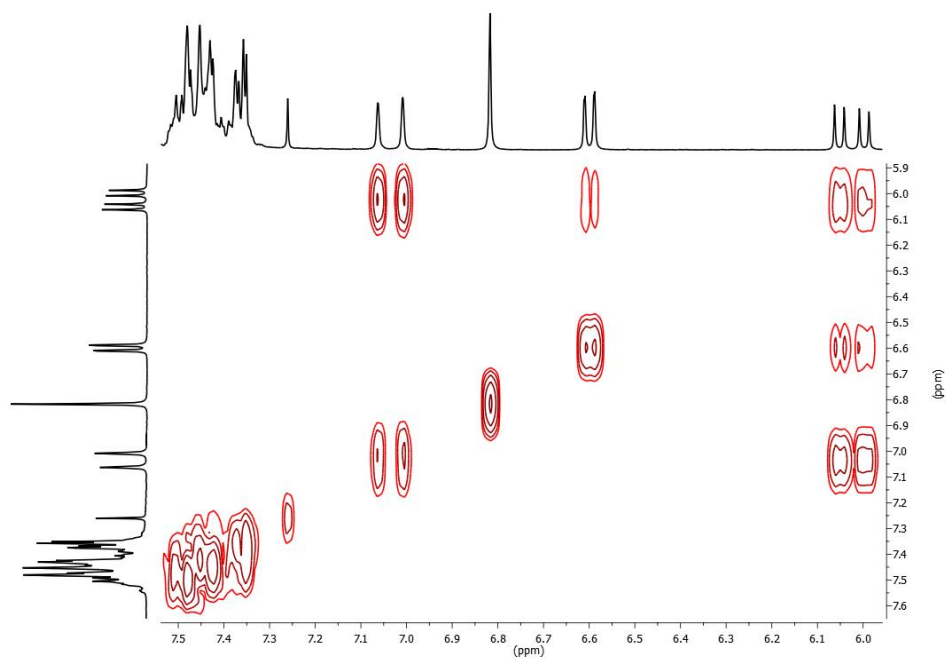
Chapter 5



Annexes

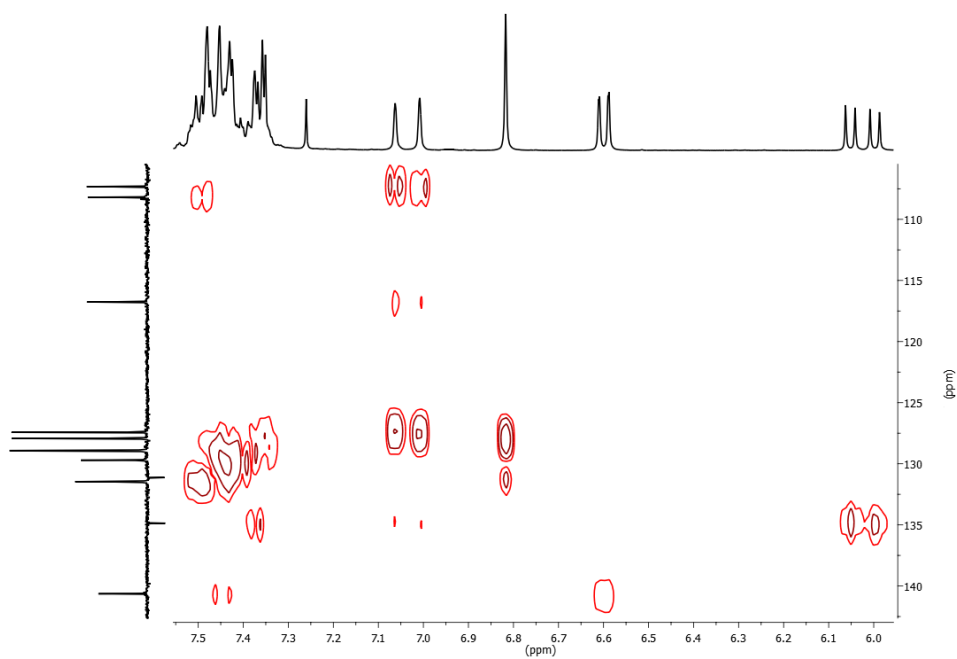
Chapter 5 - Annexes

Annex 1



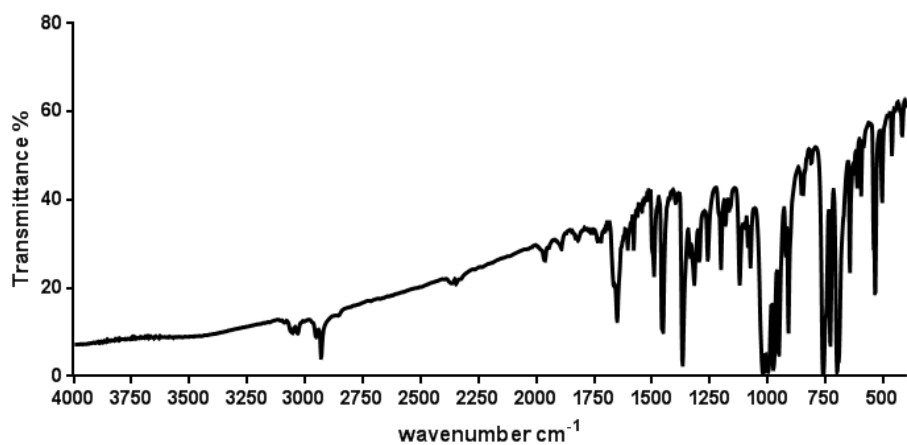
Annex 1- Benzaldehyde-tetraoxane (23) COSY specter.

Annex 2



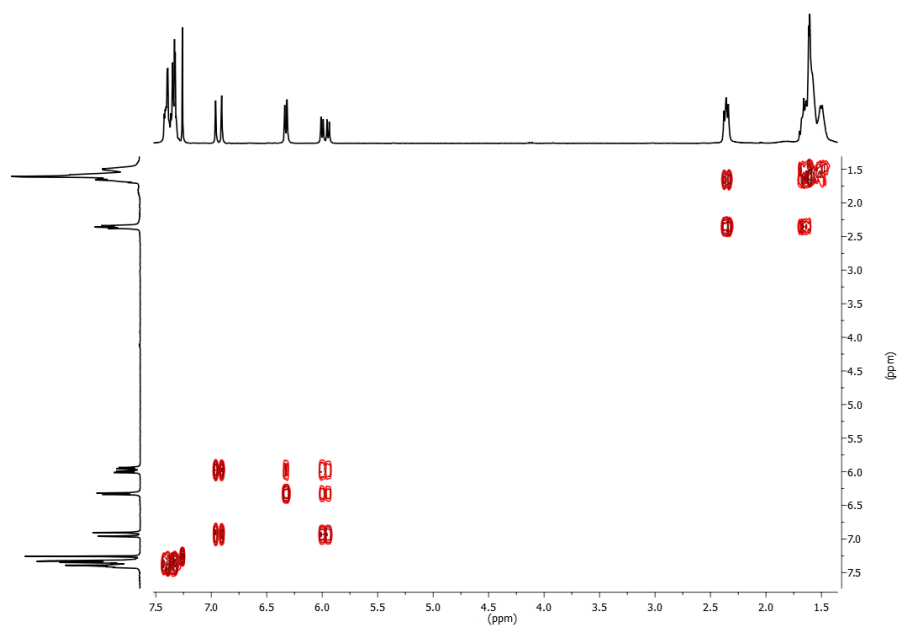
Annex 2- Benzaldehyde-tetraoxane (23) HMBC specter.

Annex 3



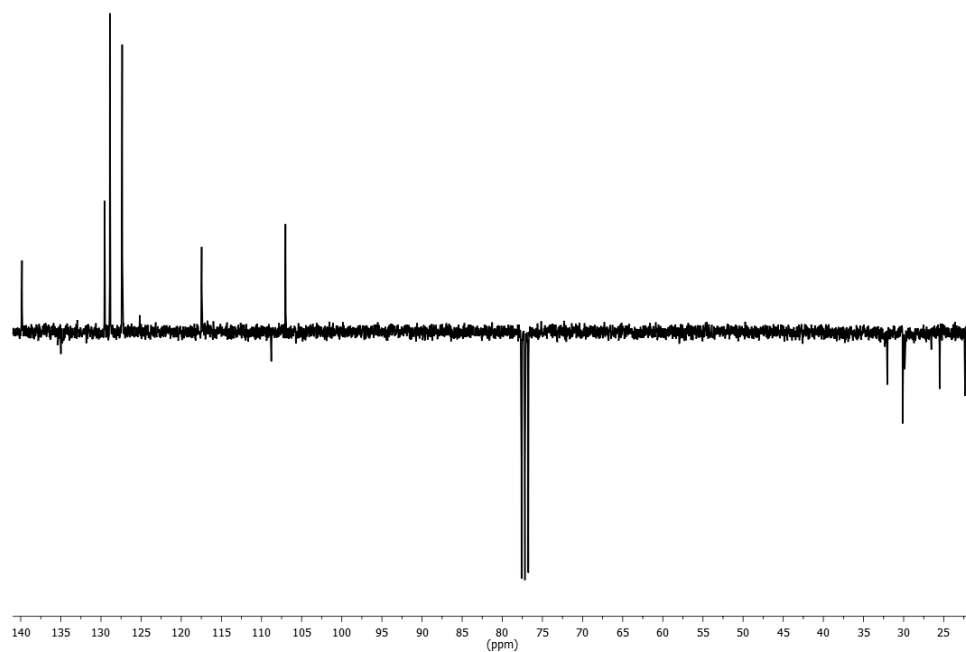
Annex 3- Benzaldehyde-tetraoxane (23) infrared specter.

Annex 4

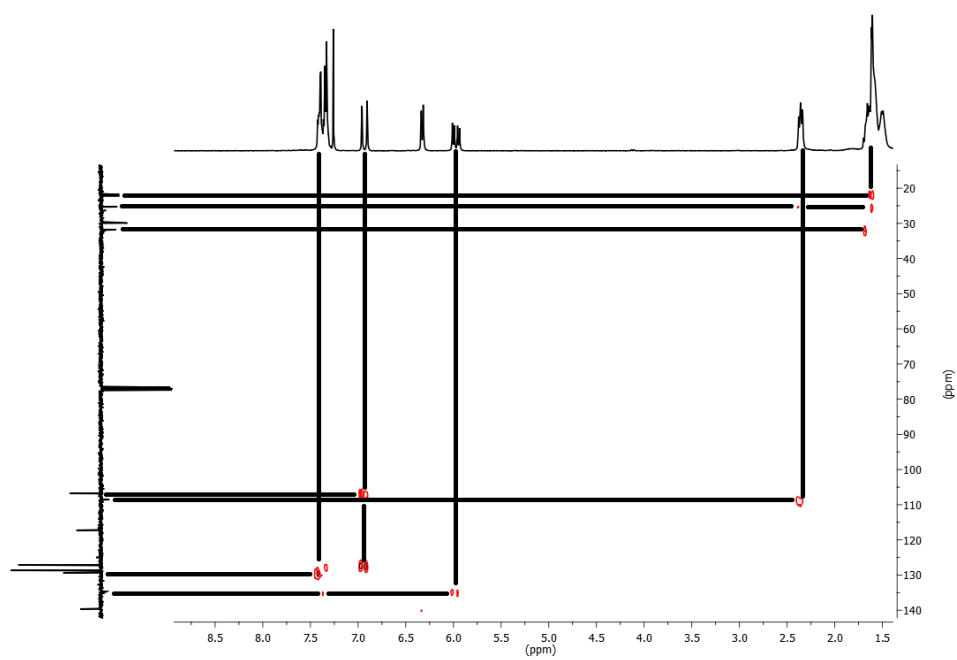


Annex 4- Cyclohexane-tetraoxane (24) COSY spectra.

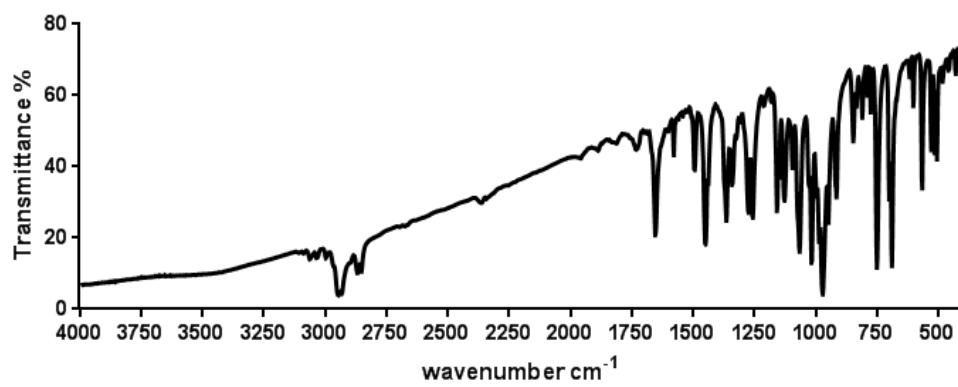
Annex 5

Annex 5- Cyclohexane-tetraoxane (**24**) ^{13}C -NMR spectra.

Annex 6

Annex 6- Cyclohexane-tetraoxane (**24**) HMBC spectra.

Annex 7



Annex 7- Cyclohexane tetraoxane (24) infrared spectra.